THESIS

SHAKE TABLE TESTING OF CONCRETE PORTAL FRAME WITH HIGH SPRAY DRYER ASH (SDA) CONTENT

Submitted by

Karthik Rechan Rudraprasad

Civil Engineering Department

In partial fulfillment of the requirements

For the Degree of Master of Science

Colorado State University

Fort Collins, Colorado

Spring 2010

COLORADO STATE UNIVERSITY

March 12, 2010

WE HEREBY RECOMMEND THAT THE THESIS PREPARED UNDER OUR SUPERVISION BY KARTHIK RECHAN, RUDRAPRASAD ENTITLED SHAKE TABLE TESTING OF CONCRETE PORTAL FRAME WITH HIGH SPRAY DRYER ASH (SDA) CONTENT BE ACCEPTED AS FULFILLING IN PART REQUIREMENTS FOR THE DEGREE OF MASTER OF SCIENCE.

Committee on Graduate Work

Rebecca Atadero

Bolivar Senior

Adviser: John W. van de Lindt

Department Head: Luis A. Garcia

ABSTRACT OF THESIS

SHAKE TABLE TESTING OF CONCRETE PORTAL FRAME WITH HIGH SPRAY DRYER ASH (SDA) CONTENT

Significant research has been conducted in replacing part of the cement content in concrete by fly ash. This thesis presents the method and results of an experiment to study the seismic behavior of a concrete portal frame with fifty percent of its cement content replaced by a spray dryer ash (SDA) , which is similar to fly ash, obtained from the Platte River Power Authority's Rawhide power plant in Northern Colorado. The behavior of the SDA portal frame under dynamic earthquake load is compared to the results obtained for the seismic behavior of ordinary Portland cement concrete. The portal frame is designed to represent the bottom story of a three-story office building in a high seismic region, e.g. Los Angeles, California. A mid bay portal frame is selected as a prototype frame and four similar 1/3 scaled down models of this frame were constructed. Two frames were constructed with fifty percent SDA concrete and the other two frames were constructed with ordinary Portland cement concrete. The frames were tested on the uni-axial shake table at the Colorado State University (CSU), Engineering Research Center (ERC), by placing two frames of the same mix type parallel to each other for stability. The scaled seismic mass is then placed on the frame and the instrumentation is installed. The concrete frames were tested first and then the SDA frames were tested using the same successive ground motions. Damage levels, and displacement response were recorded for each earthquake for both the tests and the results were compared. The basic premise of this thesis is to determine if a high SDA content frame sustains approximately the same amount of damage as a conventional concrete frame. By the results obtained from this study it has been shown that SDA frame may be considered to perform well, but not as good as conventional concrete frame. There was no significant damage or structural failure such as a collapse exhibited by the SDA frame when compared to that of conventional concrete frame. Hence about fifty percent of cement in concrete mix could be replaced by SDA for the construction of structural members in high seismic zones which leads to more economical buildings that help sustain the environment by redirecting spray dryer ash away from landfills.

Rudraprasad, Karthik Rechan
Civil and Environmental Engineering Department
Colorado State University
Fort Collins, CO 80523
Spring 2010

ACKNOWLEDGEMENTS

I would sincerely like to thank Dr. John W. Van de Lindt for his support, guidance and for accepting me as his student. His guidance has not only helped me in completing my masters but has also motivated me do more research and develop new ideas in the field of Civil Engineering. I consider myself very fortunate to have him as my mentor and would like to work under him for my doctoral studies.

I would like to thank my committee members, Dr. Rebecca Atadero for helping me by providing me information about Fly Ash and Spray Dryer Ash. I would like to thank

Dr. Bolivar Senior for accepting to be my outside committee member at the last minute. A grateful acknowledgement to Dr. Marvin Criswell for providing information and helping me in designing the frames.

I would like to thank Dr. Shiling Pei for helping me with the shake table and Platte River Authority for providing us the SDA material used in this research. I would like to thank Junior at the ERC my colleagues Sangki Park and Dao Nguyen Thang and all the people at the ERC machine shop for helping me to construct the frames.

Last but not least I would like to thank my parents, my brother Ashrith, my master Sri Parthasarathi Rajagopalachari, brothers and sisters of Sahaj Marg, friends and family for their love and support. I would specially like to thank my uncle Raveesh and aunt Shobha who supported me through my stay in the United States of America.

DEDICATION

This thesis is dedicated to my parents especially my father who encouraged me to become a Civil Engineer. Whatever I have achieved till this minute and all my future achievements is only due to the love, hard work, training, guidance and support of my parents Mr. Rudraprasad and Mrs. Ambika Prasad.

TABLE OF CONTENTS

LIST OF TABLES

LIST OF FIGURES

CHAPTER 1

INTRODUCTION

1.1 ASH IN CONCRETE

Ash is a byproduct obtained during the combustion of coal. Fly Ash is generally obtained from the chimneys of coal-fired power plants. Depending on the amount of calcium, silica, iron and alumina content of the ash there are two classes of fly ash as defined by ASTM C618 they are Class C and Class F fly ash. Class C fly ash has high calcium content and its carbon content is usually less than two percent, while Class F fly ash has a low calcium content with a carbon content usually less than five percent. Fly Ash, due to its pozzolanic properties is usually used to as an additive to Portland cement in concrete production. Pozzolans are materials which when combined with calcium hydroxide exhibit cementitious properties. The use of fly ash in concrete increases the strength and durability of the concrete and also decreases the heat of hydration and permeability in concrete. When compared to Portland cement, fly ash contains lesser amounts of iron, alumina, calcium, magnesium, sulfur, potassium, and sodium in oxidized forms. The specific gravity of fly ash ranges from 1.9 to 2.8 whereas that of Portland cement is 3.15 hence fly ash is less dense than Portland cement. The use of fly ash in concrete helps to reduce the pollution in the environment because for every ton of fly ash used to replace Portland cement in the manufacture of concrete there is a reduction of carbon dioxide emissions which is equal to the amount of carbon dioxide released from an automobile during a two month period. Since the majority of SO_2 emission into the atmosphere is due to the coal fired power plant, in recent years many coal fired power plants in the US are utilizing spray dry absorber (SDA) material for the reduction of SO_2 gas emission. In this process alkali sorbents such as lime (CaO) or calcium hydroxide ($Ca(OH)_2$) are mixed with water to form a aqueous slurry. This slurry is sprayed into the flue gas in a cloud of fine droplets. SO_2 is captured with this sorbent and is dried by the heat of flue gases. The dried mix of the sorbent and SO_2 is collected. Since most of the SDA system in U.S collect Fly ash and SDA material together the properties of the SDA material are similar to that of Fly ash. The ash obtained for our research is from Platte River Power Authority's Rawhide Power Plant (RPP) which uses the SDA system. The ash obtained from RPP power plant has a specific gravity of 2.1g/cc, due to its high sulphur content its chemical properties and mineralogical properties (Riley, 2009) are slightly different for it to be classified as Class C ash according to (ASTM, 2008).

There have been numerous studies conducted on the use of ash in concrete, several recent and relevant studies are listed in Table 1

Table 1 Studies conducted on the use of Fly Ash in Concrete

	Authors	Date	Title	Summary
1	R. N. Swamy Sami A. R. Ali D. D. Theodorakopoulos	1983	Early strength of? fly ash concrete for structural applications	Conducted tests on reinforced concrete fly ash concrete beams and slabs containing normal weight aggregates and light weight aggregates. The results of the tests showed that fly ash concrete can exhibit structural performance similar to that of conventional concrete with adequate safety factors and predicted by existing codes. The results of the study also showed that structural concrete construction can be designed to incorporate controlled quality of fly ash up to 30 percent by weight of cement.
2	Ramesh C. Joshi James M. Oswell Gurinder S. Natt	1985	Laboratory investigations on concrete and geocrete with high fly ash contents	Studied the engineering properties of non air entrained concrete. Laboratory tests were conducted on both fly ash concrete and ordinary Portland cement concrete specimens. Based on the properties such as compressive, flexural, indirect tensile strengths and additional non destructive tests it was concluded that fly ash concrete could be used as a construction material for the core of the gravity dam and pavement sub-base or base courses.
3	Hussain SE Rasheeduzzafar more name here?	1994	Corrosion resistance performance of fly ash blended cement concrete	Conducted accelerated corrosion tests on reinforced concrete specimens made of plain cement concrete and fly ash blended cement concrete. The results of the test showed superior corrosion resistance of fly ash concrete when compared to plain cement concrete.

4	Michel Pigeon V. Mohan Malhotra	1995	Frost resistance of roller-compacted high-volume fly ash concrete	In this study four high-volume fly ash-compacted concrete mixes were designed by fixing the amount of fly ash to the total cementitious material content. Laboratory investigations were carried out on air-entrained and non air-entrained concrete mixes and the results showed that frost resistance of air-entrained concrete mixes was slightly more than that of non-air entrained concrete mixes. The results of this study recommended the use of air entrainment for roller-compacted high-volume fly ash concretes.
5	G. Dinelli G. Belz C.E majorana B.A. Scherfler	1996	Experimental investigation on the use of fly ash for lightweight precast structural elements	Conducted experiments to find the possibility of partial or complete substitution of traditional aggregates in light weight concrete by aggregate made of fly ash. The results of the experiments found that the traditional aggregate could be substituted by the aggregate\ made of fly ash.
6	V. Saraswathy S. Muralidharan K. Thangavel S. Srinivasan	2002	Influence of activated fly ash on corrosion-resistance and strength of concrete	Conducted tests to study the corrosion resistance and strength of activated fly ash cement concrete. Physical, thermal and chemical activation techniques were adopted to accelerate the hydration of fly ash blended cement to improve the corrosion resistance and compressive strength.
8	A. Fernandez-Jimenez I.Garcı´a-Lodeiro A. Palomo	2006	Durability of alkali-activated fly ash cementitious materials	Studied the durability of alkali-activated fly ash (AAFA) cement under different conditions and in a number of aggressive environments such as deionized water, ASTM sea water, sodium sulphate, and acidic solutions. Studies were also made with respect to alkali-silica reaction-

				induced expansion. Weight loss, compressive strength, variations in volume, presence of the products of degradation and microstructural changes were the chief parameters which were studied. The results of the study showed that AAFA cement pastes performed satisfactorily in aggressive environments and the degradation of the materials resulting from such processes was distinctly different from that of the ordinary Portland cement paste. The AAFA mortars were found to be compliant with the 16-day expansion limit stipulated in ASTM standard C 1260-94 on potential alkali-silica reactivity.
8	J.W. van de Lindt, J.A.H. Carraro, P.R. Heyliger C. Choi	2007	Application and feasibility of coal fly ash and scrap tire fiber as wood wall insulation supplements in residential buildings	Carried out a study to investigate the possibility of increasing the thermal efficiency of a light frame residential structure through addition of fly ash-scrap tire fiber composite to traditional fiberglass insulation in light-frame wood residential construction. They found that the fly ash-scrap tire composite not only provided a sustainable supplement to traditional insulation but also helped to significantly reduce the environmental issues associated with the disposal of these composites.

1.2 SCALING PROCEDURE

Model scaling is a procedure in which a structural model is built to a reduced scale and tested. The structural model is related to the prototype structure by similitude theory. The model must be designed, loaded and the results must be interpreted as per the similitude requirements (Bracci, 1992). Similitude is developed between the model and the prototype by using dimensional analysis. The scaling procedure for our experimental study was carried out by applying the Buckingham pi theorem (Harris, 1999). The Buckingham pi theorem states that any dimensionally homogenous equation involving certain physical quantities can be reduced to an equivalent equation involving a complete set of dimensionless products. According to this theorem the solution for equation (1) of some physical quantity of interest can be expressed in the form of equation (2) as shown below.

$$F(X_1, X_2, X_3, ...X_n) = 0 \qquad (1)$$

$$G(\pi_2, \pi_2, \pi_3, ...\pi_n) = 0 \qquad (2)$$

where X_1, X_2 are the physical quantities and the pi terms are the dimensionless products of the physical quantities. The number of dimensionless products (m) is equal to the difference between the number of physical variables (n) and the number of fundamental measures(r). There are infinite number of possibilities in determining the pi terms and the solution to the unknown pi terms can be found experimentally.

1.2.1 SIMILITUDE

Structural models can be of different types which are namely true, adequate, distorted or dissimilar models depending on the similitude relations between the pi terms for the model (π_m) and those of the prototype (π_p). Using Buckingham's theorem to reduce any physical quantity to dimensionless products as shown in equation (2), the pi terms can be obtained once for the model and once for the prototype, and the equation (3) can be formed as shown below.

$$\frac{\pi_p}{\pi_m} = \frac{G(\pi_{1p}, \pi_{2p}, \pi_{3p}, \ldots \pi_{np})}{G(\pi_{1m}, \pi_{2m}, \pi_{3m}, \ldots \pi_{nm})} \qquad (3)$$

A model is said to be similar if the pi terms of the model and prototype are same. The similitude relation can be established for the corresponding pi terms by equating $\pi_p = \pi_m$ for each pi term and solving for the scale factor. The scale factor (s_i) can be defined as the ratio of the quantity (i) of the prototype (p) to that of the model (m), $s_i = i_p/i_m$. For example, the length scale can be expressed as shown in equation (4)

$$S_l = \frac{l_p}{l_m} \qquad (4)$$

where S_l = length scale factor

l_p = length of the prototype

l_m = length of the model

Appendix D shows the scale factors for different physical quantities used in this study. The Pi theorem can also be used to establish dynamic relationships between the model and prototype structure in order to satisfy the similitude requirements, which are dependent on the material properties, geometric properties and the type of loading on the structure. Length (L), force (F) and time (T) are the fundamental quantities considered for the dimensional analysis. The pi factor for the dynamic loading can be formed as show in equation (5).

$$G(Ft^2/ml) = 0 \qquad (5)$$

Complete similarity can be obtained by making the pi factor the same for both model and prototype as shown in equation (6)

$$\frac{F_m t_p^2}{m_m l_m} = \frac{F_p\, t_p^2}{m_p l_p} \qquad (6)$$

By using the scale factor definition as mentioned earlier in this chapter, the scale factors for force, length and time can be established as shown in equation (7).

$$S_F = \frac{F_p}{F_m} \qquad S_l = \frac{l_p}{l_m} \qquad S_t = \frac{t_p}{t_m} \qquad (7)$$

Since only gravity forces are considered for our experimental study it should be noted that $S_l^2 = S_t$, hence our 1/3rd scaled model will vibrate with a period 1.73 times shorter than our prototype structure.

1.3 BRIEF DESCRIPTION OF THE THESIS

The objective of this thesis was to study the seismic behavior of concrete portal frames when replacing fifty percent of their cement content by spray dryer ash (SDA) and comparing that with the seismic behavior of ordinary Portland cement concrete for the same ground motions. The SDA used for this study was obtained from the Platte River Power Authority's Rawhide power plant in Northern Colorado. Figure 1.1 shows the plan view of the three storey office building considered for this study. The building is designed for seismic load conditions as per (ASCE 7-05 (2005)) and seismic detailing is done according to (ACI 318-05 (2005)). A mid bay portal frame is selected as a prototype frame and four similar 1/3 scaled down models of this frame were constructed. Two frames were constructed with fifty percent SDA concrete and the other two frames were constructed with ordinary Portland cement concrete. Every effort was made to provide mixes of approximately the same strength. The frames were tested on the shake table by placing two frames of the same mix type at a distance of 1.6 m (5'3") in parallel for stability. The frames were tied together by wooden boards in the transverse direction so that there is no torsion and the frames behave as a space frame while testing, thus simulating the bottom story of the three-story building more closely than a single frame. The scaled down seismic mass is then placed on the frame and the instrumentation installed. Figure 1.2 shows the experimental setup of the model on the 2.44 m (8') x 4.88 m (16') shake table before the test at the Colorado State University (CSU), Engineering Research Center (ERC). The Portland cement concrete frames were tested first and then the SDA concrete frames were tested using the same successive ground motions. Chapter 2 provides a detailed description of the design and experimental setup including the mass scaling procedure for these specimens based on the scaling principle explained in section 1.2 of this chapter. Chapter 3 discusses the results obtained by comparing the damage recordings and graphs of displacement response graphs. Chapter 4 gives the summary of this study and conclusions. Based on the results obtained from this study it can be stated that concrete having high SDA content should be considered for engineered construction in seismic zones as the compressive strength of this SDA concrete is nearly equal to that of the ordinary Portland cement concrete and also the damage obtained is similar to that obtained from ordinary Portland cement concrete.

Using SDA in such construction can lead to more economical buildings that help sustain the environment by redirecting spray dryer ash away from landfills.

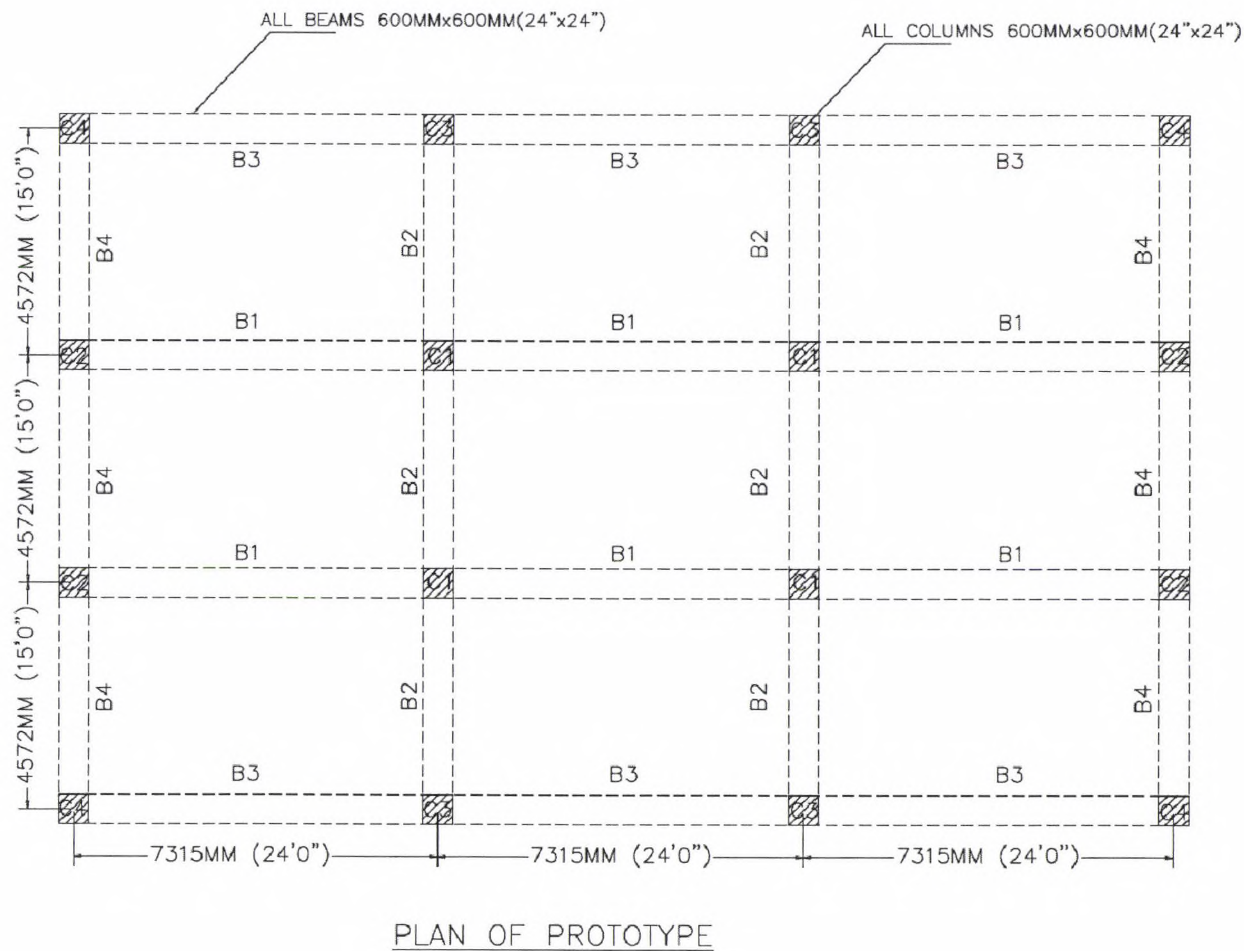

Figure 1.1 Plan of the prototype structure

Figure 1.2 Experimental setup of the model on the shake table

Chapter 2

DESIGN OF FRAMES AND EXPERIMENTAL SETUP

2.1 DESIGN OF FRAMES

The frame tested on the shake table was selected from a three storey office building having three bays in both the X and Y directions as shown in Figure 1.1. The office building was designed in such a manner that there were no plan irregularities or vertical irregularities. The frames were designed for seismic resistance and to carry gravity loads. Design loads and load factors were selected as per the seismic load combinations from ASCE 7-05 (2005). The frames were designed for seismic resistance as per seismic detailing provisions of ACI 318-05 (2005). Finite element software AxisVM9 was used for analysis of the structure.

The prototype frames selected for the design were two frames from the center of the building plan each having a span of 4.57 m (15') and height of 3.05 m (10'). An eight inch thick reinforced concrete slab was assumed for the load calculations on beams. The prototype frames were selected such that two 1/3 scaled frames could be placed parallel to each other and tested on the shake table. The frames were designed as reinforced concrete special moment frames (SMF) by using ACI chapters 1 to 18 plus ACI section 21.5. The material strengths assumed for the design were ASTM Grade 60 steel 413.68

N/mm^2 (f_y=60 ksi) and ordinary type II Portland cement concrete having a 28 days compressive strength of 27.6 N/mm^2 (4000 psi).

2.1.1 LOAD CALCULATIONS

The frames were designed for seismic resistance by taking the earthquake loading into consideration. Load combinations from Chapter 2 of ASCE 7-05 were used and the critical load of these combinations was taken for the analysis of the structure. The following load combinations from ASCE 7 were used to calculate the loading.

$$1.2\ D + 1.6\ L \qquad (2.1)$$

$$1.2\ D + 1.0\ E + L + 0.2\ S \qquad (2.2)$$

$$0.9\ D + 1.0\ E + 1.6\ H \qquad (2.3)$$

The snow load ‘S’ and load due to lateral earth pressure ‘H’ were neglected in the design.

The dead load of the 203.2 mm (8”) thick slab was calculated to be 0.0048 N/mm^2 (100 psf) by assuming the unit weight of reinforced concrete was 2.36KN/m^3 (150 lb/ft^3). The live load on the slab was found to be 0.0048 N/mm^2 (100 psf) from Table 4-1 of ASCE 7. The seismic load effect E was determined according to equations 12.4-1 and 12.4-2 of ASCE 7. The equivalent lateral load procedure 12.8 from ASCE 7 was used to calculate the seismic base shear V. The base shear V was used to calculate the seismic load effect E which was used in the above equations. The calculated values of different load combinations are listed in Appendix A. The Equivalent lateral force procedure used to determine the seismic loading, E, is explained in Appendix B.

2.1.2 DESIGN OF BEAMS

The beams are designed as the flexural members of special moment resisting frames (SMRF) according to special provisions for seismic design from chapter 21 in the ACI code (ACI, 2005). The maximum design loads for the analysis of the frame were determined from the above load combinations and the storey shear was applied to each storey as shown in the Figure 2.1. The loads were applied to the structure and the analysis was conducted using a finite element software, AxisVM9. The beam is designed for the maximum moments and shear forces obtained from the analysis. Beams having cross section (c/s) 609.6 mm X 609.6 mm (24" X 24") were designed according to section 21.3 of the ACI code. The ultimate moment (M_u), reinforcement chosen for the beam c/s, nominal moment (φM_n), and the probable moment (M_{pr}) used in the design of the beams B1 and B2 are listed in Table 2.1 and Table 2.2. The interested reader is referred to ACI 318-05 code for the detailed procedure of the beams designed in SMRF.

The design shear forces are based on the factored dead loads, live loads, plus the shear due to hinging at the ends of the beams for the frames swaying either to the left or to the right. The beams are designed for shear as per shear strength requirements of section 21.3.4 of the ACI code. V_c is taken as zero because the earthquake induced shear is more than half the value of maximum shear as per ACI section 21.3.4.2. Shear detailing is provided as per section 21.3.3.2 of the ACI code. Figure 2.2 shows the detailing of the shear reinforcement provided for the beams.

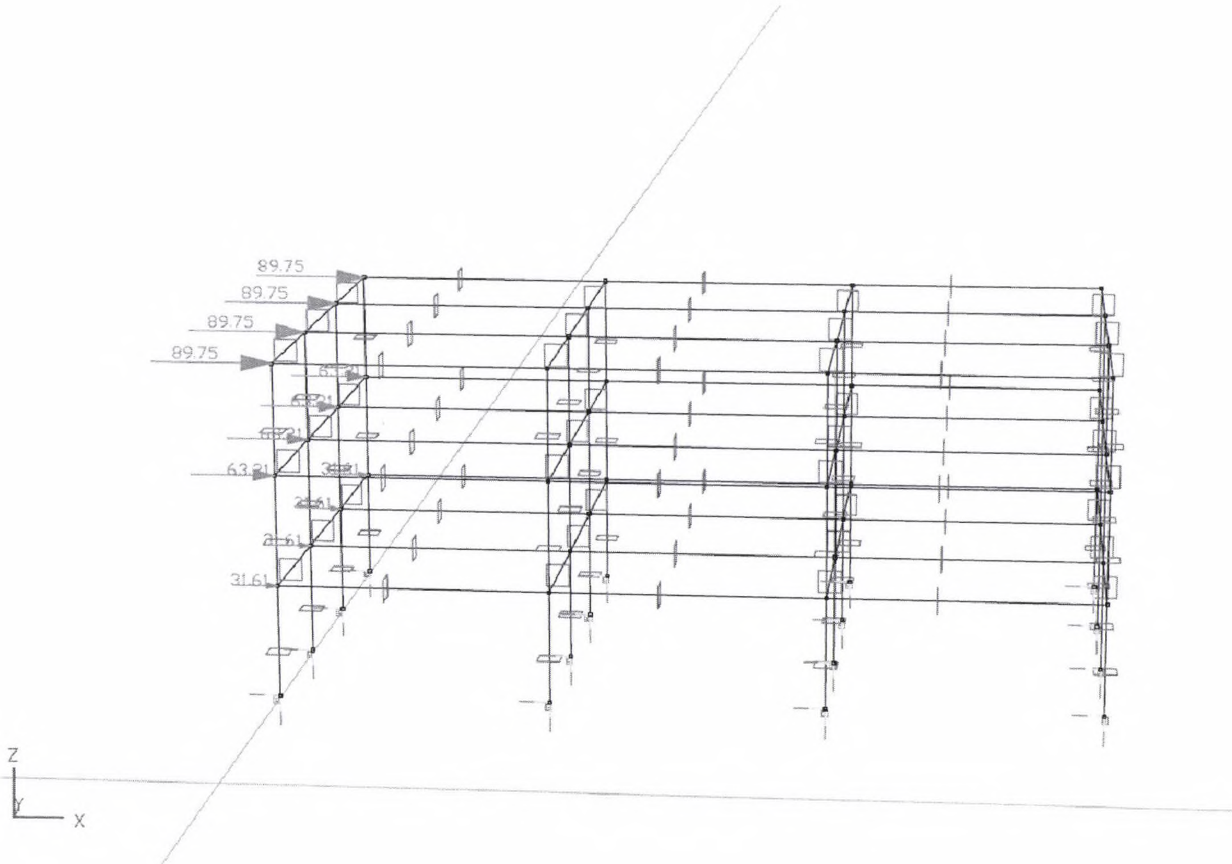

Figure 2.1 Distribution of base shear

Table 2.1 Details of Beam B1

Case	Location	Sway Direction	Mu, KN-m (kip-ft)	Reinforcement provided	As,mm^2 (in^2)	pi Mn, KN-m (kip-ft)	Mpr, KN-m (kip-ft)
1	Exterior end Negative moment	Left	-591.27 (-436.1)	7-No 8	3,567.73 (5.53)	-656.80 (-484.43)	-888.41 (-655.26)
2	Exterior end Negative moment	Right	-591.27 (-436.1)	7-No 8	3,567.73 (5.53)	-656.80 (-484.43)	-888.41 (-655.26)
3	Exterior end Positive Moment	Right	295.64 (218.05)	4-No 8	2,038.71 (3.16)	392.12 (289.21)	536.82 (395.94)
4	Exterior end Positive Moment	Left	295.64 (218.05)	4-No 8	2,038.71 (3.16)	392.12 (289.21)	536.82 (395.94)
5	Midspan Positive Moment		147.81 (109.02)	1- No 9			

Table 2.2 Details of beam B2

Case	Location	Sway Direction	Mu, KN-m (kip-ft)	Reinforcement Provided	As,mm^2 (in^2)	pi Mn, KN-m (kip-ft)	Mpr, KN-m (kip-ft)
1	Exterior end Negative moment	Left	-448.02 (-330.44)	5-No 8	2,548.38 (3.95)	-483.175 (-356.35)	-658.93 (-485.97)
2	Exterior end Negative moment	Right	-448.02 (-330.44)	5-No 8	2,548.38 (3.95)	-483.175 (-356.35)	-658.93 (-485.97)
3	Exterior end Positive Moment	Right	295.64 (218.05)	4-No 8	2,038.71 (3.16)	323.23 (238.38)	443.75 (327.27)
4	Exterior end Positive Moment	Left	295.64 (218.05)	4-No 8	2,038.71 (3.16)	323.23 (238.38)	443.75 (327.27)
5	Midspan Positive Moment		83.91 (61.89)	2-No 8			

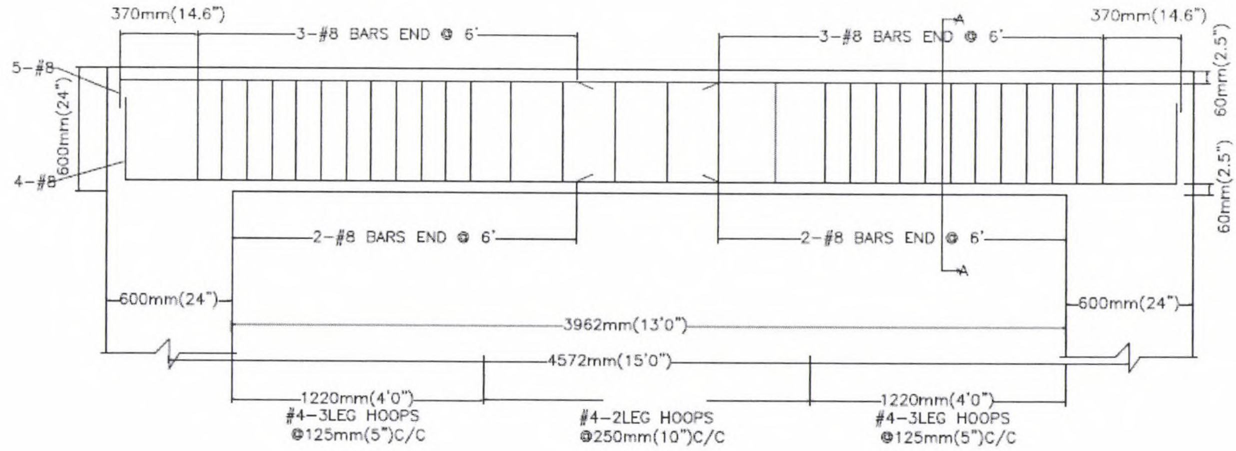

BEAM B2 PROTOTYPE

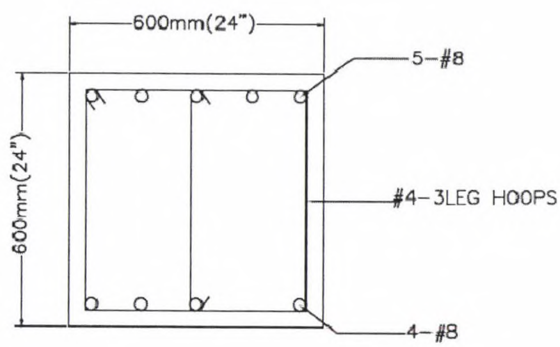

SECTION ALONG A-A

Figure 2.2 Reinforcement detail of prototype beam B2

2.1.3 COLUMN DESIGN

The Columns were designed as per ACI section 21.4.2 using the strong column weak beam concept. In this type of design plastic hinges are first formed in the beams and not in the columns, hence the damage to the columns is minimized. In this concept the nominal flexural capacity (M_{nc}) of the column should be greater than 6/5 of the sum of the nominal flexural strength (M_{nb}) of the beams framing into the joint.

For the prototype column which is a c/s 24" X 24" with 12-#8 bars the interaction diagrams are shown in Appendix E. From the interaction diagram $\sum M_{nc}$ was found to be 1,721.89 KN-m (1270 kip-ft) which is greater than six fifth times $\sum M_{nb}$ which was found to be 967.62 KN-m (713.676 kip-ft) . #4 diameter, three leg hoop in each direction was provided as per the requirements of the ACI code to resist shear and for the confinement of longitudinal bars in the column. The beam column joint was designed as per section 21.5 of the ACI code. The detailing of the prototype column is show in Figure 2.3.

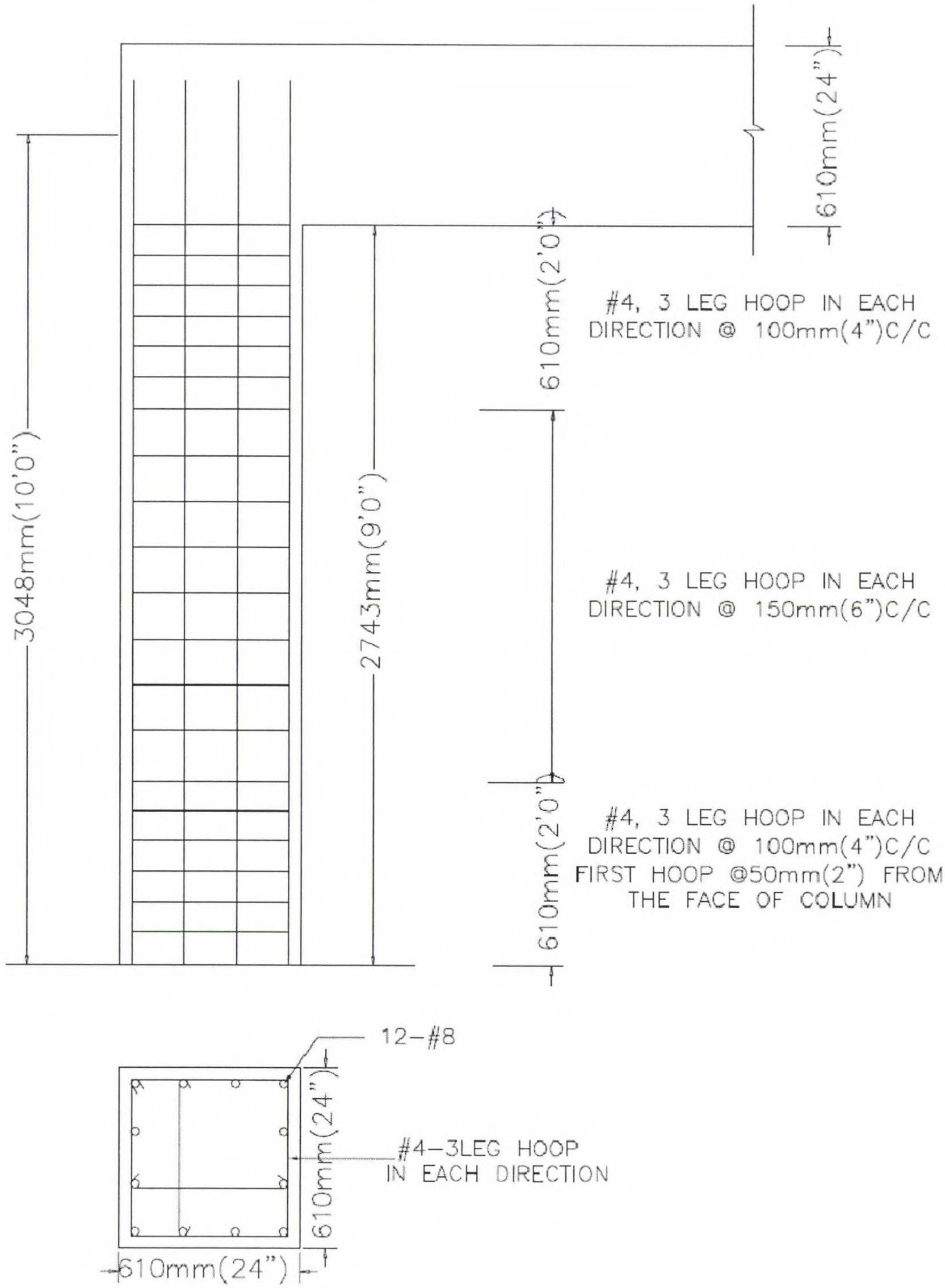

Figure 2.3 Reinforcement detail of the prototype column

2.2 SCALING OF THE MODEL

The model was scaled by using the Buckingham pi theorem as mentioned in chapter 1.2. Figure 2.4 shows the plan for the one-third scale model of the prototype. Design and properties of one third scale model structures have been tested successfully before (see e.g. Bracci, 1992). The length factor used for scaling is 3 and Appendix D shows the scale factors for other quantities. The reinforcement bars provided for the prototype beams and columns to resist flexure and shear are #8 and #4 bars having yield strength of 413.68 Mpa (60 ksi). The c/s areas of #8 and #4 grade 60 bars are 509.68 mm^2 (0.79 in^2) and 129.03 mm^2 (0.2 in^2). Hence by referring to Appendix D yield force scale factor of 9 is used to find the required area of bars used as reinforcing steel in the model. Thus bars having areas of 56.8 mm^2 (0.088 in^2) and 14.2 mm^2 (0.022 in^2) must be provided for reinforcement in the model. 9.52 mm (3/8") all-thread steel rods having c/s area of 71 mm^2 (0.11 in^2) and 5.08 mm (0.2") diameter galvanized steel wires having c/s area of 20.3 mm^2 (0.0314 in^2) were used as flexural and shear reinforcement in model, respectively. All-thread rods were used instead of #3 rebar as the effective area excluding threads is less than that of #3 rebar and close to the required area of 56.8 mm^2 (0.088 in^2). Figure 2.5 and Figure 2.6 show the reinforcement details of the model.

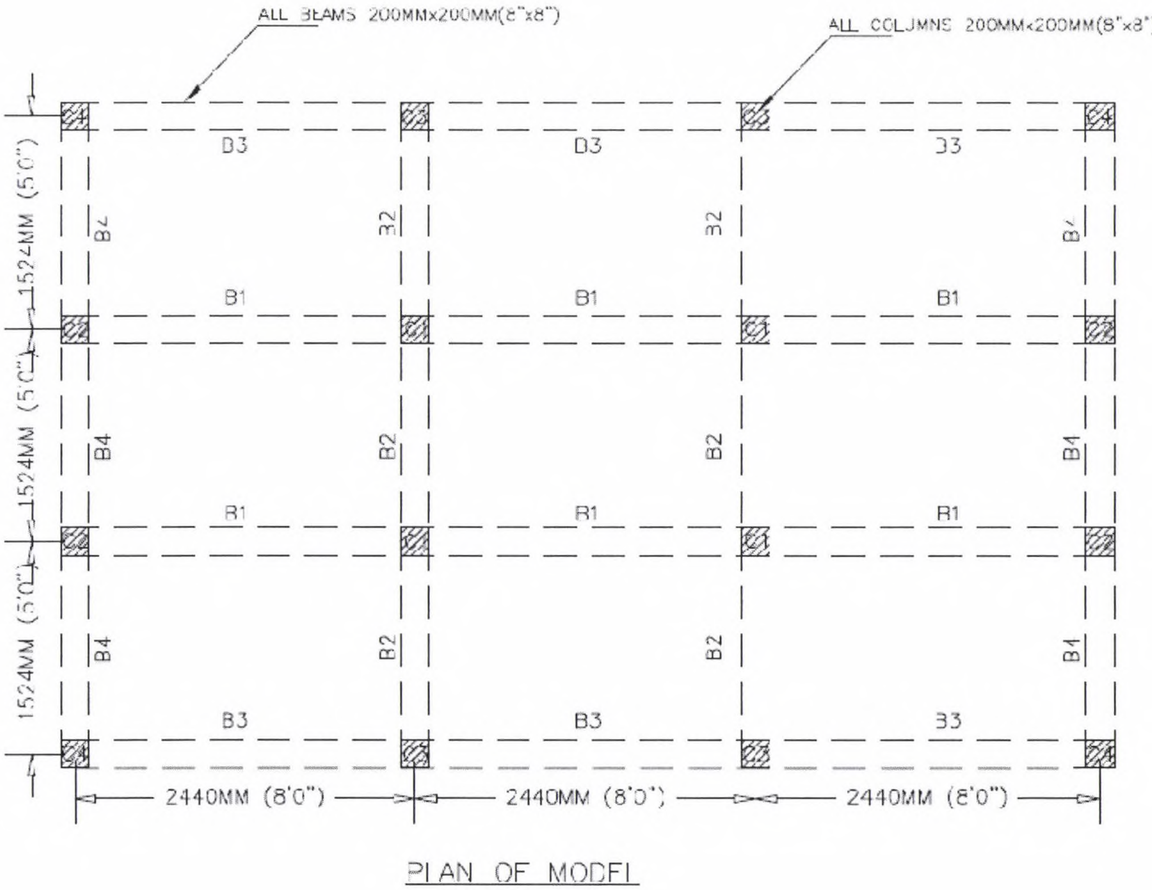

Figure 2.4 Plan of the 1/3rd scaled model

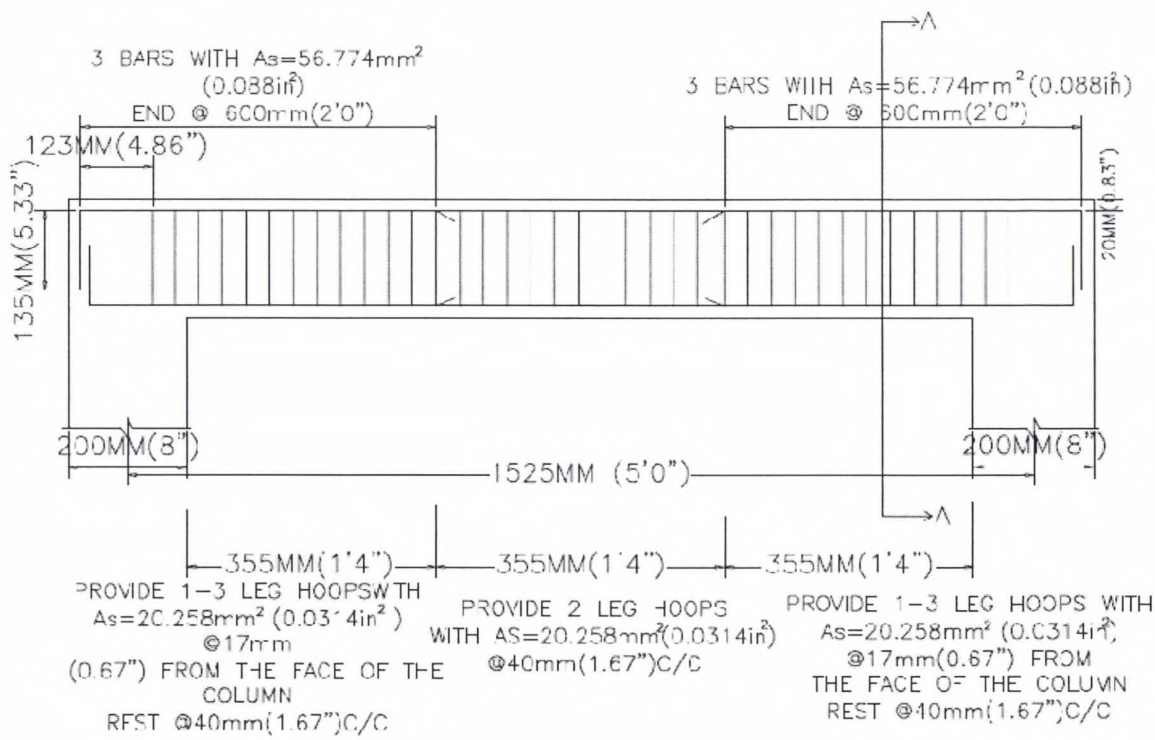

BEAM DETAIL OF MODEL

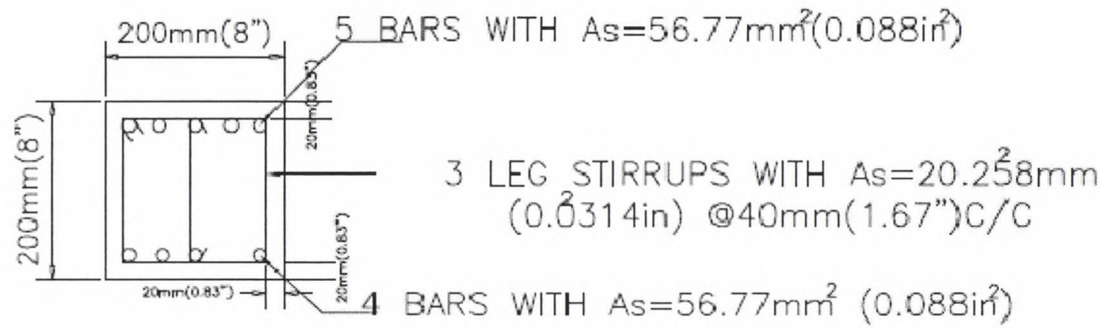

SECTION ALONG A-A

Figure 2.5 Reinforcement details of the 1/3rd scaled beam B2

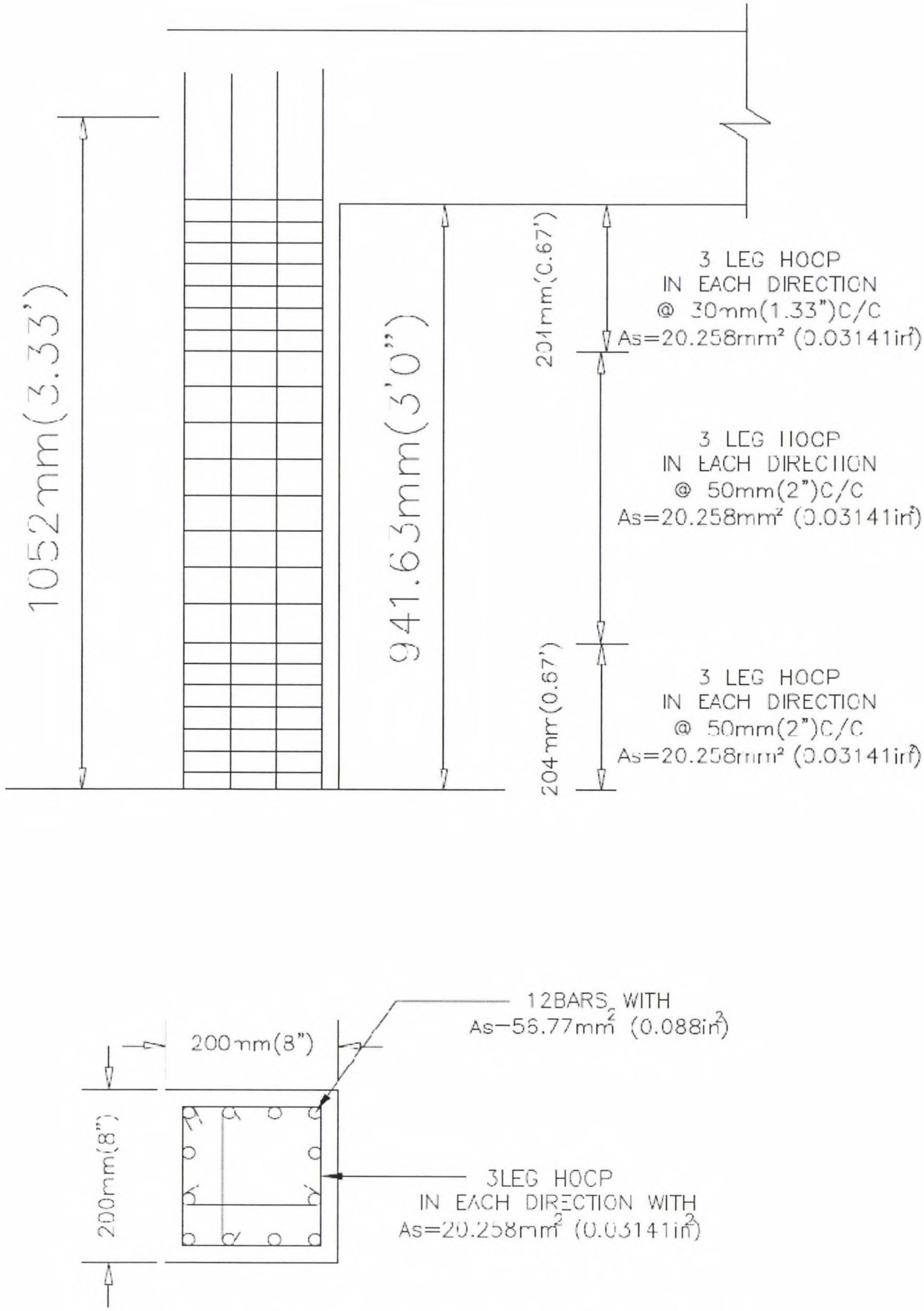

Figure 2.6 Reinforcement detail of the 1/3rd scaled column

2.3 MIX DESIGN

The material properties and compressive strength of the model and the prototype are considered to be the same, hence the scale factor of one is considered for the mix design since the acceleration and the materials of the model and the prototype are the same. Type II Portland cement, SDA from Rawhide power plant and ¾" coarse aggregates, sand and high range water reducing agent from a local RMC plant were used for the concrete mixes in the model. The compressive strengths of the concrete mixes were obtained by testing the concrete cylinders in compression testing machine, after 7, 21 and 28 days from the day the respective models were cast.

The mix design for the spray dryer ash (SDA) concrete mix was obtained from the study by King(2005). A few modifications were made to the mix design, SDA was used instead of Class F fly ash as mentioned in the original mix design. SDA is similar to Class C fly ash but has a slightly different chemical composition. Fifty percent of cement and fifty percent of SDA were used for the mix instead of 45% of cement and 55% of fly ash as mentioned in the original mix design. Only ¾" coarse aggregate was used and high range water reducers were used as mentioned in the mix design. The mix design and the obtained compressive strengths of the SDA concrete are shown in Table 2.2. The compressive strength obtained was greater than the desired compressive strength mentioned in the original mix design.

The mix design for Portland cement concrete was obtained from the PCA mix design software developed by CSU. The mix design was done for the desired 28 days compressive strength of 31.03 N/mm^2 (4500 psi). The Table 2.4 shows the mix design and the obtained compressive strength of the concrete mix used in the model. The compressive strength obtained exceeded the desired compressive strength of the concrete mix.

Table 2.3 SDA Concrete Mix Design

Weights for1 cubic foot of 50% SDA concrete

Type II Portland cement	49.69 N (11.17 lbs)
Spray Dryer Ash	49.69 N (11.17 lbs)
Sand	237.43 N (53.38 lbs)
3/4" Coarse aggregate	318.58 N (71.62 lbs)
Water	33.18 N (7.46 lbs)
High range water reducer	3.3 ml
W/CM ratio	0.33

Compressive Strength	N/mm^2 (psi)
7 days	20.04 (2907)
21 days	37.79 (5482)
28 days	46.91 (6803)

Table 2.4 Type II Portland cement concrete mix design

Weights for 1 cubic foot of Concrete

	N (lbs)
Water	63.10 (14.19)
Cement	146.48 (32.93)
3/4" Coarse aggregate	222.41 (50.00)
Fine aggregate	44.88 (199.64)

W/C ratio 0.43

Compressive Strength	N/mm^2 (psi)
7 days	42.64 (6184)
21 days	51.23 (7436)
28 days	56.33 (8170)

2.4 EXPERIMENTAL SETUP

A 4.57 meter (15') long 1/3 scale portal frame from the center bay of the plan (see Figure 2.4) was selected for construction and testing. Four portal frames were constructed in total for the experiment, out of which two frames were made of ordinary Portland cement concrete having a compressive strength of 56.33 N/mm^2 (8170 psi) (Table 2.4). The other two frames were made of concrete in which 50% of the cement was replaced by SDA, having a compressive strength of 46.91 N/mm^2 (6803 psi), (Table 2.3). The formwork was made using ½" thick plywood boards and 3" X 4" wooden blocks. Figure 2.7 shows the setup of the formwork.

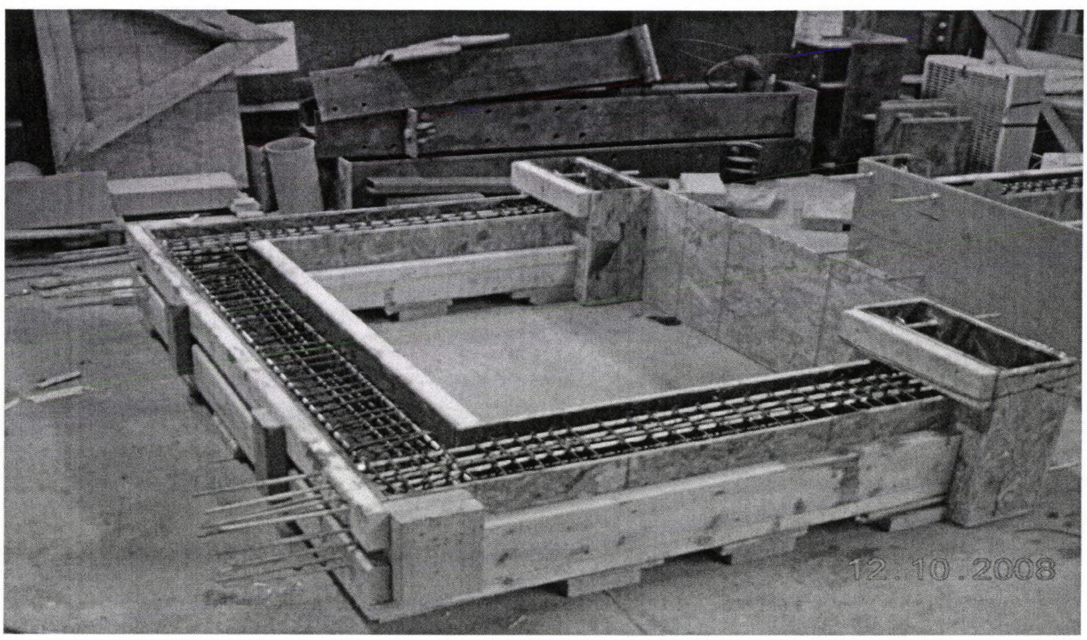

Figure 2.7 Formwork before pouring of concrete

The reinforcement bars were tied as per the detailing shown in Figures 2.5 and 2.6 using a two end loop steel wires as used in the actual construction. The size and type of bars used for the longitudinal and transverse reinforcement were as discussed in section

2.2 of this chapter. The reinforcement was placed in the formwork by keeping the formwork flat on the ground. The column bars were extended about 6" out of the formwork such that two frames could be tied together while testing thus restricting them from accidental torsion. Concrete was poured on two days. First SDA concrete was poured in two of the formworks, then plain cement concrete was poured into the remaining two formworks on the next day. The concrete was mixed in a 9 ft^3 capacity concrete mixer and was compacted using a needle vibrator having a 1" thick head. The concrete was poured in two batches per model as per the mix design shown in Table 2.3 and Table 2.4 for 50% SDA and plain cement concrete, respectively. The concrete was allowed to cure for 28 days, water was sprinkled for curing for the first fourteen days and the model was left open in the lab to cure for the remaining days. A total of 18 cylinders were cast to test the compressive strength of concrete, 9 cylinders were of plain cement concrete and the other 9 were of SDA cement concrete. The cylinders were tested in the compression testing machine in the CSU concrete lab.

The formworks were removed after 28 days and the models were ready for testing. The seismic mass was calculated using a mass similitude factor of 9, by referring to the table in Appendix D and by using the mass similitude procedure outlined in Bracci (1992). The seismic mass to be placed on the model was found to be 17,605 lbs with details shown in Appendix C. Two frames at a time were placed on the shake table with the help of a fork lift. First the Portland cement concrete frames were placed and tested, followed by the testing of the two SDA concrete frames. Figure 2.7 and figure 2.8 shows the setup of the concrete and SDA concrete models with the seismic mass on the shake table before testing. As the seismic weight was 17605 lbs, two steel fork lift counter balances weighing 5000 lbs each, two concrete blocks of 1800 lbs each and a concrete block of 4000 lbs were used as the seismic weights. Three displacement gauges were used to measure the displacement of the frames. Figure 2.9 shows the instrumentation of the experimental setup. The comparison of damages, and displacement responses obtained after the tests are discussed in detail in the next chapter.

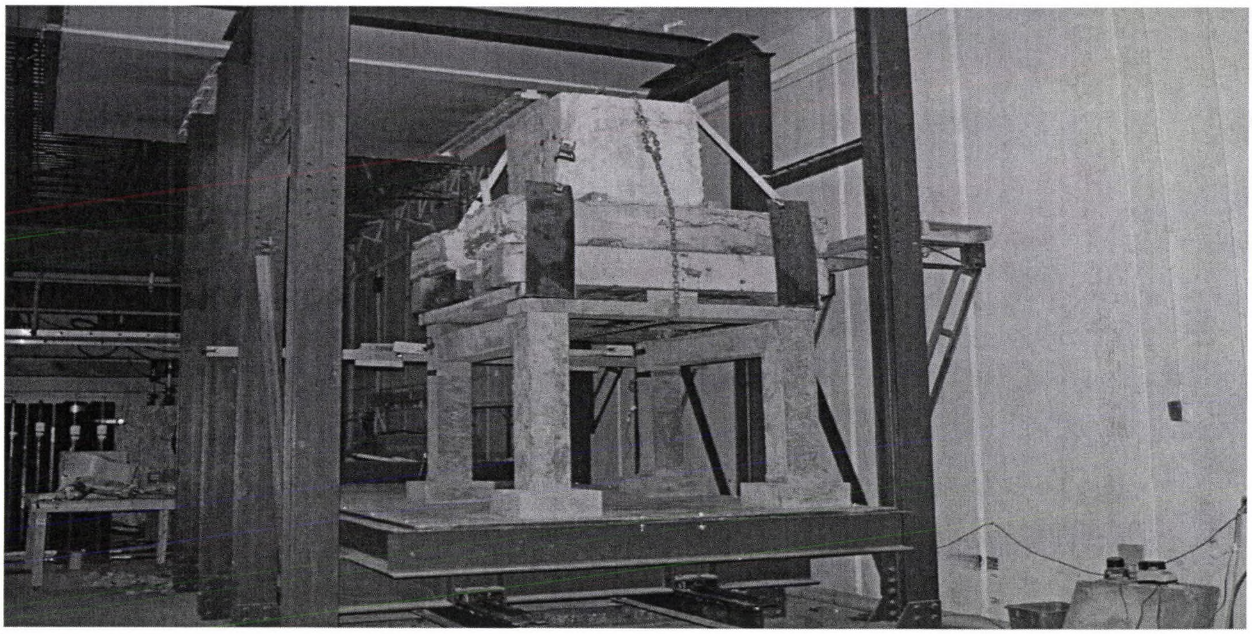

Figure 2.8.a Experimental setup of the Portland cement concrete frames before the test

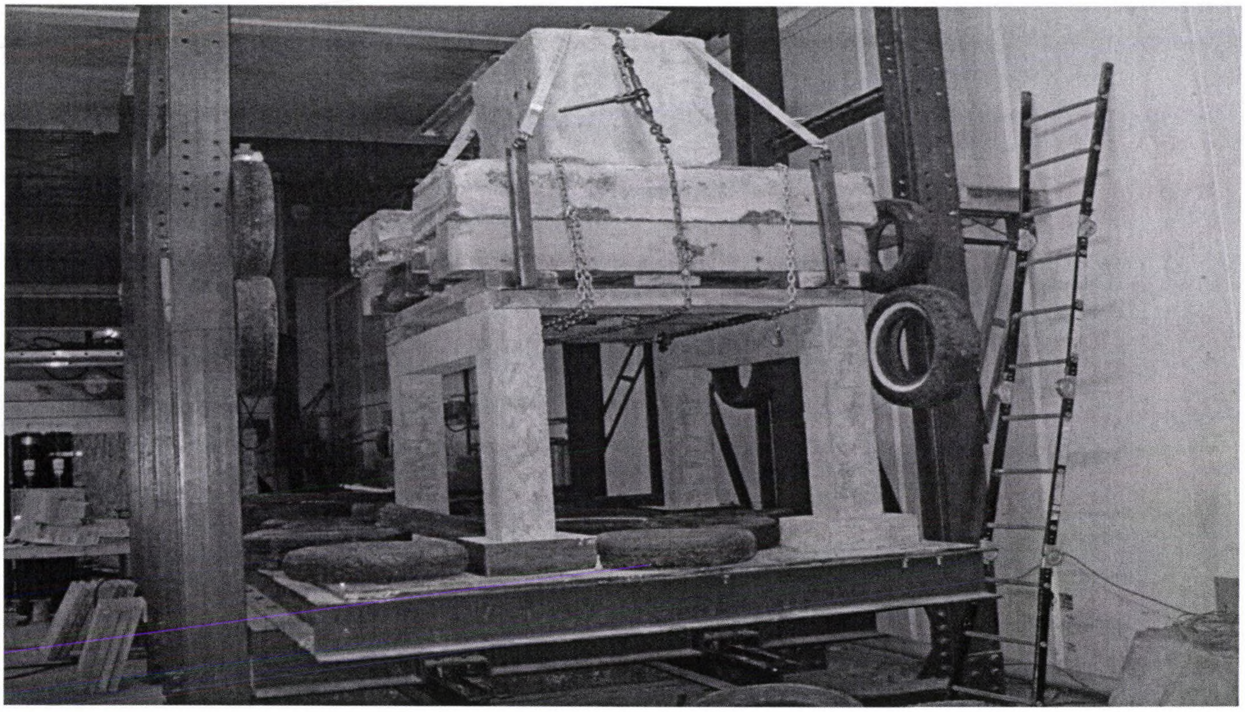

Figure 2.8.b Experimental setup of the 50% SDA concrete frames before the test

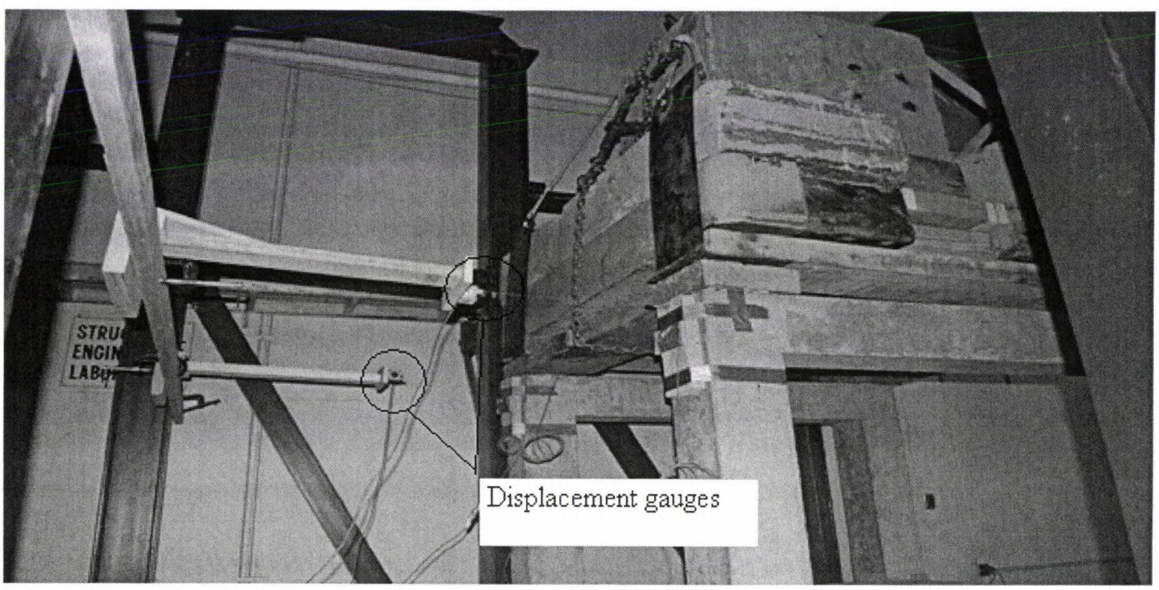

Figure 2.9 showing the instrumentation setup

CHAPTER 3

EXPERIMENTAL RESULTS

3.1 INPUT MOTION

The portal frames were both tested on the uni-axial shake table at Colorado State University using a total of five different earthquakes in succession. The parent office building for the portal frame was designed based on the seismic intensity requirement for Los Angeles, California. The 1994 Northridge, California earthquake and 1992 Landers earthquake were selected as input ground motions for the shake table to excite the structure. Table 3.1 provides the peak ground motion details for the scaling of the records used to excite the structure.

Table 3.1 Ground motion details of Earthquakes used to excite the structure

Earthquake Event & Year	File name	Station	Peak Ground Acceleration(g)
Northridge (1994)	Nor5	LA – Hollywood Storage	0.778
Landers (1992)	Lan1	Desert Hot Springs	0.875

The 1992 Landers earthquake ground motions were selected as the first ground motion to excite the structure. Table 3.2 shows the name, peak ground acceleration and the test sequence of the earthquakes used to run the test.

Table 3.2 Test sequence

Test Sequence	Ground Motions	Peak Ground Acceleration (g)
1	Lan1	0.875
2	Nor5	0.778
3	Nor5	0.778
4	Nor5	0.778
5	Nor5	0.973

Figures 3.1 and 3.3 show the acceleration response for the 1992 Landers earthquake and 1994 Northridge earthquake. Figures 3.2, 3.4a and 3.4b show the time compressed acceleration response of the ground motions used to run the shake table. Referring to Appendix D the time was scaled by a square root of the length factor. Since the scale factor for acceleration is 1, acceleration values remain unchanged for the acceleration response and the time compressed acceleration response as shown in the figures below.

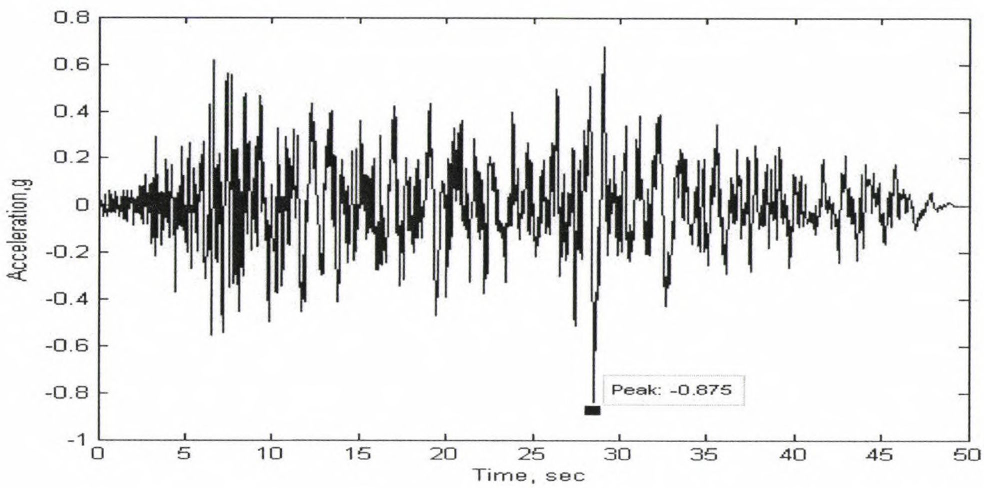

Figure 3.1 Acceleration response of the 1992 Landers earthquake

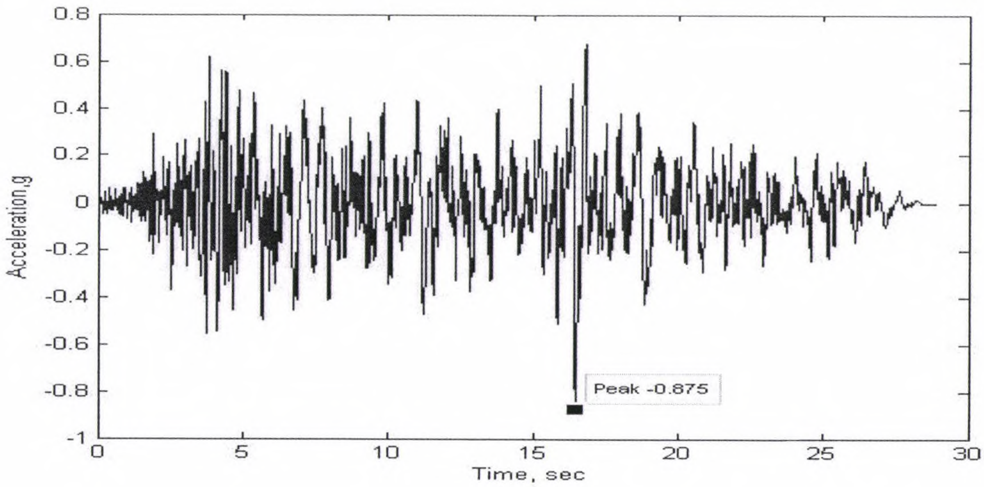

Figure 3.2 Time compressed acceleration response of 1992 Landers earthquake

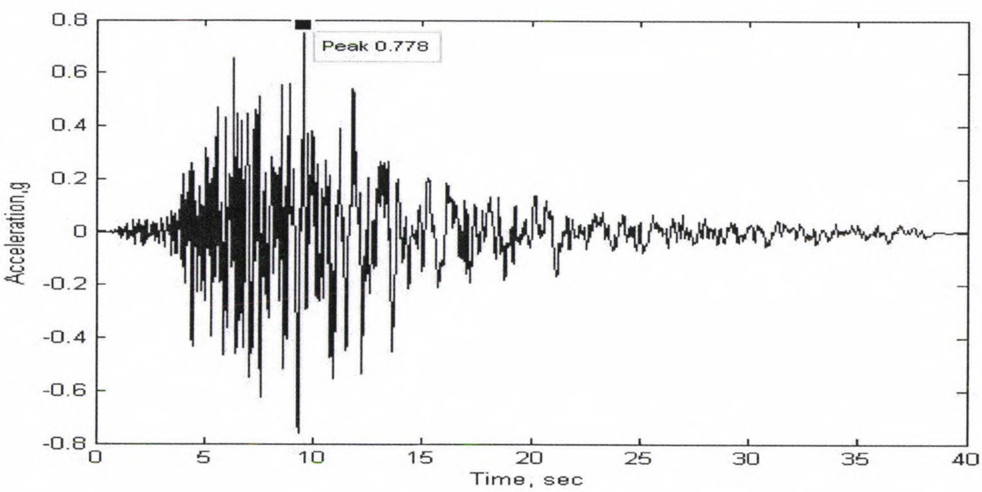

Figure 3.3 Acceleration response of the 1994 Northridge earthquake

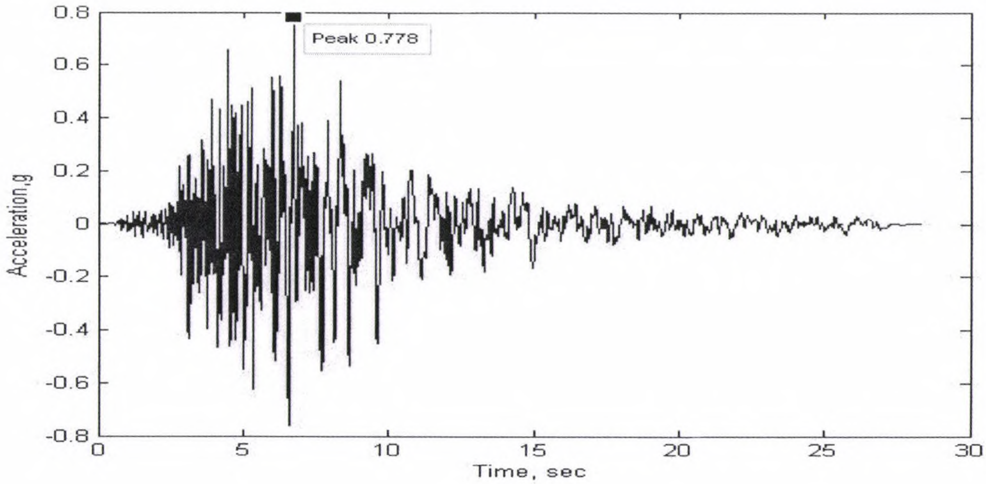

Figure 3.4a Time compressed acceleration response of 1994 Northridge earthquake

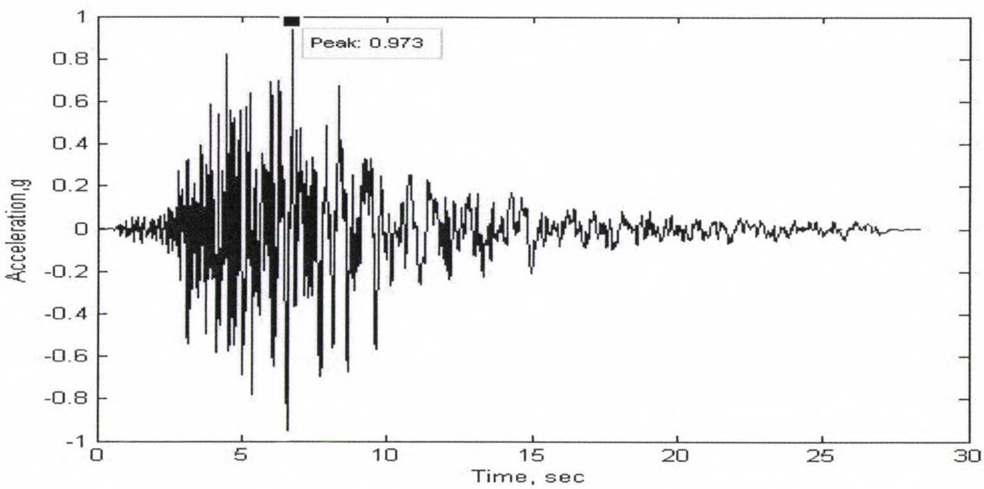

Figure 3.4b Time compressed acceleration response of 1994 Northridge earthquake

3.2 PLOTS OF RESPONSE AND DAMAGE IMAGES

Recall that the objective of this project was to demonstrate that the performance of a high content SDA frame is similar to a conventional reinforced concrete frame under strong earthquake motion. The concrete and SDA frame models were tested on the shake table in the same sequence as shown in Table 3.2. After each test sequence damage inspection was carried out and the damages were marked and recorded by taking photographs. There were no damages observed on the concrete frames for test sequence 1. A complete damage analysis of both concrete and SDA frames are presented in section 3.3 of this Chapter. At the end of the test the displacement data from the sensors were collected. Selected pictures of the damages and displacement response curves are presented in this Chapter and those not presented here appear in Appendix F and Appendix G, respectively.

3.2.1 DAMAGE IMAGES

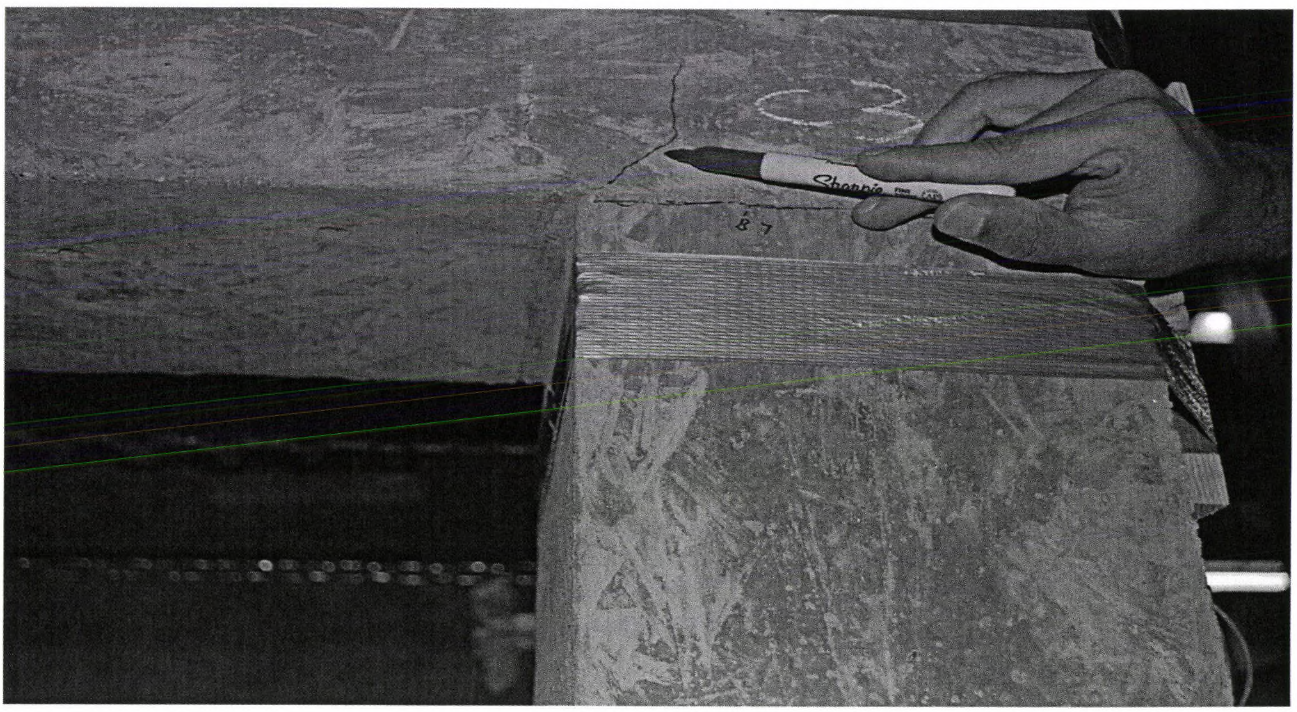

Figure 3.5 Shear crack at the beam-column joint of the concrete frame after test sequence

Figure 3.6 Vertical cracks on the concrete beam and extended shear crack on the column after test sequence 3

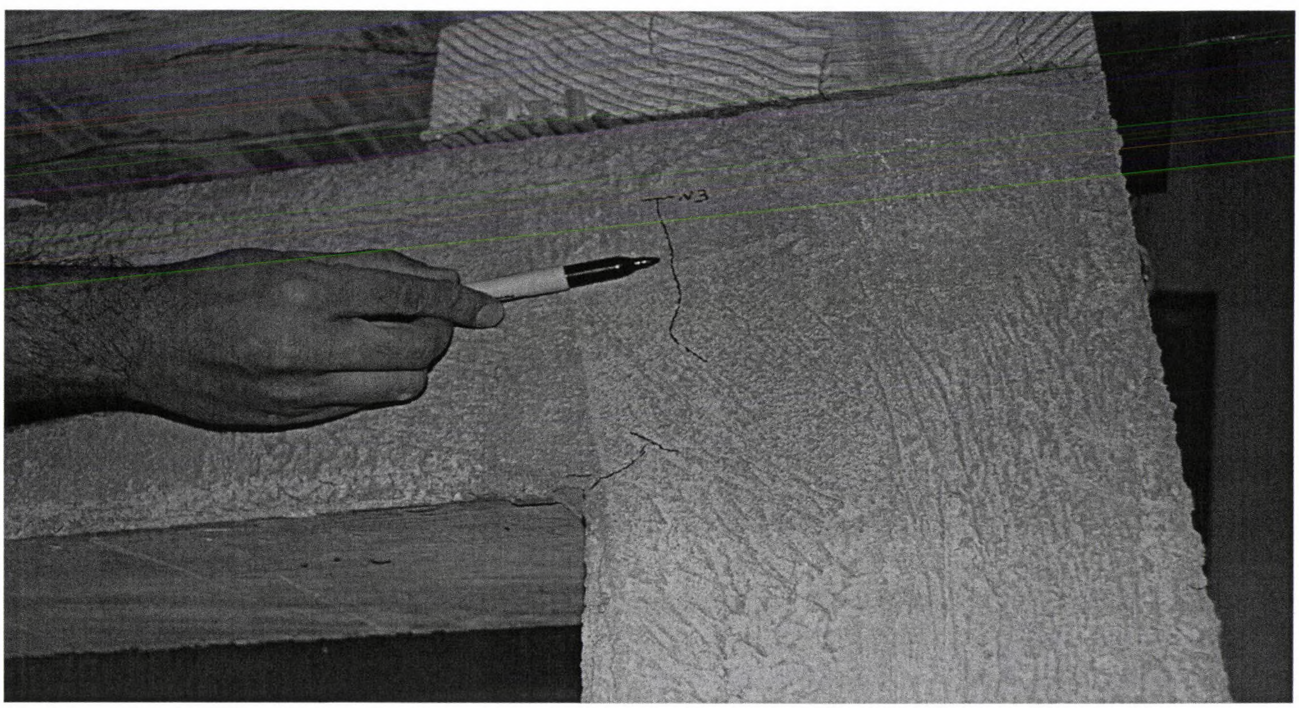

Figure 3.7 Vertical crack on the concrete column after test sequence 4

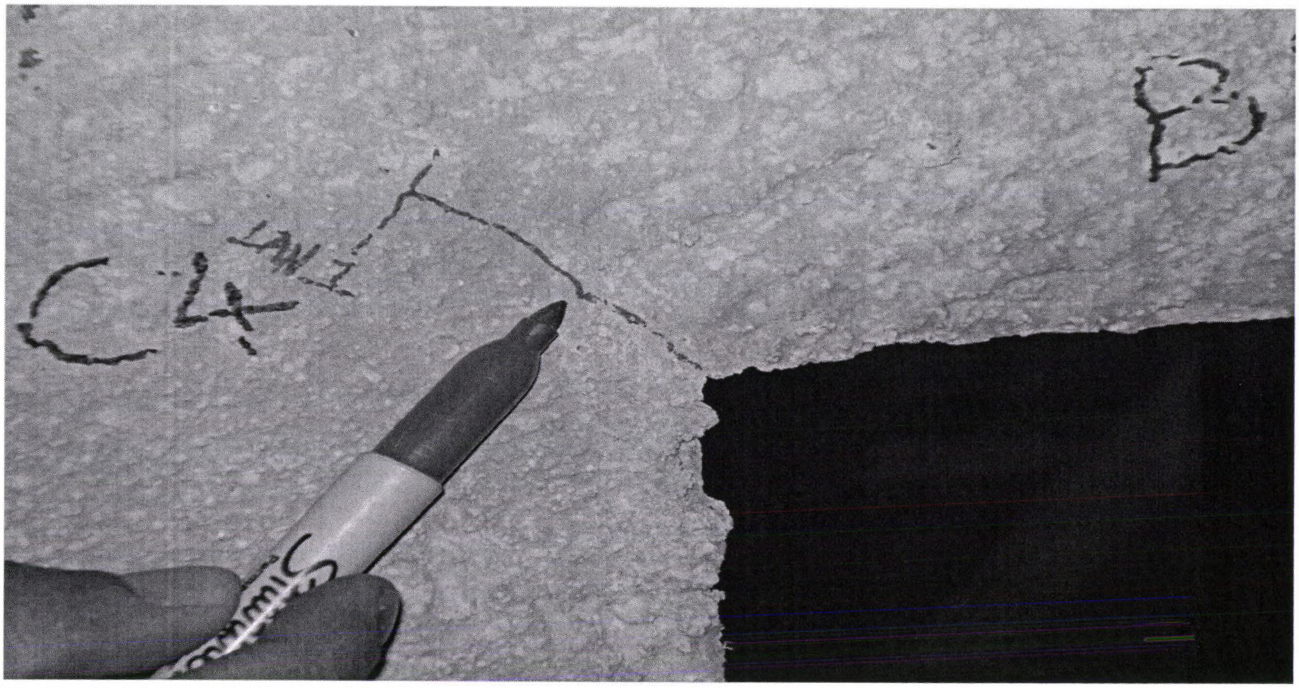

Figure 3.8 Shear crack at the beam column joint of the SDA concrete frame after test sequence 1

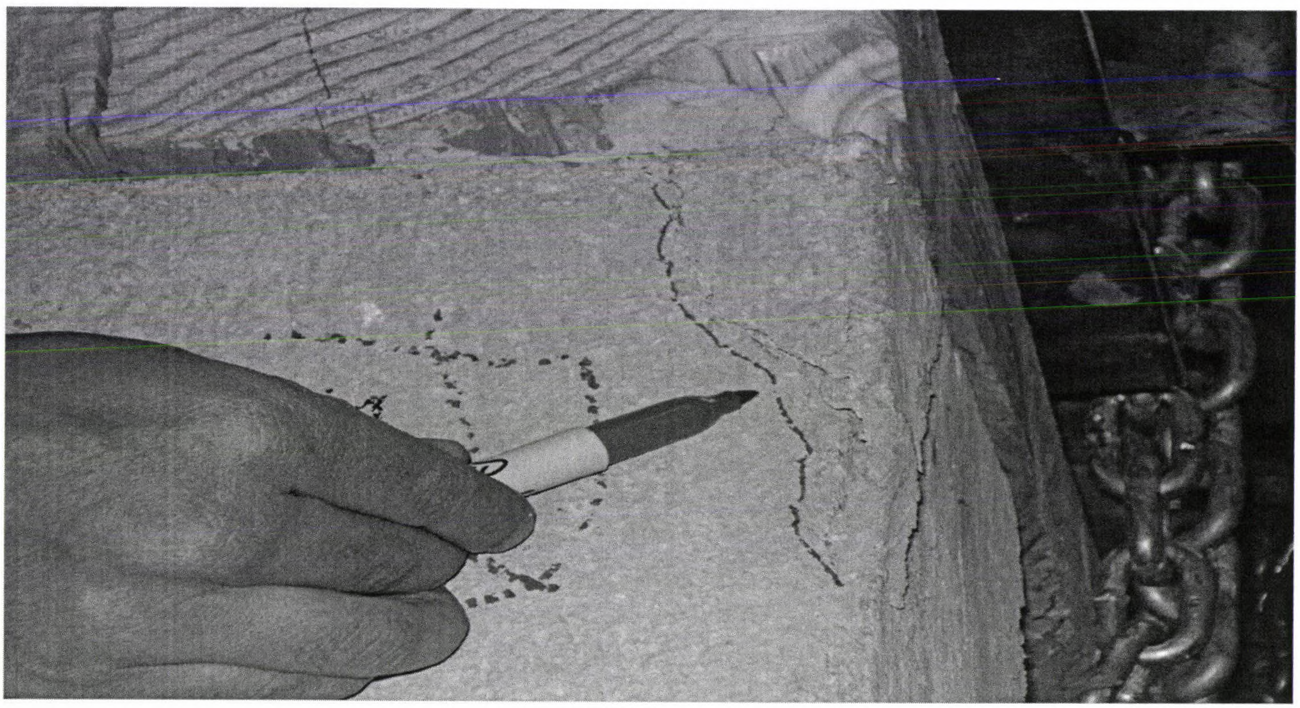

Figure 3.9 Damage at the column edge of the SDA concrete frame after test sequence 1

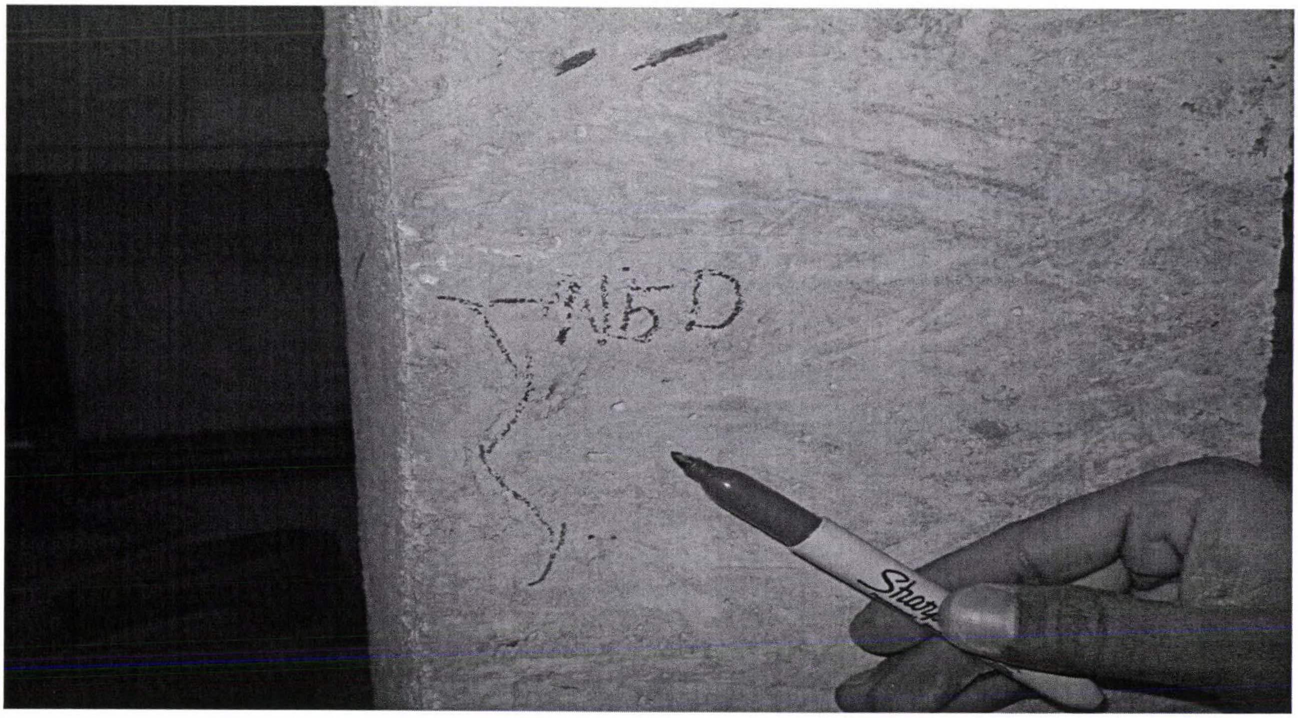

Figure 3.10 Vertical crack at mid height of SDA concrete column after test sequence 5

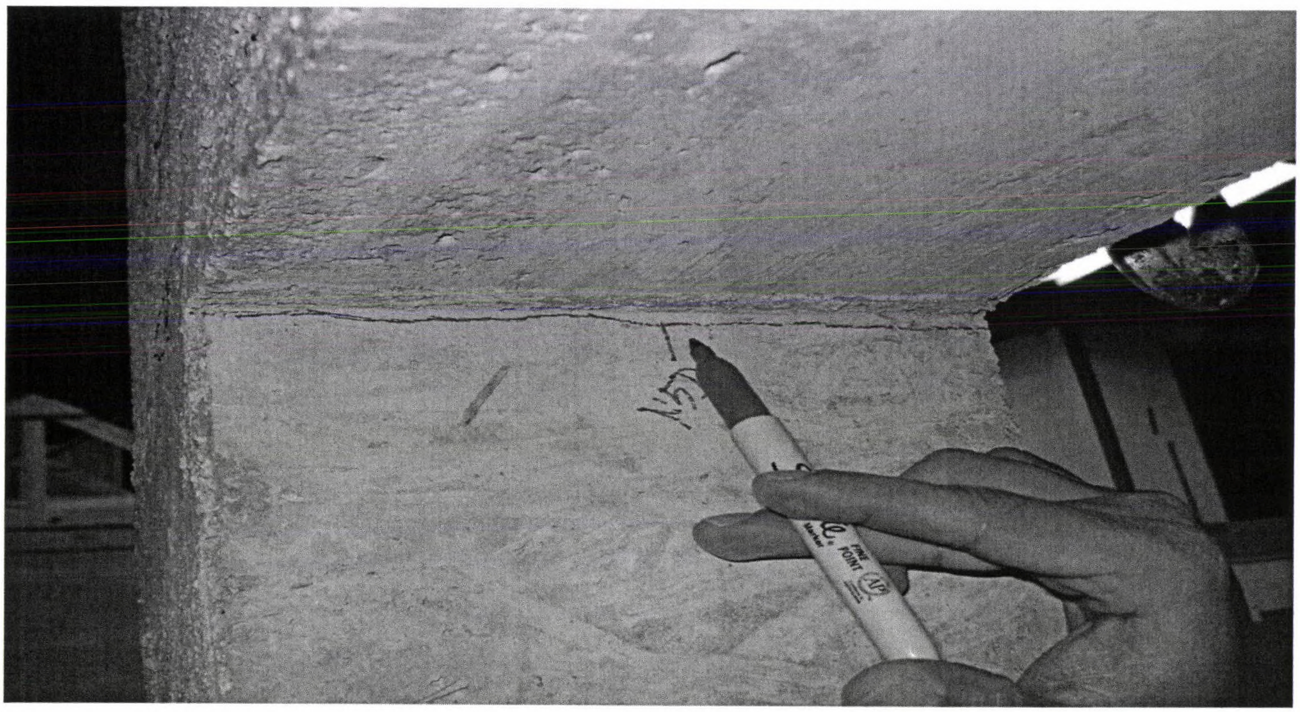

Figure 3.11 Horizontal crack at the beam-column joint of the SDA concrete frame after test sequence 5

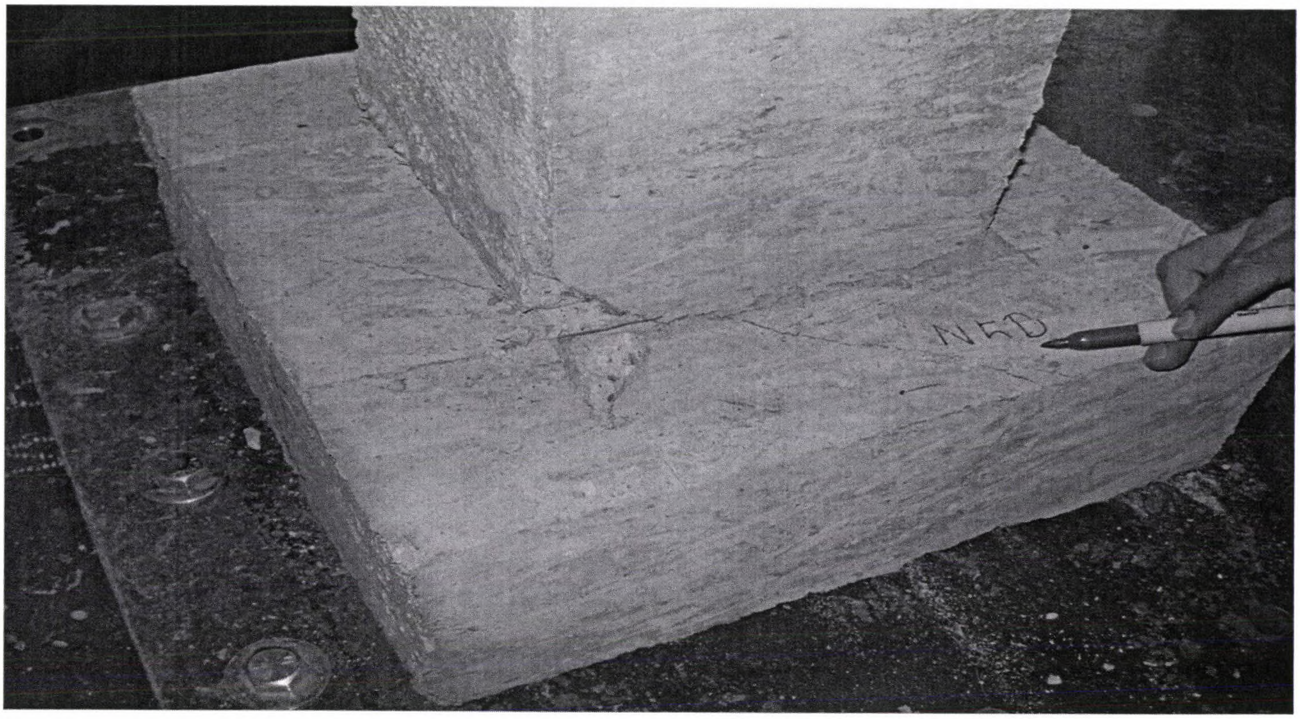

Figure 3.12 Damaged SDA concrete column base after test sequence 5

3.2.2 DISPLACEMENT RESPONSE

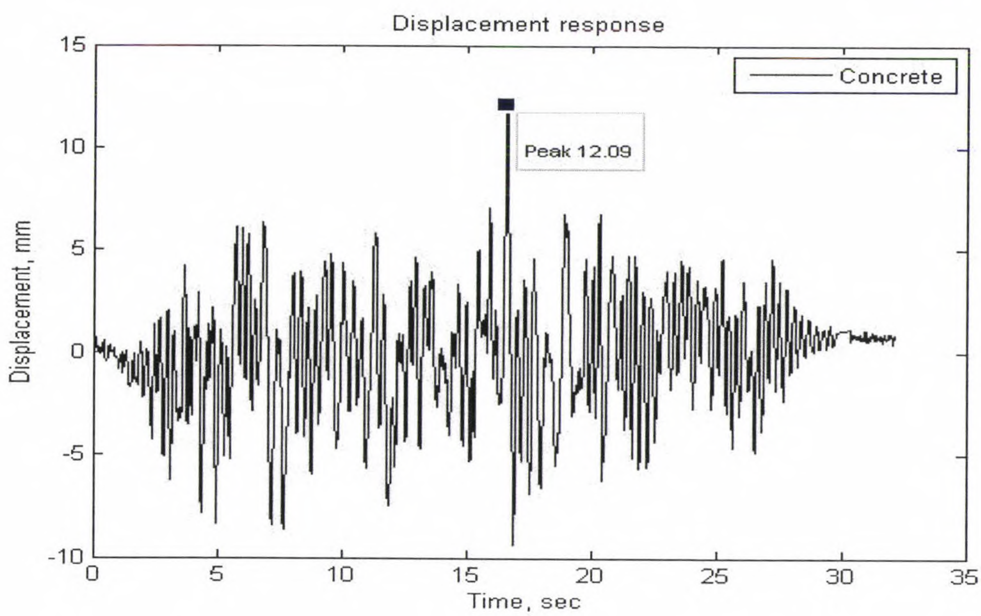

Figure 3.13 Displacement response of concrete frame, Column C2 after test sequence 1

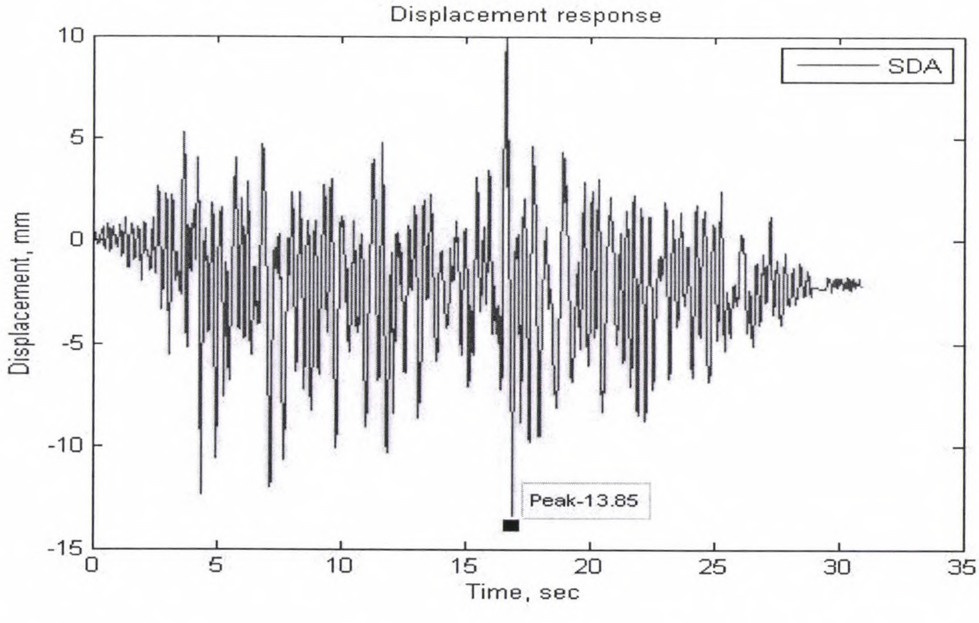

Figure 3.14 Displacement response of SDA concrete frame, Column C2 after test sequence 1

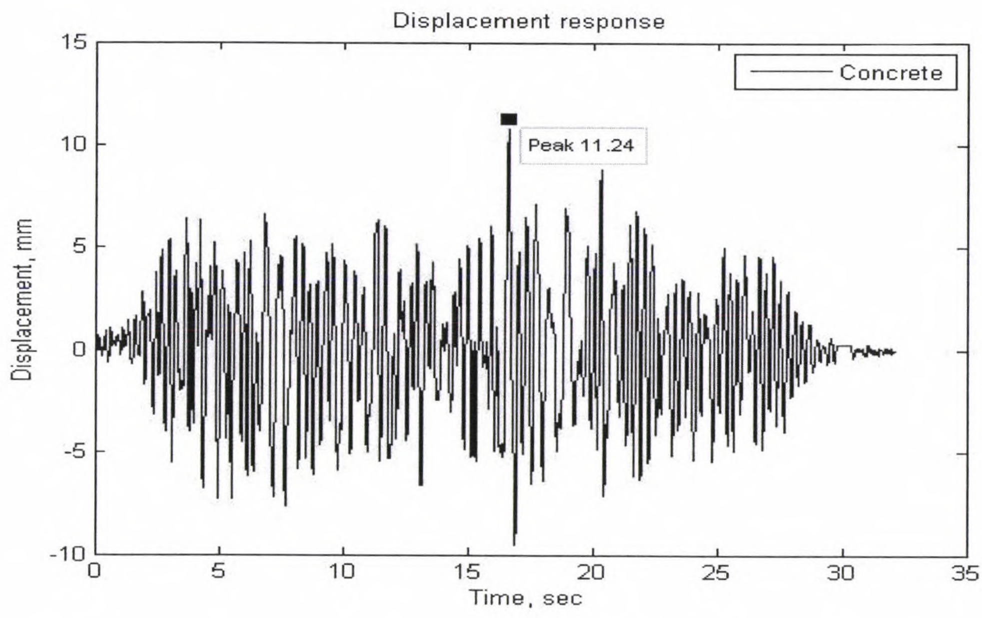

Figure 3.15 Displacement response of concrete frame, Column C3 after test sequence 1

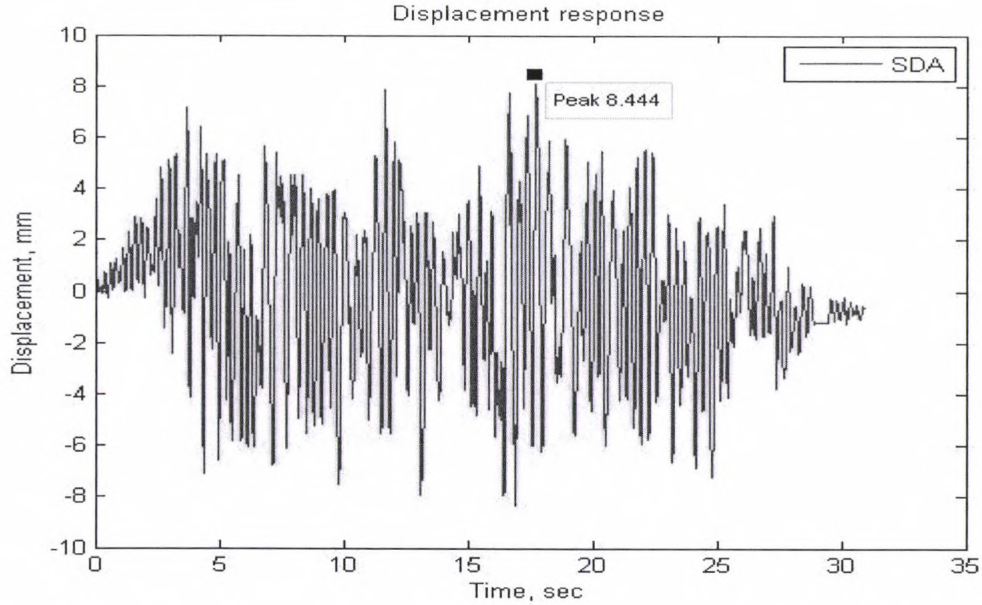

Figure 3.16 Displacement response of SDA concrete frame, Column C3 after test sequence 1

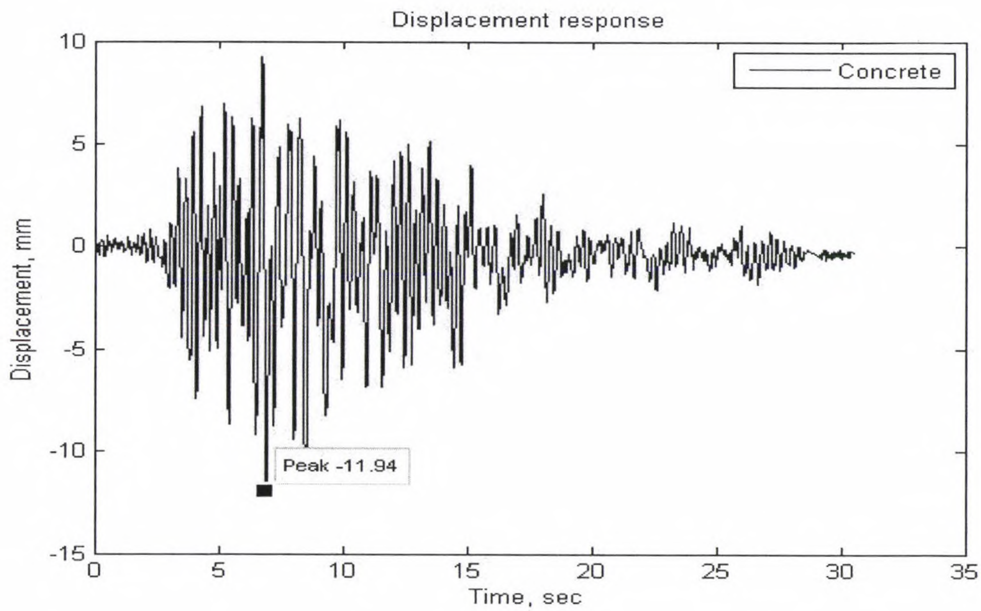

Figure 3.17 Displacement response of concrete frame, Column C2 after test sequence 2

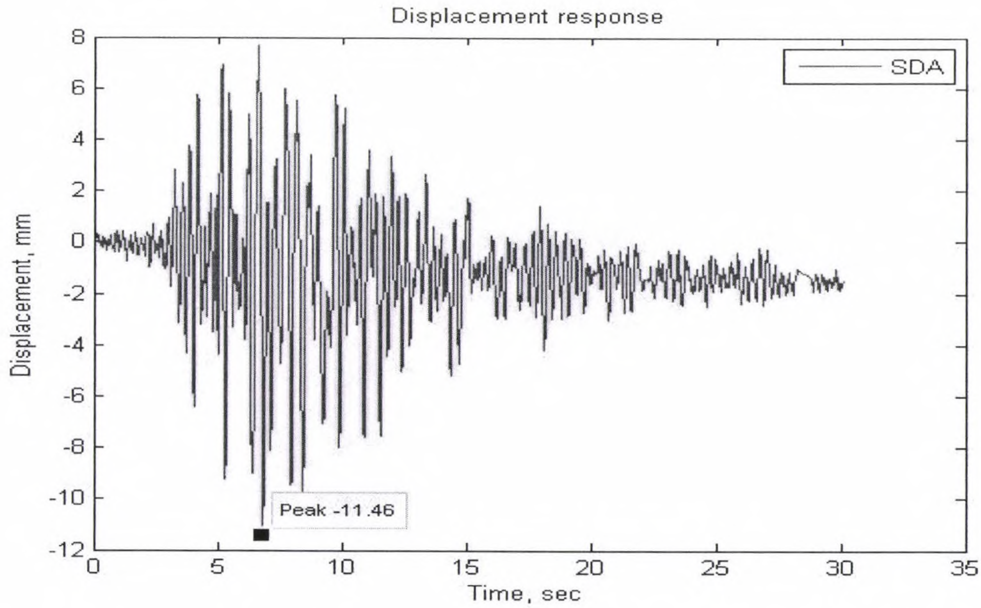

Figure 3.18 Displacement response of SDA concrete frame, Column C2 after test sequence 2

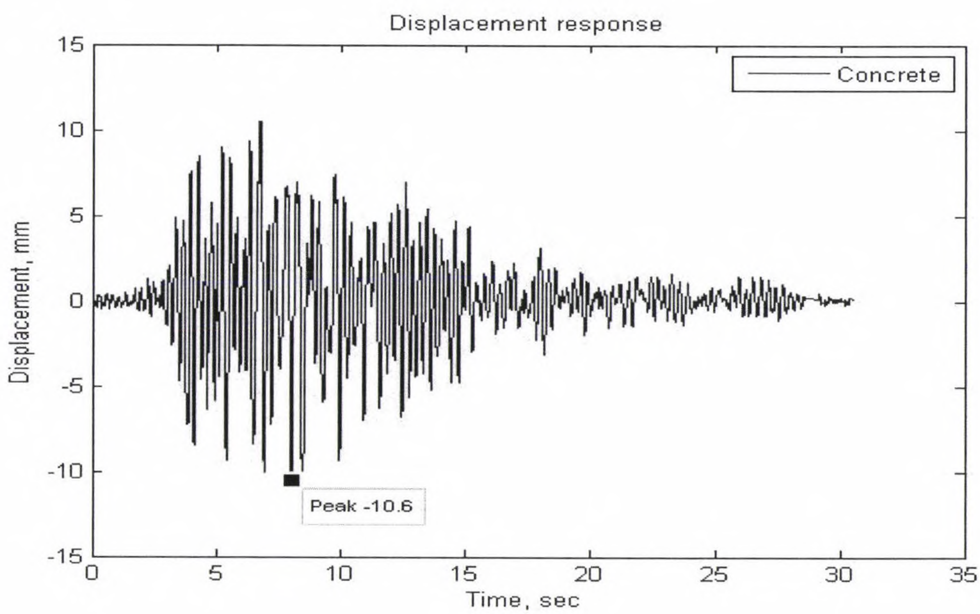

Figure 3.19 Displacement response of concrete frame, Column C3 after test sequence 2

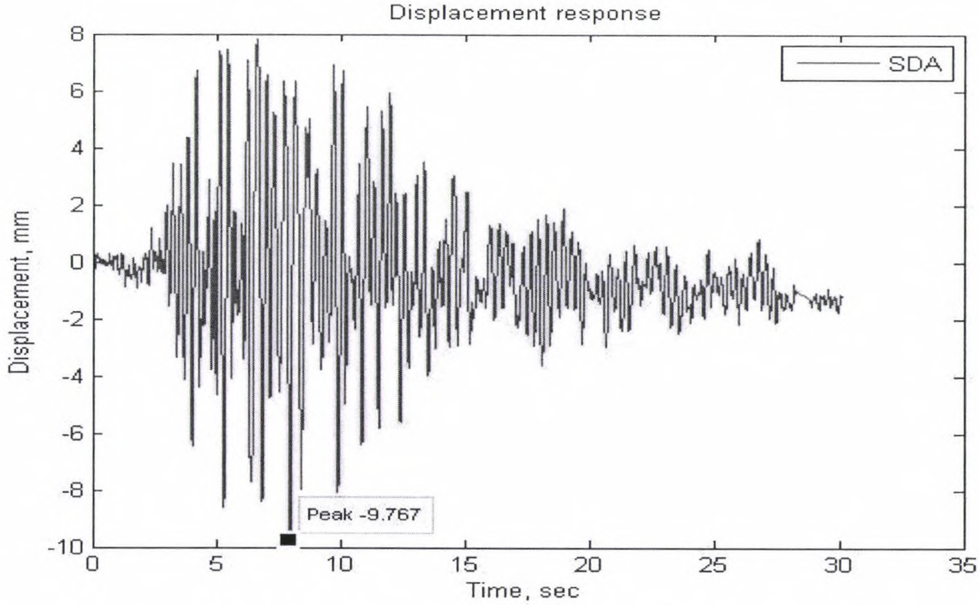

Figure 3.20 Displacement response of SDA concrete frame, Column C3 after test sequence 2

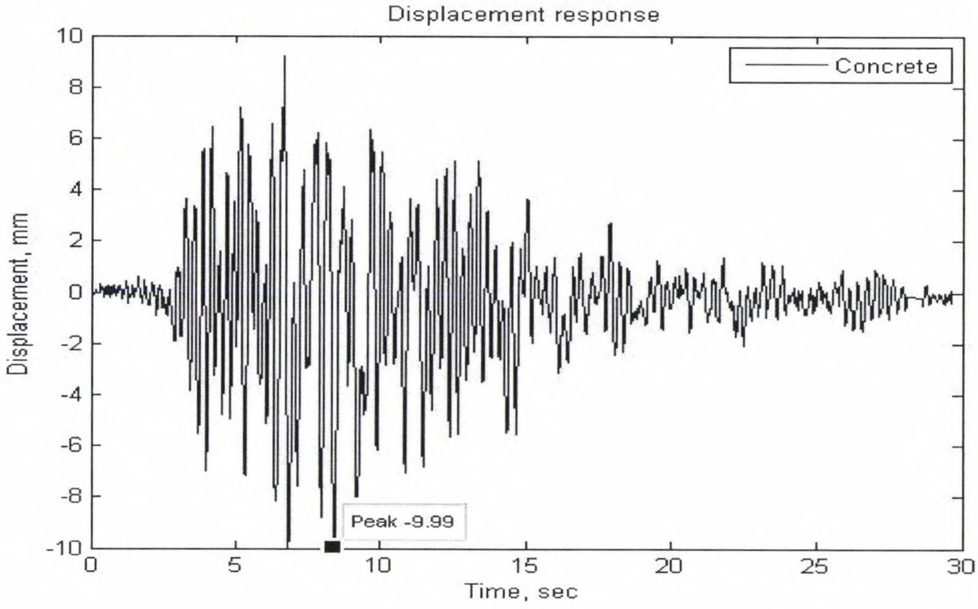

Figure 3.21 Displacement response of concrete frame, Column C2 after test sequence 3

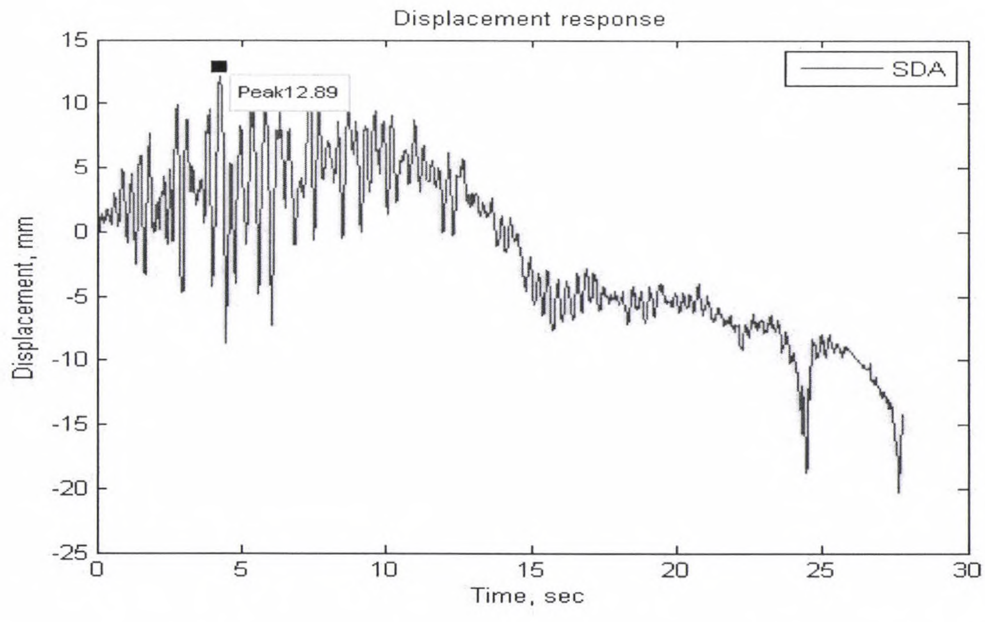

Figure 3.22 Displacement response of SDA concrete frame, Column C2 after test sequence 3

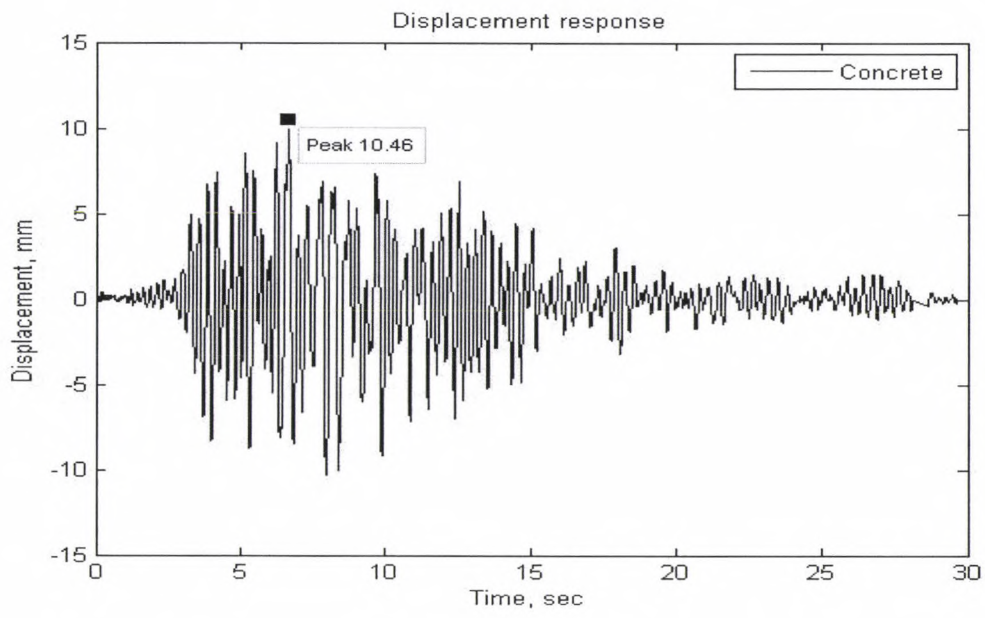

Figure 3.23 Displacement response of concrete frame, Column C3 after test sequence 3

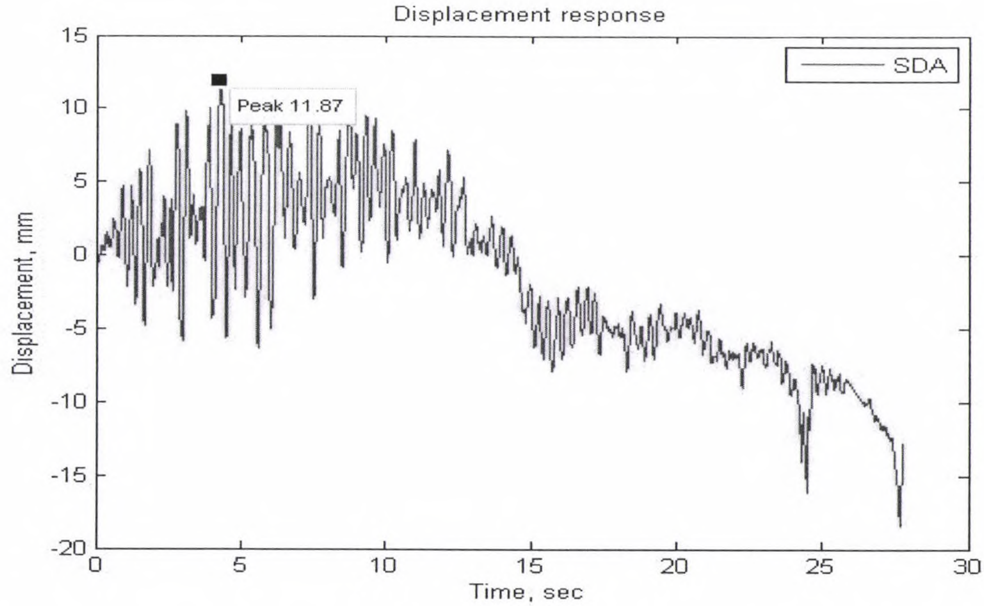

Figure 3.24 Displacement response of SDA concrete frame, Column C3 after test sequence 3

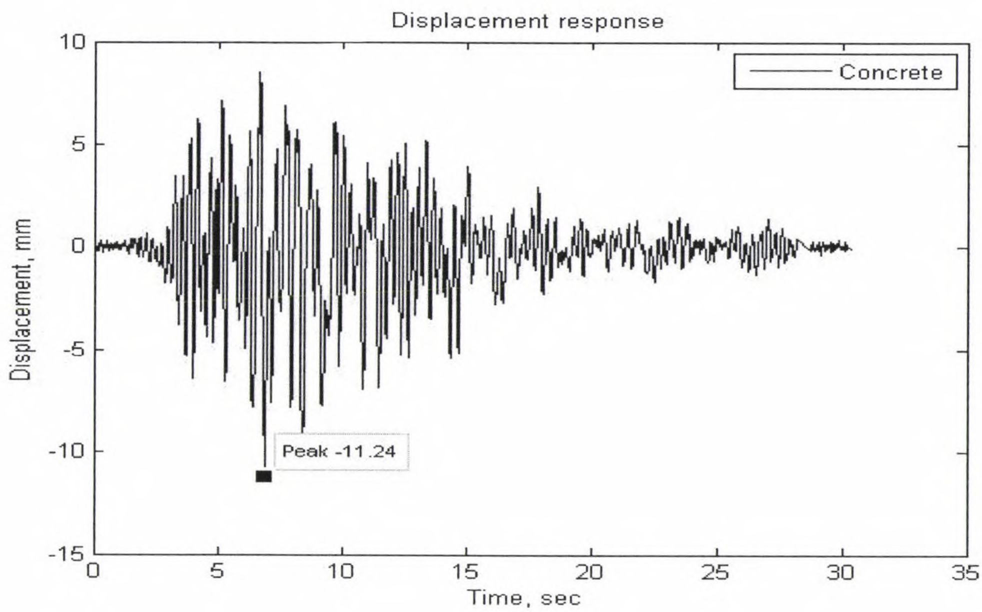

Figure 3.25 Displacement response of concrete frame, Column C2 after test sequence 4

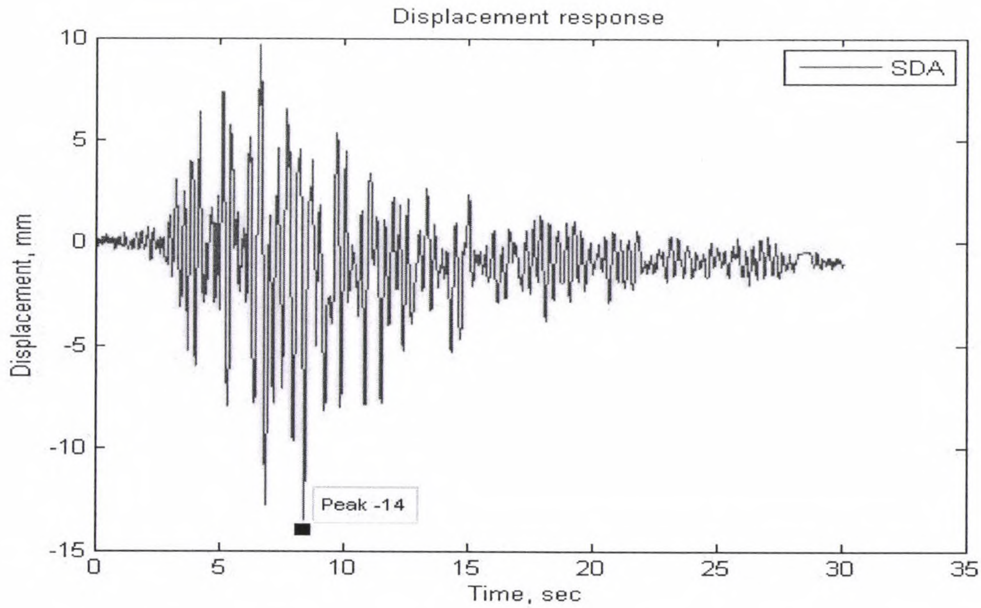

Figure 3.26 Displacement response of SDA concrete frame, Column C2 after test sequence 4

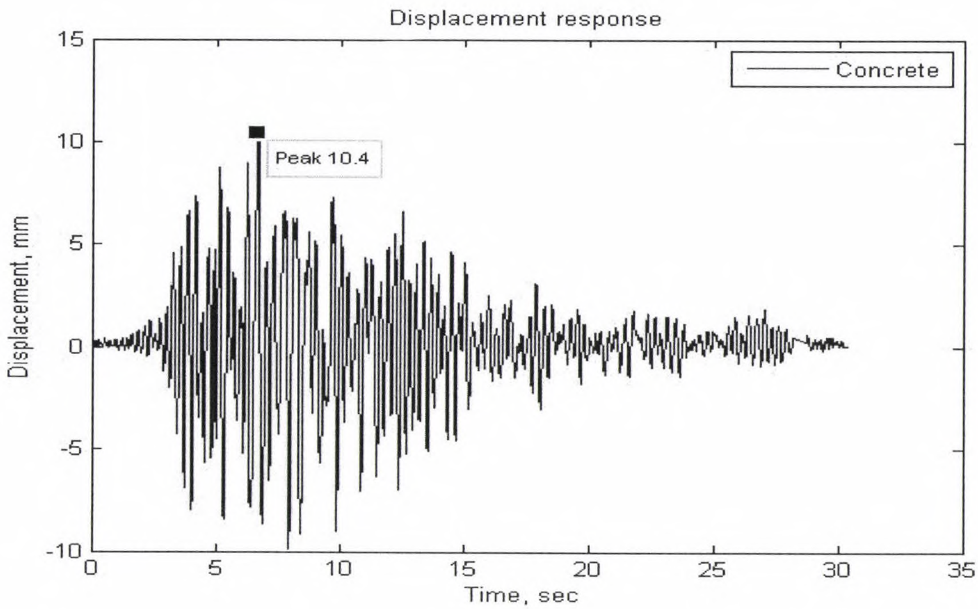

Figure 3.27 Displacement response of concrete frame, Column C3 after test sequence 4

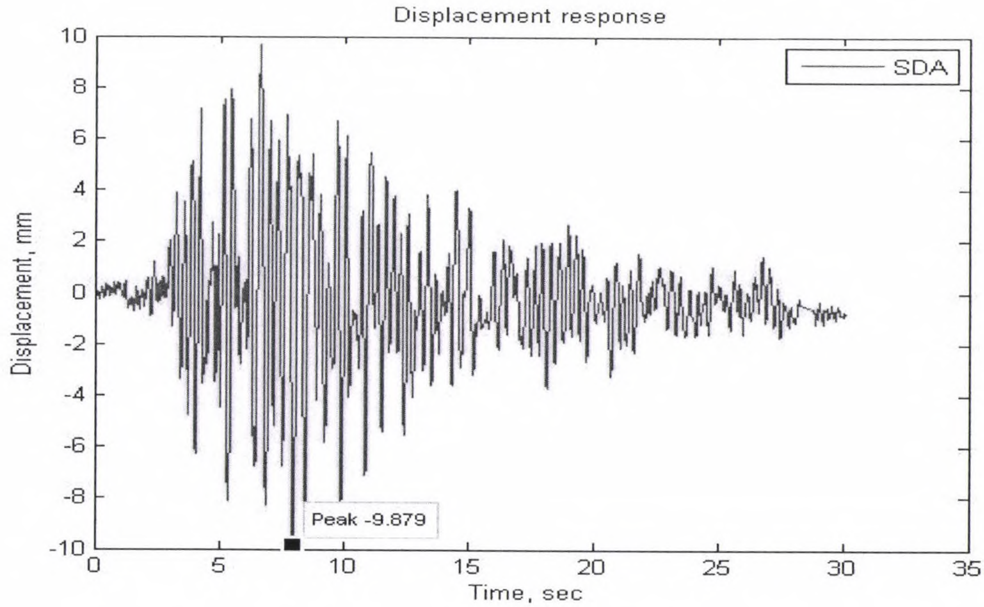

Figure 3.28 Displacement response of SDA concrete frame, Column C3 after test sequence 4

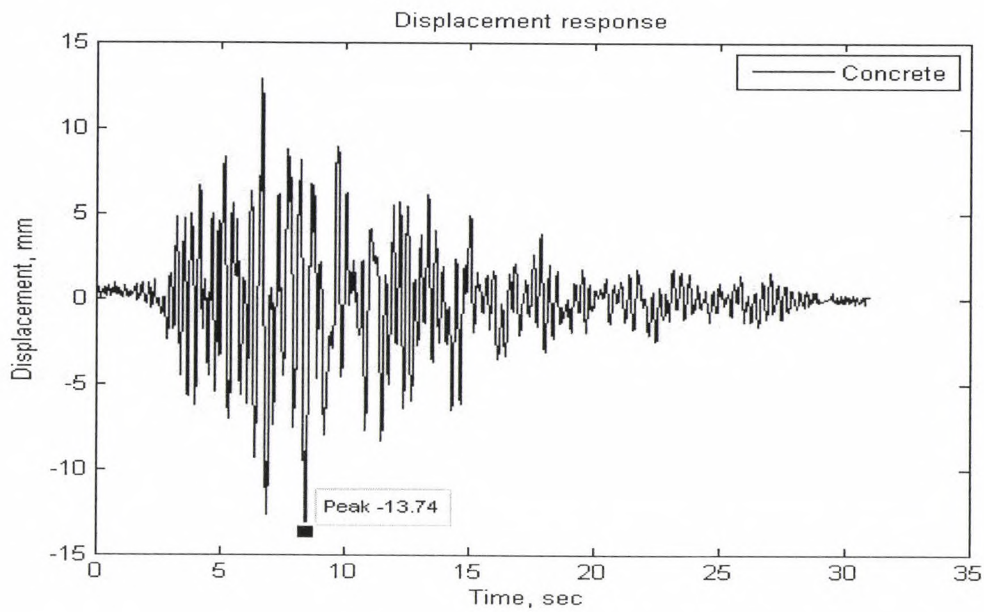

Figure 3.29 Displacement response of concrete frame, Column C2 after test sequence 5

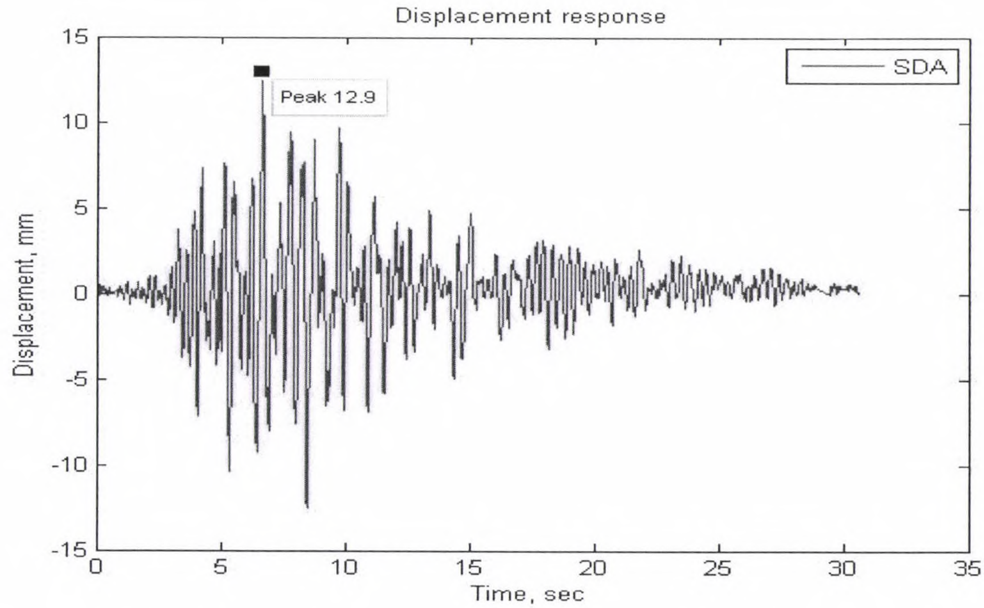

Figure 3.30 Displacement response of SDA concrete frame, Column C2 after test sequence 5

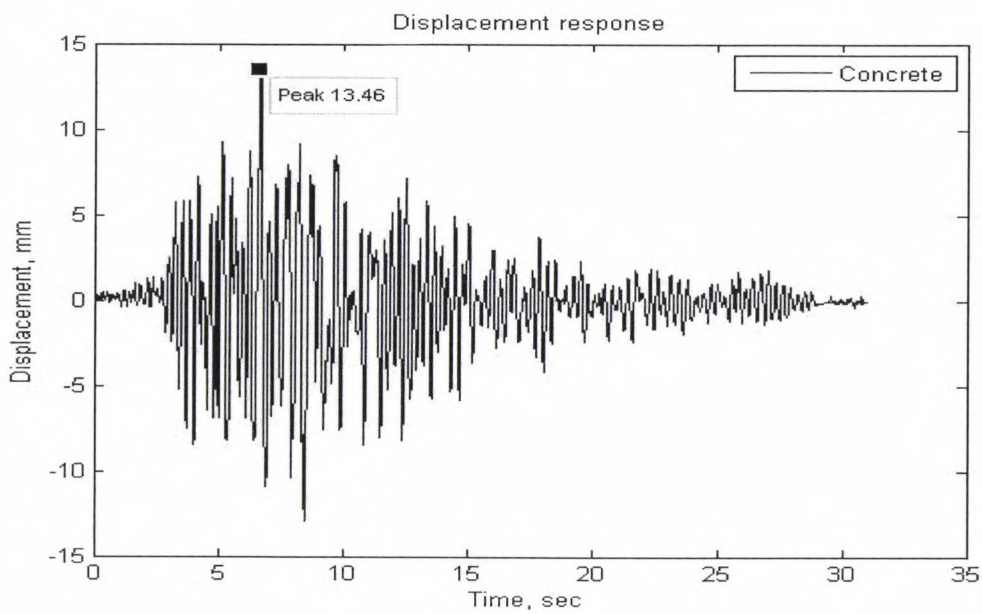

Figure 3.31 Displacement response of concrete frame, Column C3 after test sequence 5

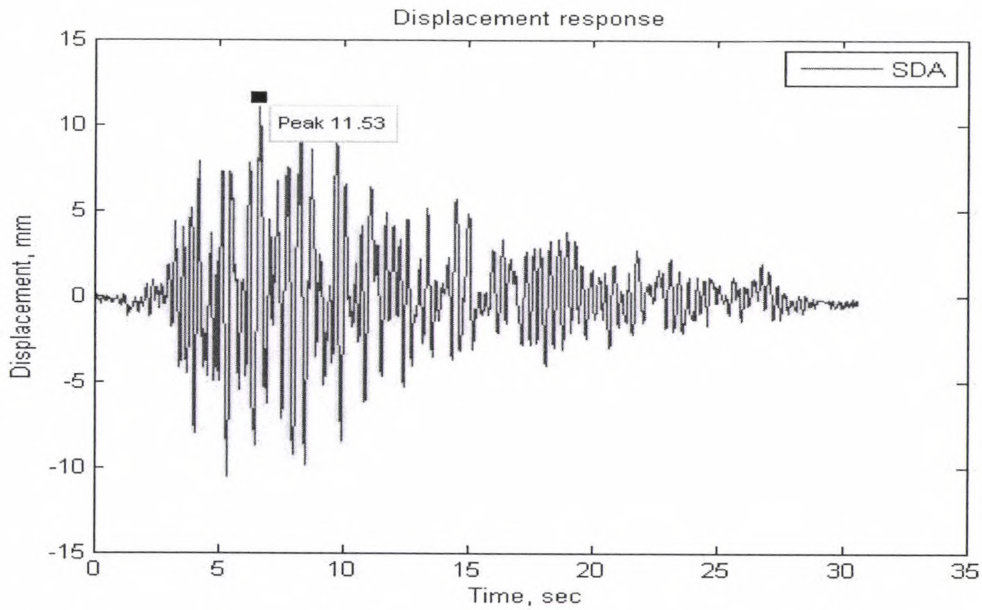

Figure 3.32 Displacement response of SDA concrete frame, Column C3 after test sequence 5

3.3 DAMAGE ASSESSMENT

A detailed damage inspection is carried out by referring to the Figures in section 3.2 and Figures from Appendix F. Tables 3.3 and 3.4 shows the damage assessment after each test sequence for the Portland cement concrete and SDA concrete frames, respectively.

Table 3.3 Damage assessment of Portland cement concrete frame

Test Sequence	Portland cement concrete frame					
	Columns				Beams	
	C1	C2	C3	C4	B1	B2
1	-	-	-	-	-	-
2	-	Shear crack at the outer face of the beam-column joint as shown in Figure F.1 of Appendix F	Shear crack at both inner and outer faces of the beam-Column joints as shown in Figure F.2 and Figure F.3 of Appendix F	Shear crack at the inner face of the beam-column joint as shown in Figure 4 of Appendix F	-	-
3	Shear Crack at the outer face of the beam-column joint as shown in Figure F.5 of Appendix F	Vertical crack extension towards the end of outer face of the column as shown in Figure F.6 of Appendix F	Vertical crack extending till the end of the outer face of the column as shown in Figure F.7 of Appendix F	-	-	Vertical crack at the end of the beam near column C3 as shown in Figure F.7 of Appendix F
4	Vertical crack on the outer face of the column as shown in Figure F.8 of Appendix F	-	-	Shear crack at the outer face of the beam-column joint as shown in Figure F.9 of Appendix F	-	-
5	-	-	-	-	-	-

Table 3.4 Damage assessment of SDA concrete frame

Test Sequence	SDA concrete frame					
	Columns				Beams	
	C1	C2	C3	C4	B1	B2
1	A thick crack at the outer face of the column edge as shown in Figure F.10 of Appendix F	-	-	Shear crack at the inner face of the beam-column joint as shown in Figure F.11 of Appendix F	-	-
2	-	-	2 Vertical cracks on the outer face of the column as shown in Figure 12 of Appendix F	Vertical crack on the outer face of the column as shown in Figure 13 of Appendix F	-	-
3	Diagonal Crack at the outer face of the column as shown in Figure 14 of Appendix F	-	Vertical crack on the outer face of column as shown in Figure F.15 of Appendix F	-	-	-
4	-	-	Shear crack at the inner face of the beam-column joint as shown in Figure F.16 of Appendix F	Shear crack at the inner face of the beam-column joint as shown in Figure F.17 of Appendix F	-	Vertical crack on the inner face of the beam near column C4 as shown in Figure F.17 of Appendix F
5	-	-	a) Horizontal crack exactly below the beam-column joint of	a) Extended vertical crack on the outer face of the column as	-	-

			column C3 and beam B2 as shown in Figure F.18 of Appendix F b) Vertical crack at mid height on outer face of the column as shown in the Figure F.19 of Appendix F	shown in Figure F.20 of Appendix F b) Base of the column damaged as shown in the Figure F.21 of Appendix F c) Vertical crack at the mid height of the column as shown in the Figure F.22 of Appendix F d) Horizontal crack exactly below the beam column joint of the column and beam B2 as shown in Figure F.23 of Appendix F		

3.4 DISCUSSION

In this chapter displacement graphs of the concrete and SDA concrete frames are compared with reference to the damage inspection after each test sequence. Table 3.5 shows the peak displacement values of concrete and SDA concrete frames based on the displacement response curves shown in section 3.2.

Table 3.5 Peak displacement response values of concrete and SDA concrete frames

Test Sequence	Peak displacement response values			
	Concrete frames		SDA Concrete Frames	
	Column C2, mm	Column C3, mm	Column C2, mm	Column C3, mm
1	12.09	11.24	13.85	8.44
2	11.94	10.6	11.46	9.77
3	9.99	10.46	12.89	11.87
4	11.24	10.4	14	9.88
5	13.74	13.46	12.9	11.53

Referring to the damage assessment Table 3.5 the peak displacement values of column C3 and Column C2 after test sequence 1 for the concrete frame were 11.24 mm and 12.09 mm respectively. Peak displacement values of Column C3 and Column C2 in SDA concrete frame were 8.44 mm and 13.85 mm The reason for the comparatively high values of displacement for the SDA frame when compared to that of the concrete frame may be due to the shear crack in column C4 Figure F.11, no damage was observed on the concrete frame at the end of the test sequence 1. After test sequence 2, not much difference was found in peak displacements of column C2 in both concrete and SDA concrete frames. . Development of a shear crack in column C2, as seen in Figure F.1, of the concrete frame may be the reason for the concrete frame to have higher displacement value when compared to the displacement of SDA frame at column C2. The SDA concrete frame had no damage in column C2. From Figure F.2, Figure F.3 and Figure F.4 it can be seen that shear cracks were developed on columns C3 and C4 of the concrete frame, could be the reason for a greater displacement when compared to the displacement in Column C3 of SDA concrete frame, though SDA frame had cracks on Column C3 and C4 as shown in Figure F.12 and Figure F.13 of Appendix F.

After test sequence 3, damages in the concrete frame as seen in figures F.5 and F.6 of Appendix 6 was more than that of the SDA frame. The damage observed in the SDA frame as shown in Figure F.14 (Appendix F) was only to the reinforcement cover for column C1. Column C2 of SDA frame showed greater displacement when compared to column C2 of concrete frame. Effect of damages from previous test sequences may be the reason for greater displacement in the SDA concrete frame when compared to that of ordinary Portland cement concrete frame. Same reason could be given to column C3 as the displacement of SDA frame is slightly more when compared to that of concrete frame, though cracks were developed both on beam B2 and column C3 of the concrete frame as seen in Figure F.7 (Appendix F) and only a single crack on column C3 as seen Figure F.15 (Appendix F) of SDA frame.

Figures F.8 and F.9 show that cracks developed on column C1 and beam-column joint of column C4 of the concrete frame after test sequence 4. It can be seen from the Figure F.16 and F.17 (Appendix F) that cracks developed on columns C3, C4 and beam B2 for the SDA concrete frame. Total damage to the SDA frame was slightly more when compared to the total damage to the concrete frame.

There was no additional damage found in any part of the concrete frame following test 5. Referring to figures F.18 and F.19 (Appendix F) for the SDA frame it can be seen that a new crack had developed at the beam column joint of beam B2 and column C3 also a vertical crack was found on column C3. Figure F.20, Figure F.22 and Figure F.23 (Appendix F) show the cracks on column C4. Base of the column C4 was damaged as shown in the Figure F.21 (Appendix f) which may be the cause for low displacement (Table 3.41) value of the SDA frame when compared to that of the concrete frame.

From the above discussions it can be seen that until test sequence 2 both the SDA concrete frame and Portland cement concrete frame behaved in a similar manner with respect to their damage levels for the same ground motions. From test sequence 3 to sequence 4 it can be seen that Portland cement concrete frame performed better than the SDA concrete frame, though similar damage was observed in both the frames. After test sequence 5 the SDA frame had suffered more damage overall when compared to that of the concrete frame.

CHAPTER 4

SUMMARY, CONCLUSIONS AND RECOMMENDATIONS

4.1 SUMMARY

The objective of this thesis was to test and compare the performance of 1/3 scaled high SDA content concrete portal frames to conventional Portland cement concrete portal frames for the same series of earthquake ground motions. In order to accomplish this, a three bay, three storey office building was designed based on the seismic intensity requirements for Los Angeles, California. The portal frame to be constructed for testing was selected from the mid bay of the first storey plan. The prototype frame was scaled down to 1/3 scale by applying the Buckingham pi theorem in order to maintain dynamic similitude between the model and the prototype. After scaling the model, the reinforcement bars were tied together according to the seismic detailing specified in the ACI code. The tests were carried out in the ERC structural lab at CSU. Each set of frames was subjected to the same sequence of five different earthquakes. Portland cement concrete frames were tested first followed by SDA concrete frames. Damage inspection was performed and photographs of damage taken after each shake. Time histories of the deformation were plotted for each earthquake. The photographs of the damages and displacement time history for the SDA concrete frames were compared to that of Portland cement concrete frames and the conclusions were made based on these comparisons.

4.2 OBSERVATIONS LEADING TO CONCLUSIONS

Referring to the damage assessment and discussion in section 3.2 of Chapter 3 where the damage assessment is done based on the photographs taken after each earthquake and discussion is based on comparing damages and displacement response. It was observed that both the SDA concrete and Portland cement concrete frames behaved in a similar manner with respect to their damage levels until test sequence 2. After test sequences 3 and 4 the SDA frame was observed to not perform as well when compared to the concrete frame. But the key observation may be after test sequence 5 where no damage was observed on the concrete frame but the SDA frame suffered significant damage to the column base, cracking at the beam column joint, and damage at other parts of the structure as mentioned in Table 3.2 of Chapter 3. Through these observations the SDA frame may be considered to perform well, but not as good as the Portland cement concrete frame.

4.3 CONCLUSIONS

By comparing the damage levels and displacement response plots of the SDA frame to that of the Portland cement concrete frame after each earthquake, not much difference was found in the response of the frames since both SDA concrete frames and Portland cement concrete frames behaved in a similar manner for the first two test sequences (refer Table 3.31 and Table 3.32). It was only after the third test sequence that the SDA frame did not perform as well when compared to that of the Portland cement concrete frame. One possible reason for this was that the SDA concrete frame 28 day compressive strength was 46.91 N/mm^2 while that of Portland cement concrete was 56.33 N/mm^2, hence the SDA concrete was 18% weaker when compared to the compressive strength of

Portland cement concrete. The frames were designed as per strong column-weak beam concept, according to which the plastic hinges induced due to the seismic forces are formed at the end of the beams (Macgregor, 2005). Development of shear cracks at the beam column joints in both Portland cement concrete frames and SDA concrete frames after each test sequence indicates that the frames behaved as per the designed strong column-weak beam concept. Regardless, there was no significant damage or structural failure such as a collapse exhibited by the SDA frame. From a strictly structural standpoint, it can be stated that up to fifty percent of cement could be replaced by SDA in a concrete mix in place of ordinary Portland cement concrete for the construction of structural members in high seismic zones. Obviously work in the area of durability and corrosion of reinforcement is needed prior to actual implementation of such a high SDA content. However, if this can be studied and contents as high as 50% utilized the cost of construction can be reduced and SDA can be recycled and diverted from landfills, thus moving towards greener construction.

4.4 RECOMMENDATIONS FOR FURTHER STUDY

During this research significant time was allotted for construction and testing of the frames, and therefore further research could be performed to investigate the use of high percentage SDA in concrete in the following areas:

1.) Numerical models could be calibrated for the models in this study and numerical investigation performed on the prototype

2.) Further research could be performed on the mix design to obtain a mix of SDA concrete and Portland cement concrete having equal strength.

3.) Since the SDA was the locally available type of ash, similar research could be performed with using Class C or Class F Fly Ash. All the three stories could be constructed and tested on the shake table for more accurate results, i.e. a full building model.

BIBILOGRAPHY

1. Early strength fly ash concrete for structural applications. 1983. N. Swamy, Sami A. R. Ali, D. D. Theodorakopoulos,
2. Laboratory investigations on concrete and geocrete with high fly ash contents. 1985. Ramesh C. Joshi, James M. Oswell,Gurinder S. Natt,
3. Seismic resistance of reinforced concrete frame structures designed only for gravity loads: Part I – Design and properties of one-third scale model structure. J.M. Bracci, A.M. Reinhorn and J.B Mander. 1992 Technical Report NCEER -92-0027
4. Seismic Design of Reinforced Concrete and Masonry Buildings. T. Paulay, M.J.N. Priestley,. 1992 John Wiley & Sons, INC.
5. Design of Concrete Buildings for Earthquake & Wind Forces. S.K. Ghosh, August W. Domel, Jr.. 1992, pca, Skokie, Illinois 60077-1083
6. Corrosion-resistance performance of fly-ash blended cement concrete. Hussain,SE and Rasheeduzzafar, . 1994 ACI Materials Journal, 91 .
7. Frost resistance of roller-compacted high-volume fly ash concrete.Michel Pigeon, V. Mohan Malhotra. Journal of Materials in Civil Engineering, 1995, pg. 216,
8. Experimental investigation on the use of fly ash for lightweight precast structural elements. Materials and Structures/Mat6riaux et Constructions. G. Dinelli, G. Belz, C. E. Majorana and B. A. Schrefler. Vol. 29, December 1996, pp 632-638
9. Structural Modeling and Experimental Techniques. Harry G. Harris and Gajanan M. Sabnis,. 1999, Second Edition.
10. Anil K. Chopra. *Dynamics of Structure.* 2001, Prentice Hall, Upper Saddle River, NJ.
11. V. Saraswathy , S. Muralidharan, K. Thangavel and S. Srinivasan, *Influence of activated fly ash on corrosion-resistance and strength of concrete.* 2002 Concrete Structures and Failure Analysis Group. Tamilnadu, India
12. Robert E. Englekirk, *Seismic Design of Reinforced and Precast Concrete Buildings.* 2003 John Wiley & Sons, INC
13. Bruce King, P.E. *Making of better concrete, Guidelines to using Fly Ash for high quality eco-friendly structures.* 2005.
14. James G. Macgregor, James K. Wight, *Reinforced Concrete Mechanics and Design*, 2005, Prentice Hall, Upper Saddle River, NJ.
15. Building Code Requirements for Structural Concrete, ACI 318-05
16. Minimum Design Loads for Buildings and other Structures, ASCE/SEI 7-05

17. A. Fernandez-Jimenez, I. García-Lodeiro and A. Palomo, *Durability of alkali-activated fly ash cementitious materials.* 2006 Journal Mater Science 42:3055–3065
18. *A Review of Literature Related to the Use of Spray Dryer Absorber Material*, 2007 Electric Power Research Institute
19. J.W. van de Lindt, J.A.H. Carraro, P.R. Heyliger and C. Choi, *Application and feasibility of coal fly ash and scrap tire fiber as wood wall insulation supplements in residential buildings.* 2008 Colorado State University, Department of Civil and Environmental Engineering, Fort Collins, CO, USA
20. Charles E. Riley, *High-volume use of Self-Cementing Spray Dry Absorber Material for Structural Applications.* 2009 Colorado State University, Fort Collins, CO

APPENDIX A
DESIGN LOADS ON THE FRAME

Dead Load on slab (8" thick slab)	4.788 KN/m^2 (100 psf)
Live Load on slab	4.788 KN/m^2 (100 psf)
Load Combinations	
1.2D+1.6L	13.41 KN/m^2 (280 psf)
1.2D+1.0E+L+.2S	10.53 KN/m^2 (220 psf)
.9D+1E	4.31 KN/m^2 (90 psf)
Additional dead load	
Self weight of beams	3.74 KN (840 lbs)
Self weight of columns	37.37 KN (8400 lbs)

APPENDIX B

EQUIVALENT LATERAL FORCE PROCEDURE

Building Height h_n = 9.14 m (30 ft)

Seismic Weight W = 11981.06 KN (2693.45 kips)

Design Response spectral acceleration at 0.2 s S_{DS} = 0.2 for Los Angeles California

Site Class D $F_a = 1$

Response modification factor R = 8 for special reinforced concrete moment frames (Table 12-2-1 of ASCE 7-05)

Occupancy factor I = 1 for occupancy category II

Approximate fundamental period of building $T_a = C_t h_n^x = (0.016)(30)^{0.9} = 0.342$ s

Seismic coefficient $C_s = 0.2741$

Base Shear $V = C_s W = 3284.03$ KN (738.274 kips)

Table showing Vertical distribution of seismic design forces

Storey Level	wx, KN (kips)	hx, m (ft)	wx*hx	Cvx	Fx, KN (Kips)
3	3780.14 (849.81)	9.14 (30 ft)	34550.48 (25494.47)	0.486267	1596.90 (358.9983)
2	3993.7 (897.82)	6.1 (20)	24361.57 (17956.31)	0.342489	1124.73 (252.85)
1	3993.7 (897.82)	3.05 (10)	12180.79 (8978.16)	0.171244	562.39 (126.43)
Total	11767.55 (2645.45)		71092.84 (52428.94)		3284.03 (738.28)

The lateral force obtained for each storey as shown in the above table is distributed equally to all the column line frames in that storey

APPENDIX C

SEISMIC WEIGHT CALCULATIONS

Seismic mass was calculated by referring to Bracci (1992). From table in Appendix D the scale factor for mass is 9.

$W_{mr} = W_p * 1/S_l^2$

Were W_{mr} = Required weight of the model

W_p = Weight of the prototype

S_l = Length scale factor = 3

The weight of the prototype was calculated by considering only the dead load of the prototype. The total weight of the frame was calculated to be 171 kips.

Hence, $W_{mr} = W_p * 1/S_l^2 = 171 / 3^2 = 19$ kips

$W_{am} = 1.39$ kips

Where W_{am} = The Actual weight of the constructed model

$W = W_{mr} - W_{am} = 19 – 1.39 = 17.6$ kips

Where W = The required weight to be placed on the model

APPENDIX D

SCALE FACTORS USED FOR MODELING

Quantity	General case	Same material and Acceleration (Model)	
		Required	Provided
Geometric Length, l	$S_l = ?$	$S_l = 3.0$	$S_l = 3.0$
elastic Modulus, E	$S_E = ?$	$S_E = 1.0$	$S_E = 1.0$
Acceleration ,a	$S_a =?$ ($= 1/S_l*S_E/S_\rho$)	$S_a = 1.0$	$S_a = 1.0$
Density, ρ	$S_\rho = S_E/(S_lS_a)$ (=?)	$S_\rho = .33$	$S_\rho = 1.0$
Velocity, v	$S_v = \sqrt{(S_l\ S_a)}$	$S_v = 1.73$	$S_v = 1.73$
Forces, f	$S_f = S_ES_l^2$	$S_f = 9.0$	$S_f = 9.0$
Stress, σ	$S_\sigma = S_E$	$S_\sigma = 1.0$	$S_\sigma = 1.0$
Strain, ε	$S_\varepsilon = 1.0$	$S_\varepsilon = 1.0$	$S_\varepsilon = 1.0$
Area, A	$S_A = Sl2$	$S_A = 9$	$S_A = 9.0$
Volume, V	$S_V = S_l^3$	$S_V = 27$	$S_V = 27.0$
Second Moment of Area, I	$S_I = S_l^4$	$S_I = 81$	$S_I = 81.0$
Mass, m	$S_m = S_\rho S_l^3$	$S_m = 9$	$S_m = 27$
Impulse, i	$S_i = S_l^3\sqrt{(S_\rho S_E)}$	$S_i = 15.59$	$S_i = 27$
Energy, e	$S_e = S_eS_l^3$	$S_e = 27.0$	$S_e = 27.0$
Frequency, ω	$S_\omega = 1/S_s \sqrt{(S_E/S_\rho)}$	$S_\omega = 0.58$	$S_\omega = 0.33$
Time (Period), t	$S_t = \sqrt{S_l}/S_a$	$S_t = 1.73$	$S_t = 1.73$
Gravitational Acceleration , g	$S_g = 1.0$	$S_g = 1.0$	$S_g = 1.0$
Gravitational Force, fg	$S_{fg} = S_\rho S_l^3$	$S_{fg} = 9.0$	$S_{fg} = 27.0$
Critical Damping, ξ	$S_\xi = 1.0$	$S_\xi = 1.0$	$S_\xi = 1.0$

Note: All the scale factors are obtained from (Bracci, 1992)

APPENDIX E

INTERACTION DIAGRAM OF THE COLUMN

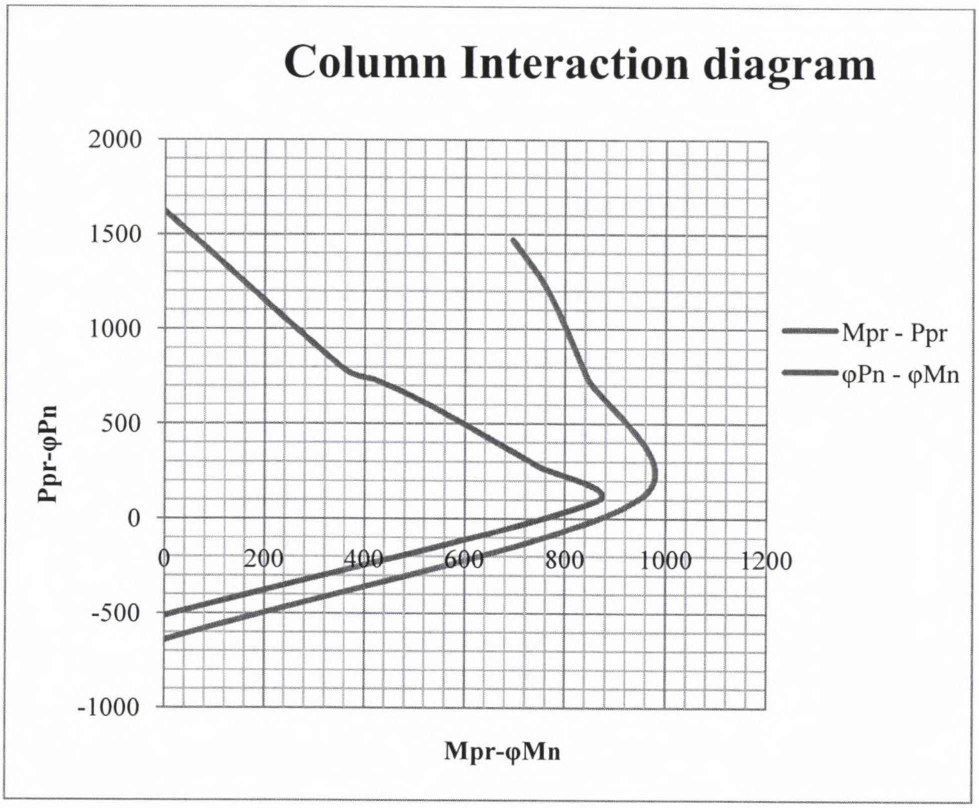

APPENDIX F

PICTURES OF DAMAGES AFTER EACH TEST SEQUENCE

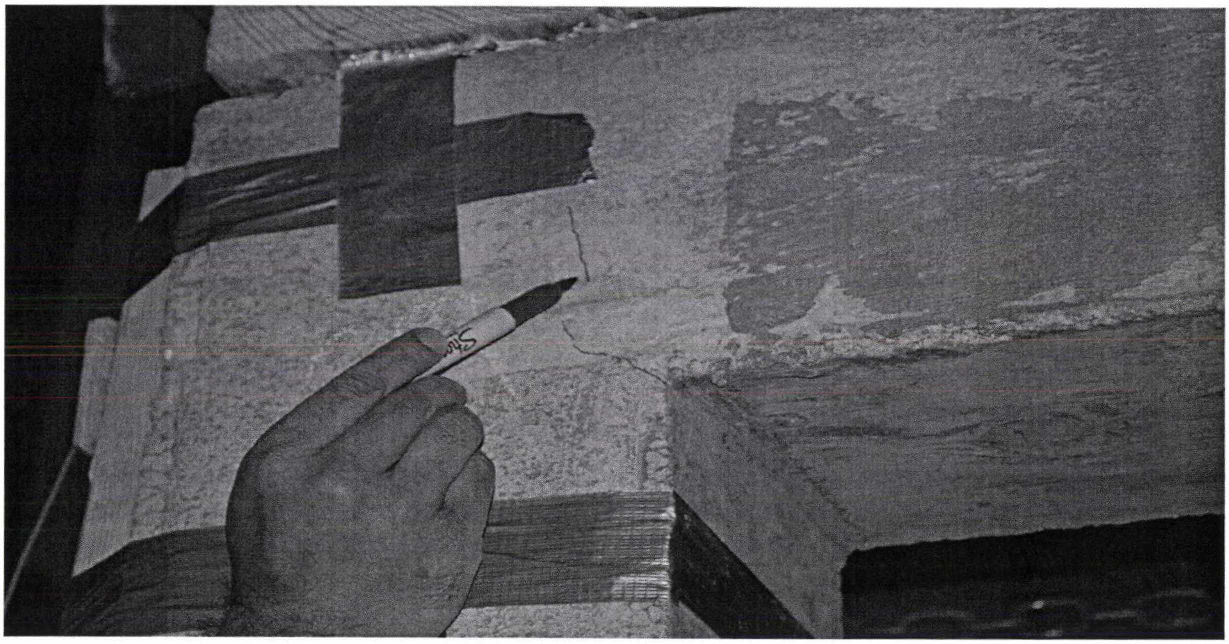

Figure F.1 Shear crack in column C2 of concrete frame after test sequence 2

Figure F.2 Shear crack in column C3 of concrete frame after test sequence 2

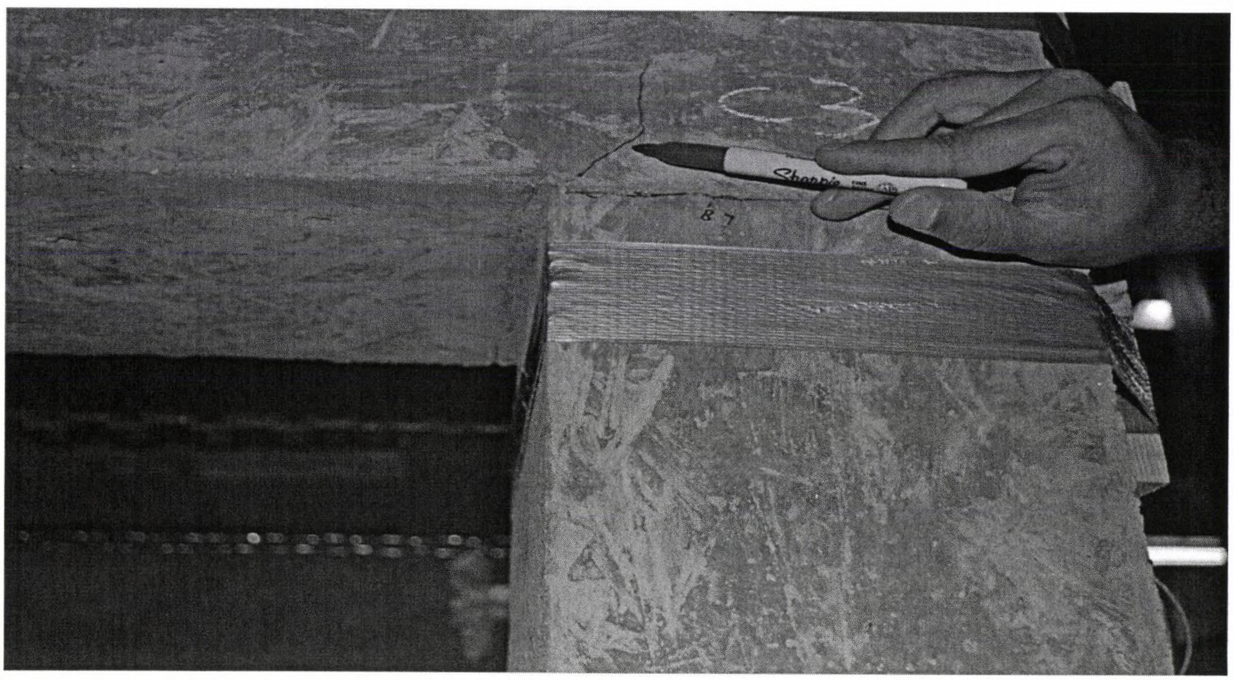

Figure F.3 Shear crack in column C3 of concrete frame after test sequence 2

Figure F.4 Shear crack in column C4 of concrete frame after test sequence 2

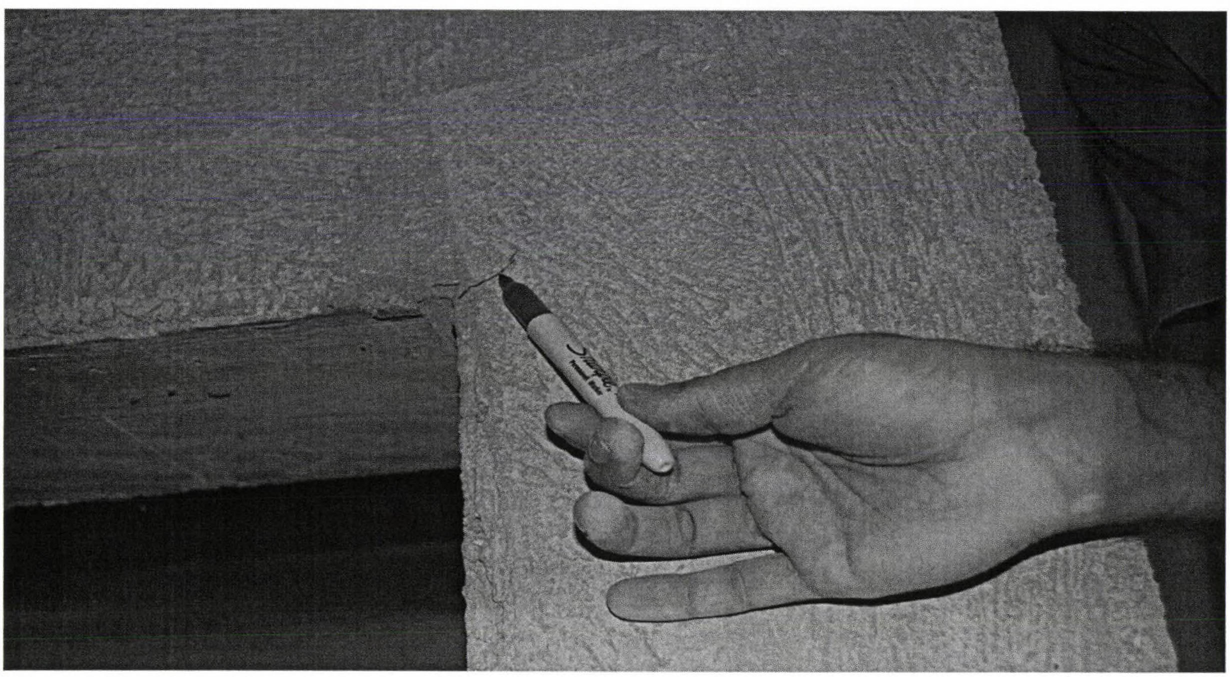

Figure F.5 Shear crack in column C1 of concrete frame after test sequence 3

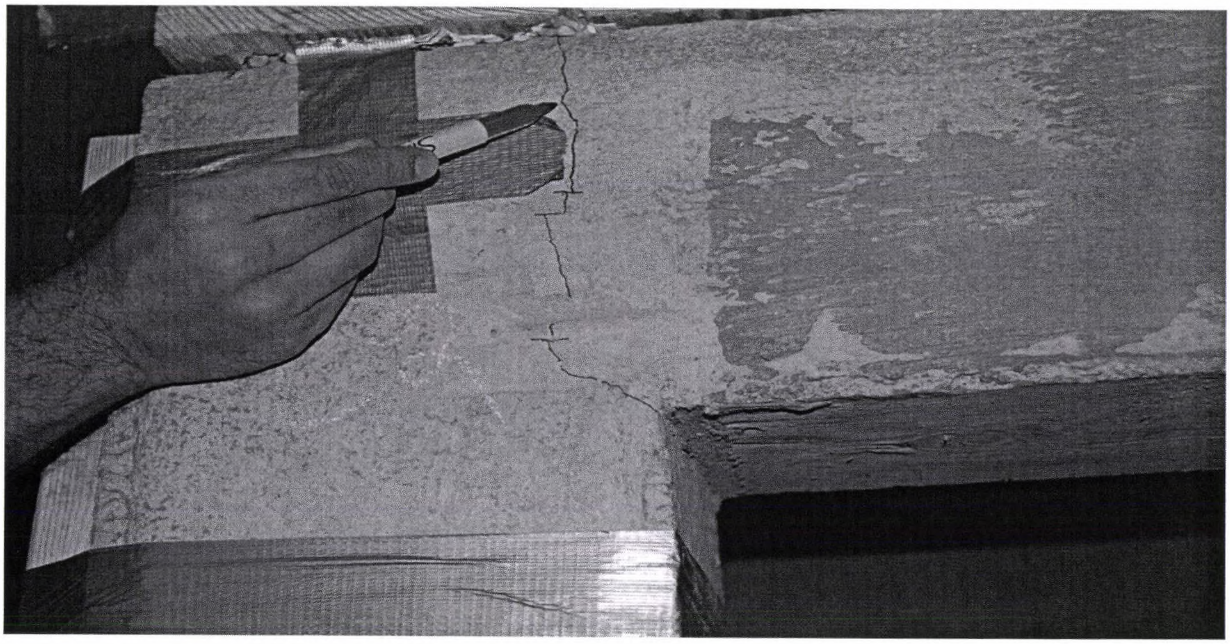

Figure F.6 crack in column C2 of concrete frame after test sequence 3

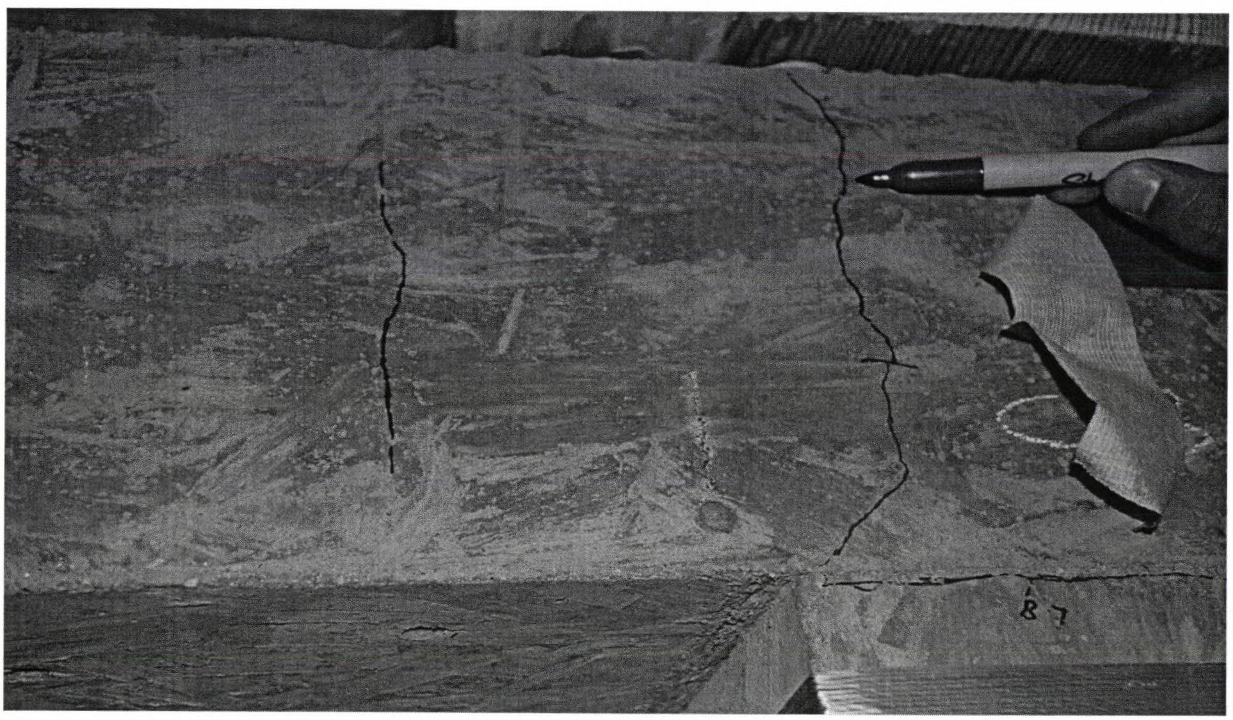

Figure F.7 crack in column C3 and beam B2 of concrete frame after test sequence 3

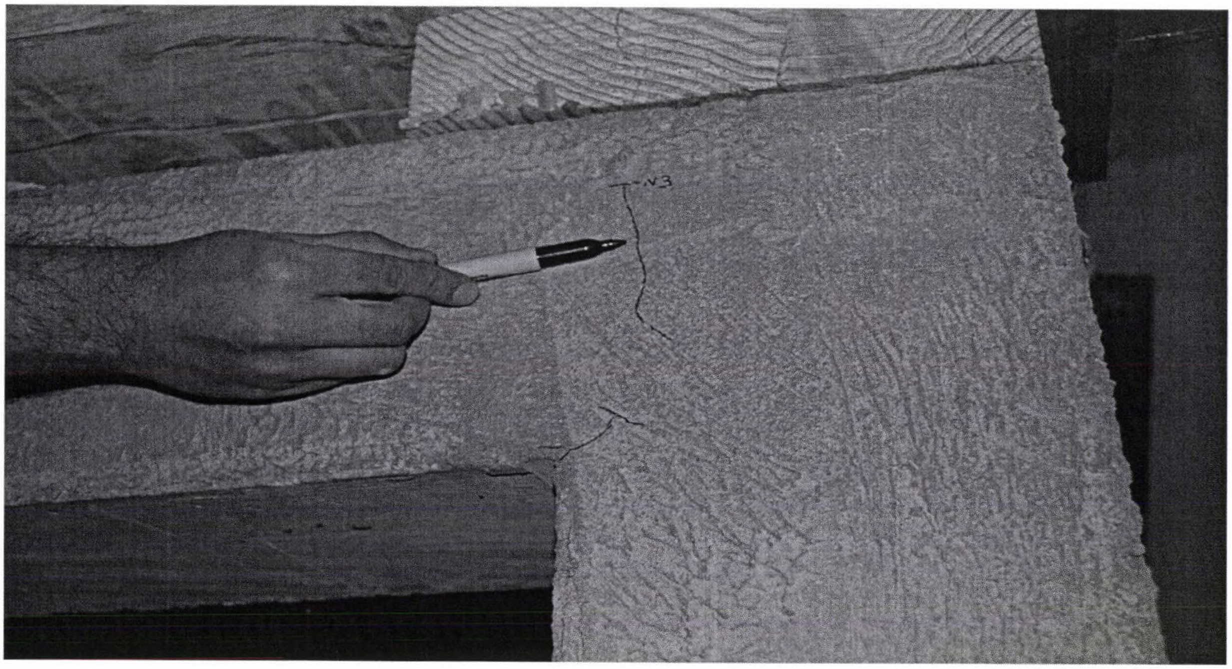

Figure F.8 crack in column C1 of concrete frame after test sequence 4

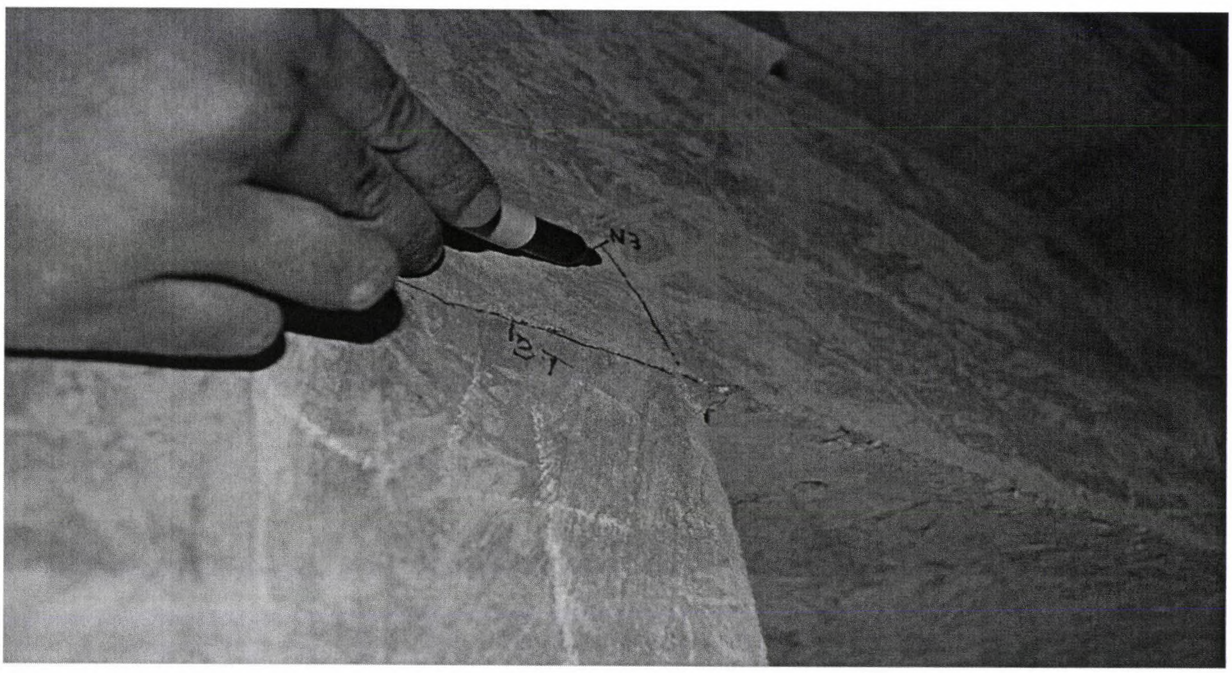

Figure F.9 Shear crack in column C4 of concrete frame after test sequence 4

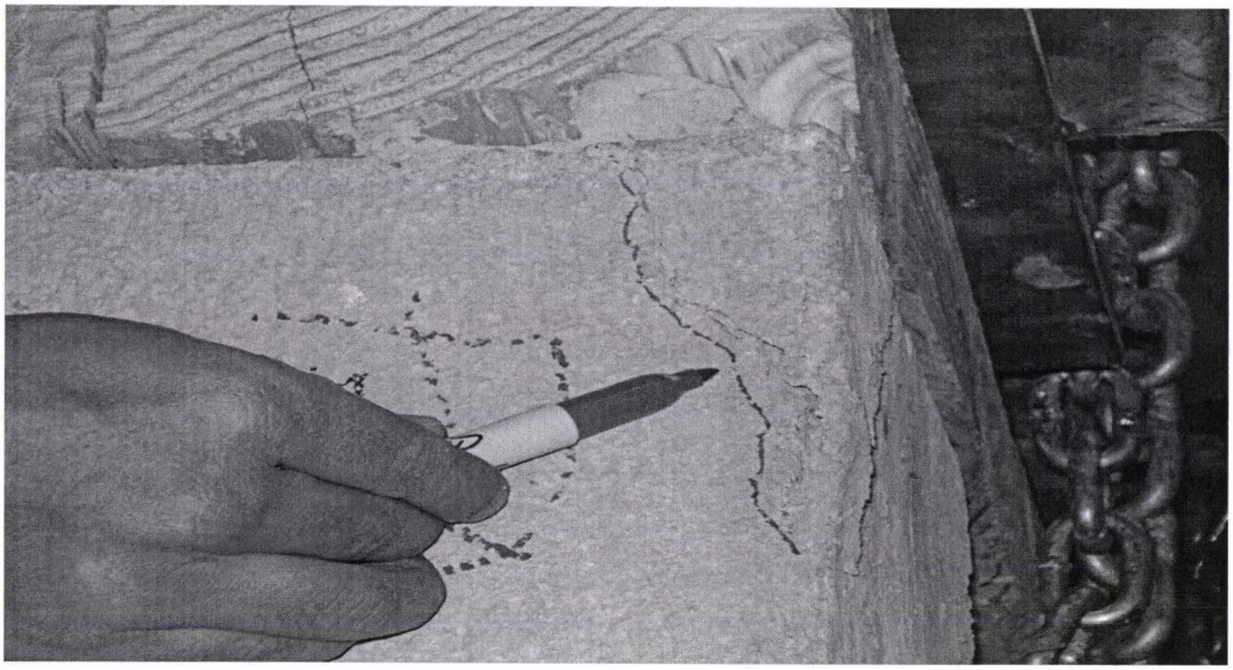

Figure F.10 Crack in column C1 of SDA concrete frame after test sequence 1

Figure F.11 Shear crack in column C4 of SDA concrete frame after test sequence 1

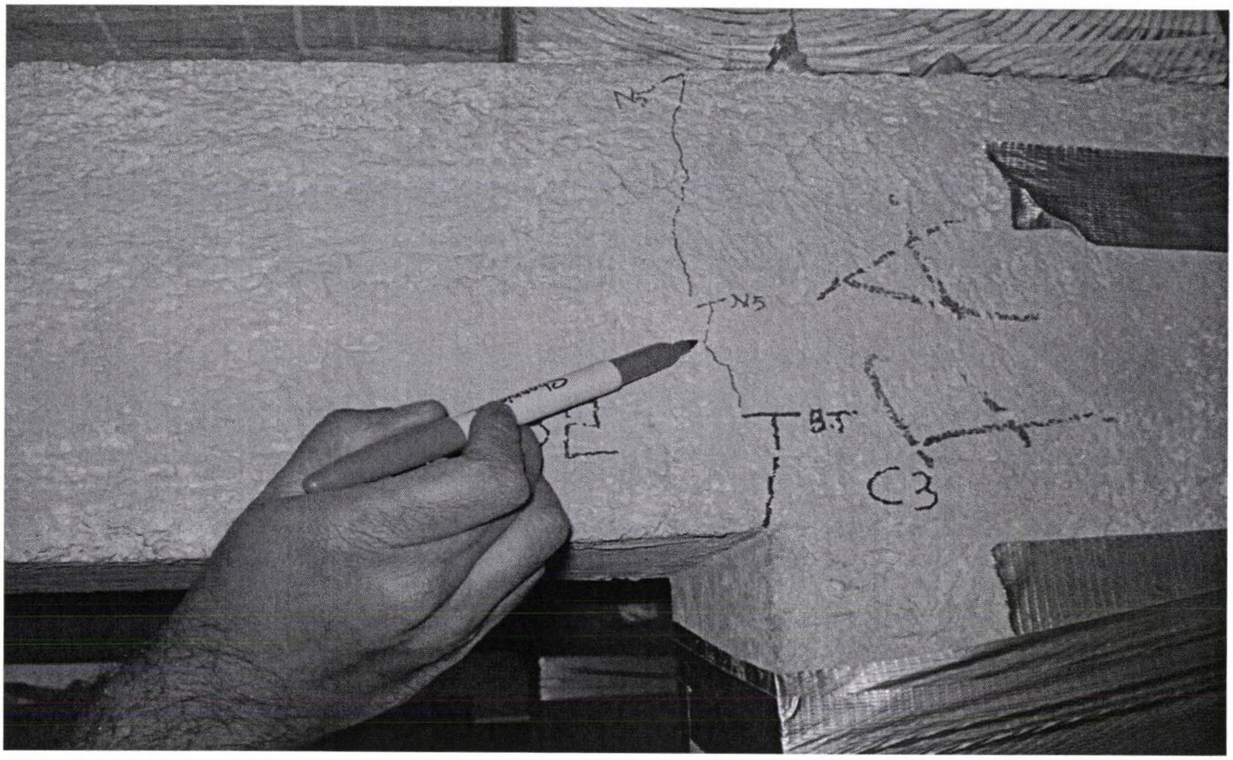

Figure F.12 Crack in column C3 of SDA concrete frame after test sequence 2

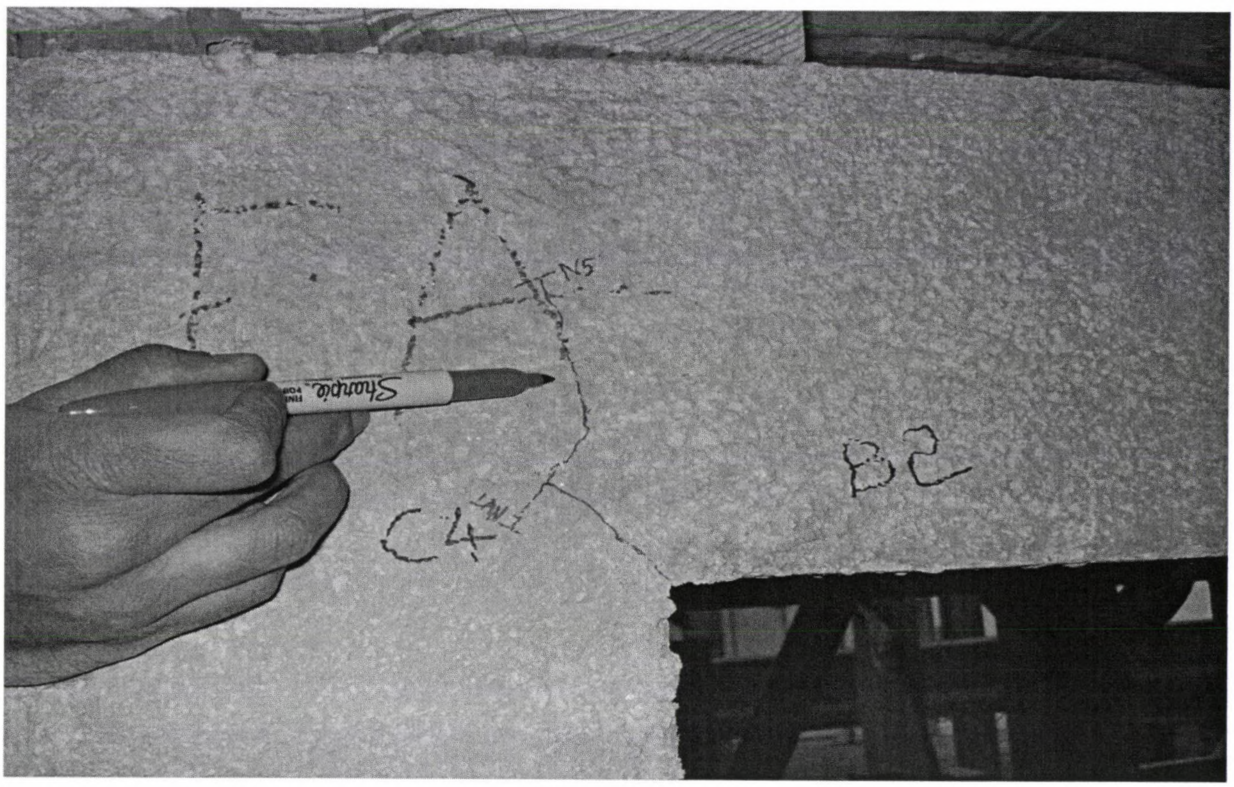

Figure F.13 Crack in column C4 of SDA concrete frame after test sequence 2

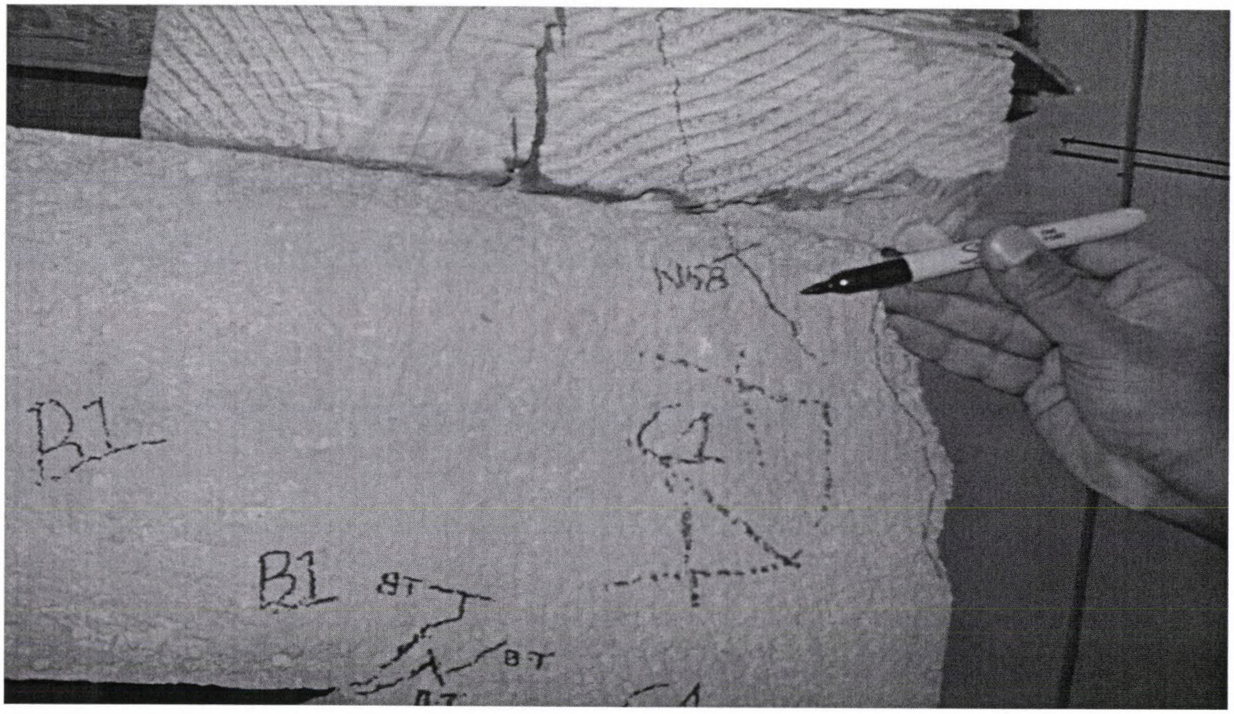

Figure F.14 Crack in column C1 of SDA concrete frame after test sequence 3

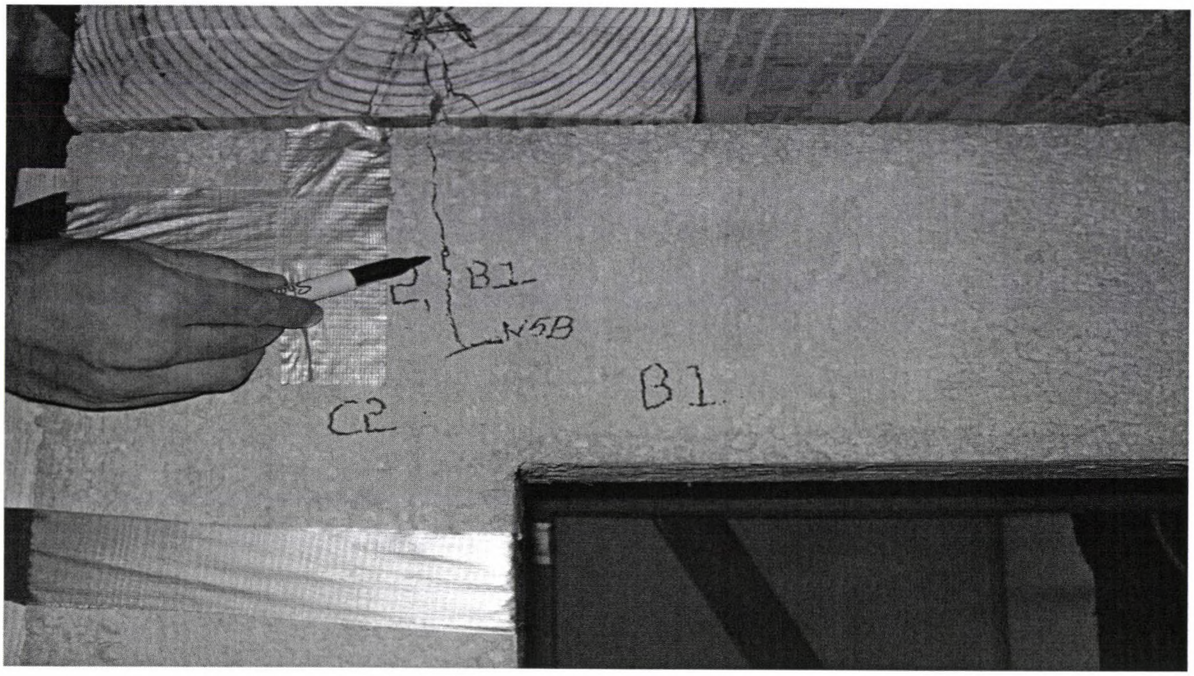

Figure F.15 Crack in column C2 of SDA concrete frame after test sequence 3

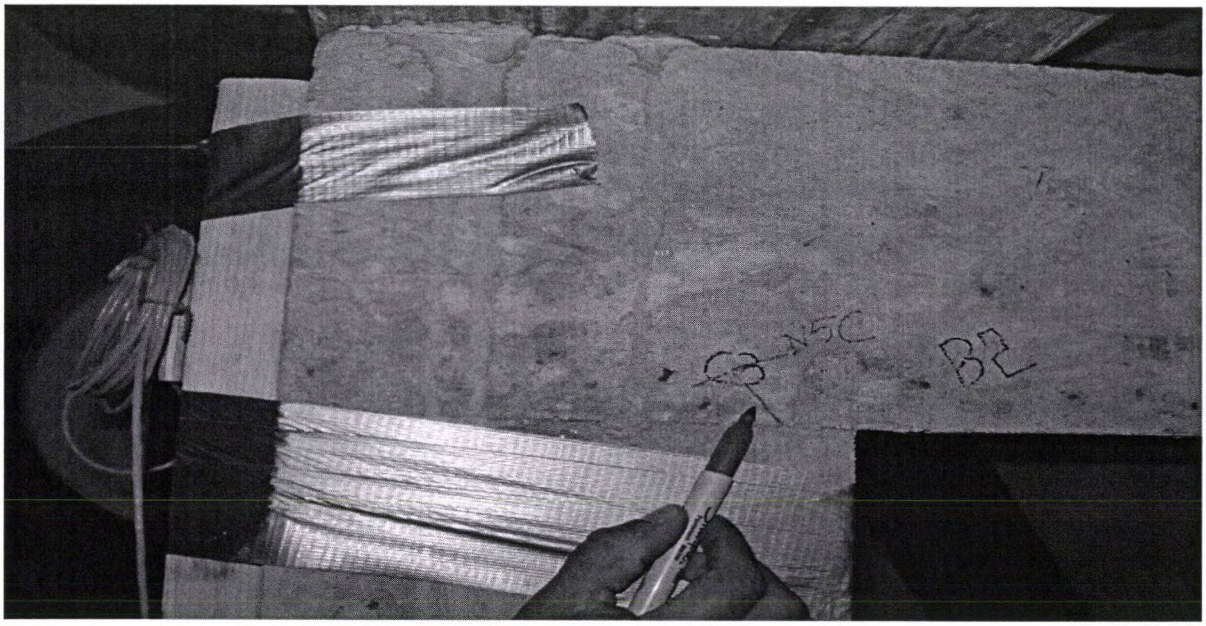

Figure F.16 Shear crack in column C3 of SDA concrete frame after test sequence 4

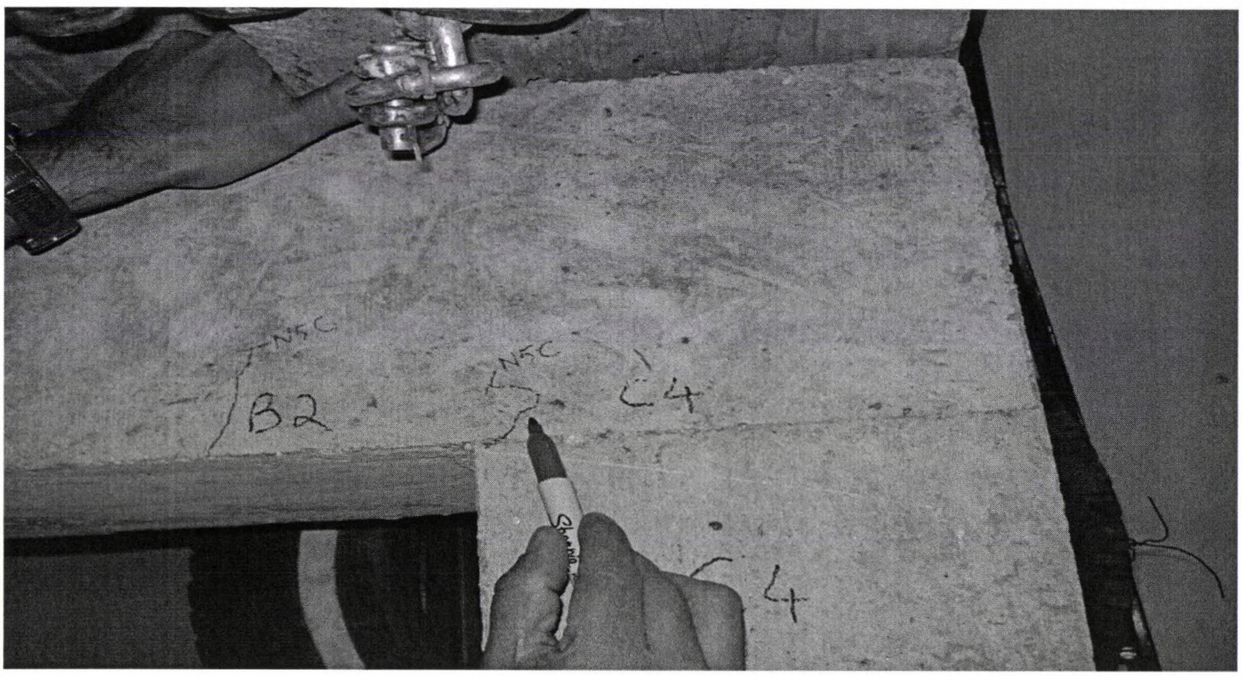

Figure F.17 Shear crack in column C4 and beam B2 of SDA concrete frame after test sequence 4

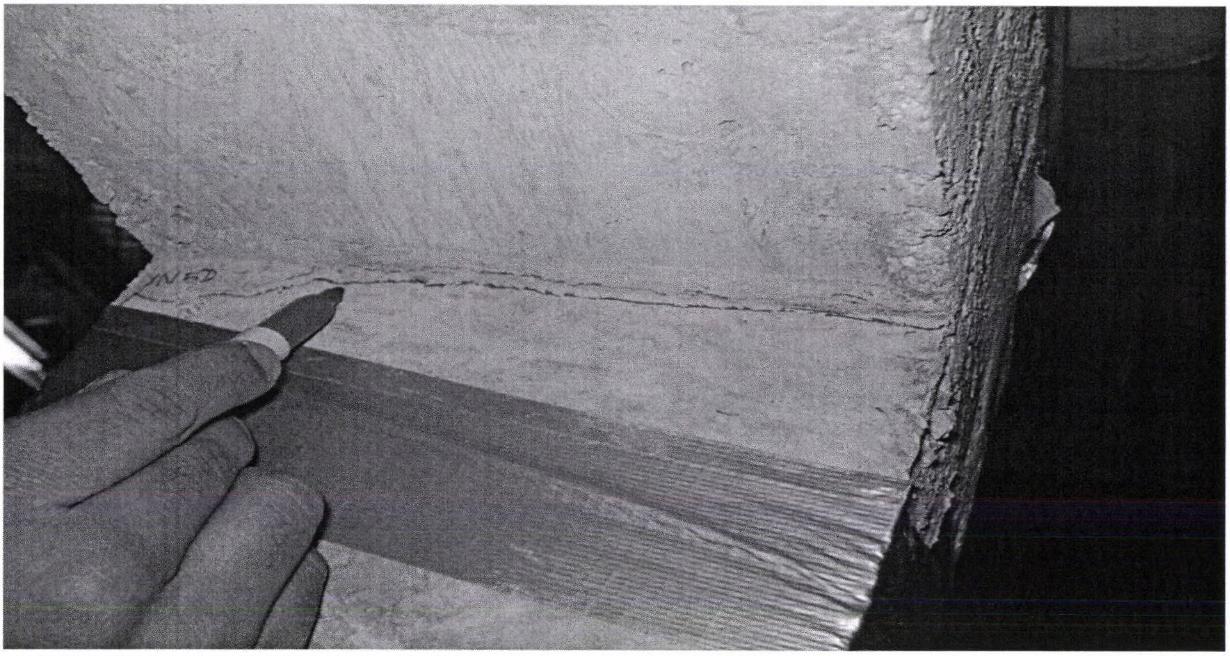

Figure F.18 Crack in beam-column joint at column C3 of SDA concrete frame after test sequence 5

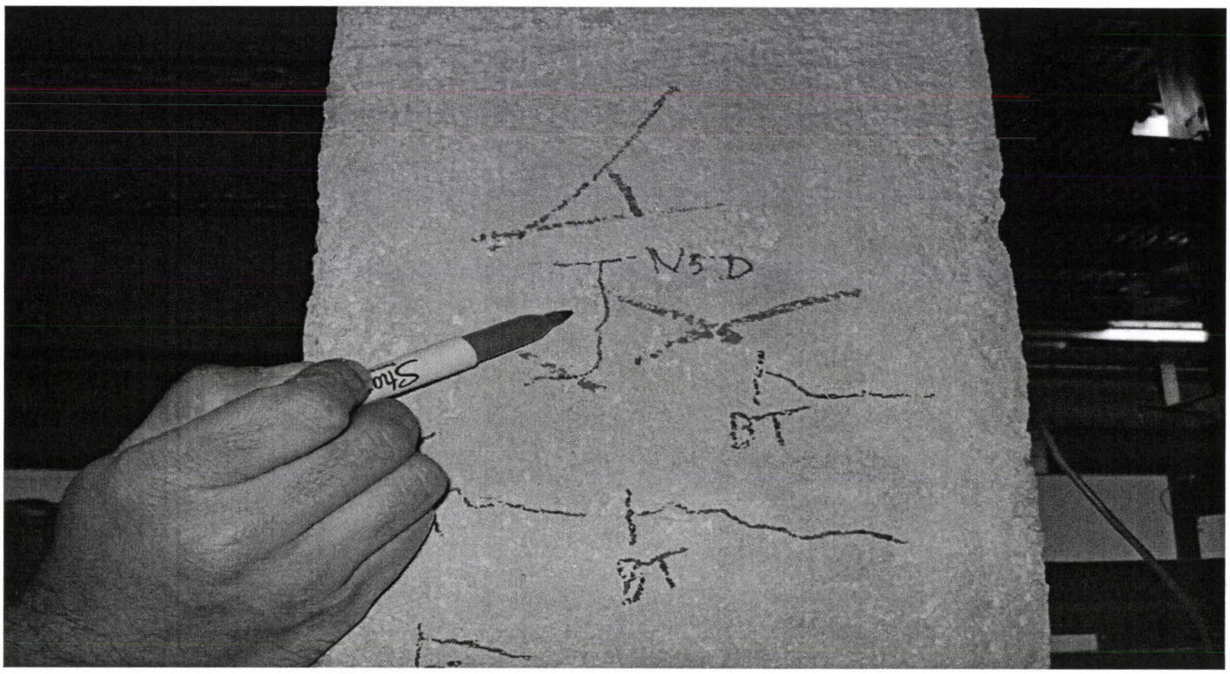

Figure F.19 Crack in column C3 of SDA concrete frame after test sequence 5

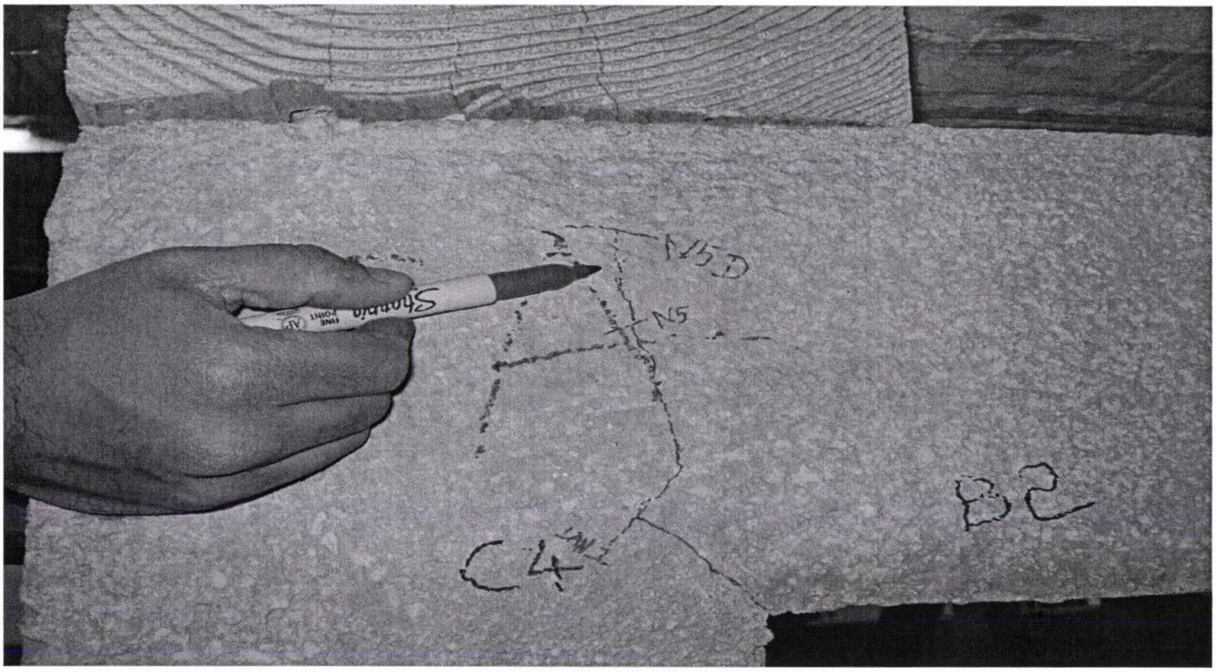

Figure F.20 Crack in column C4 of SDA concrete frame after test sequence 5

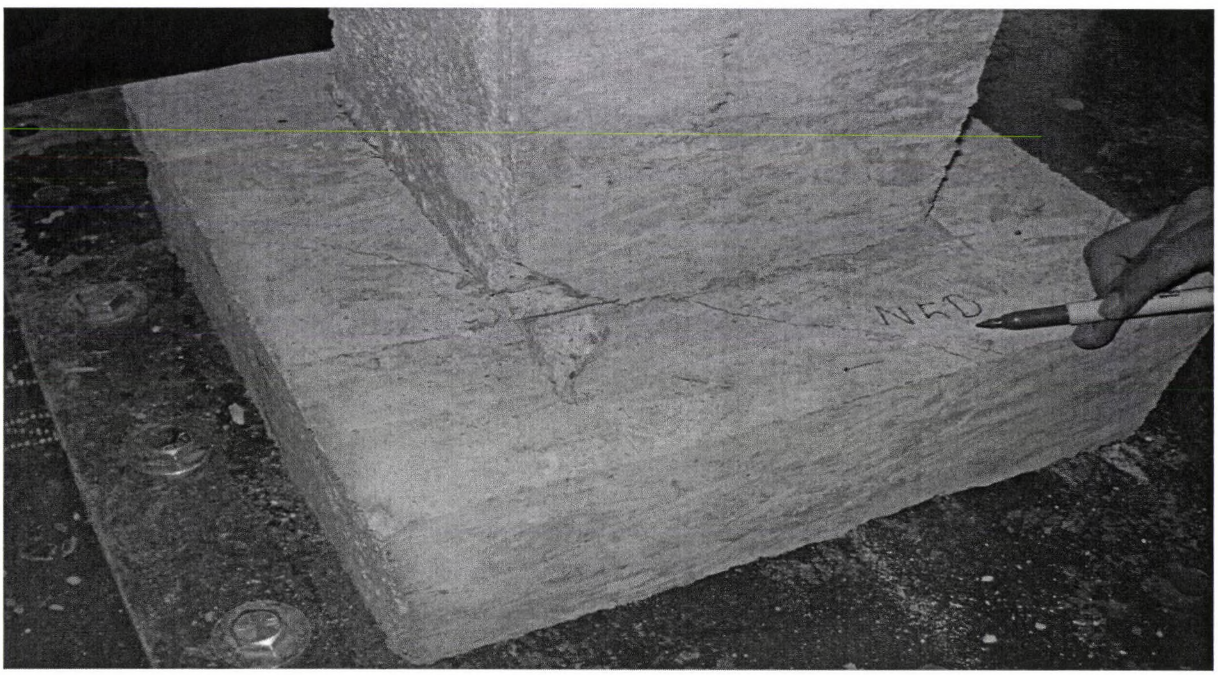

Figure F.21 Crack in column base C4 of SDA concrete frame after test sequence 5

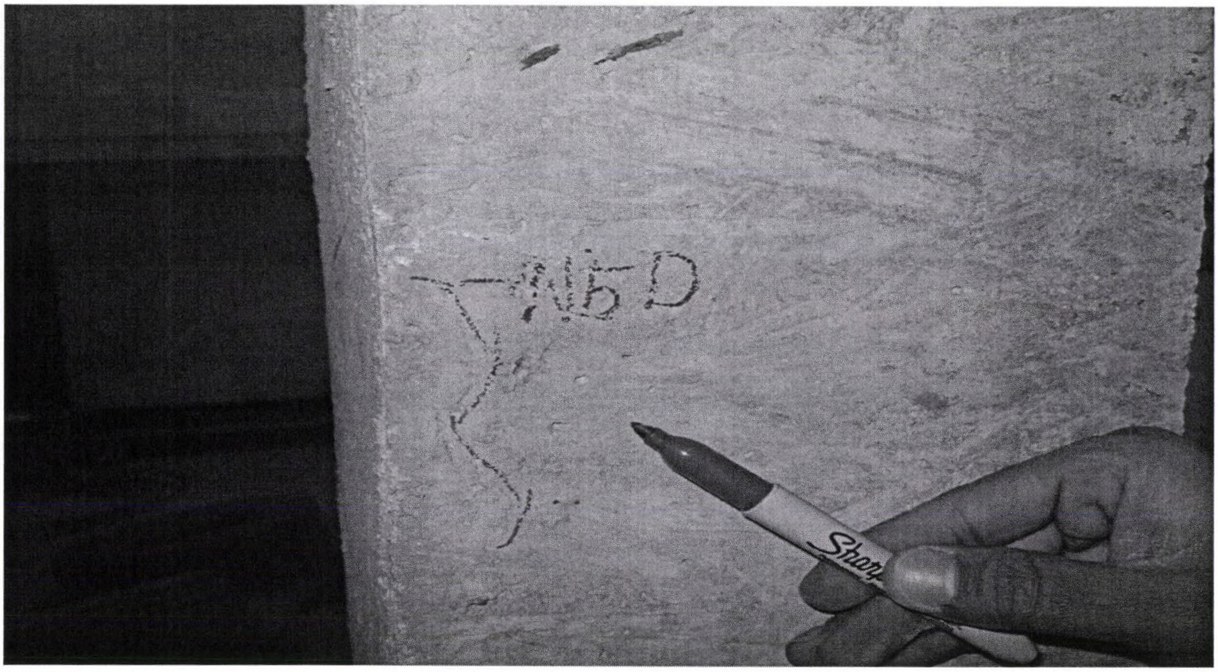

Figure F.22 Crack in column C4 of SDA concrete frame after test sequence 5

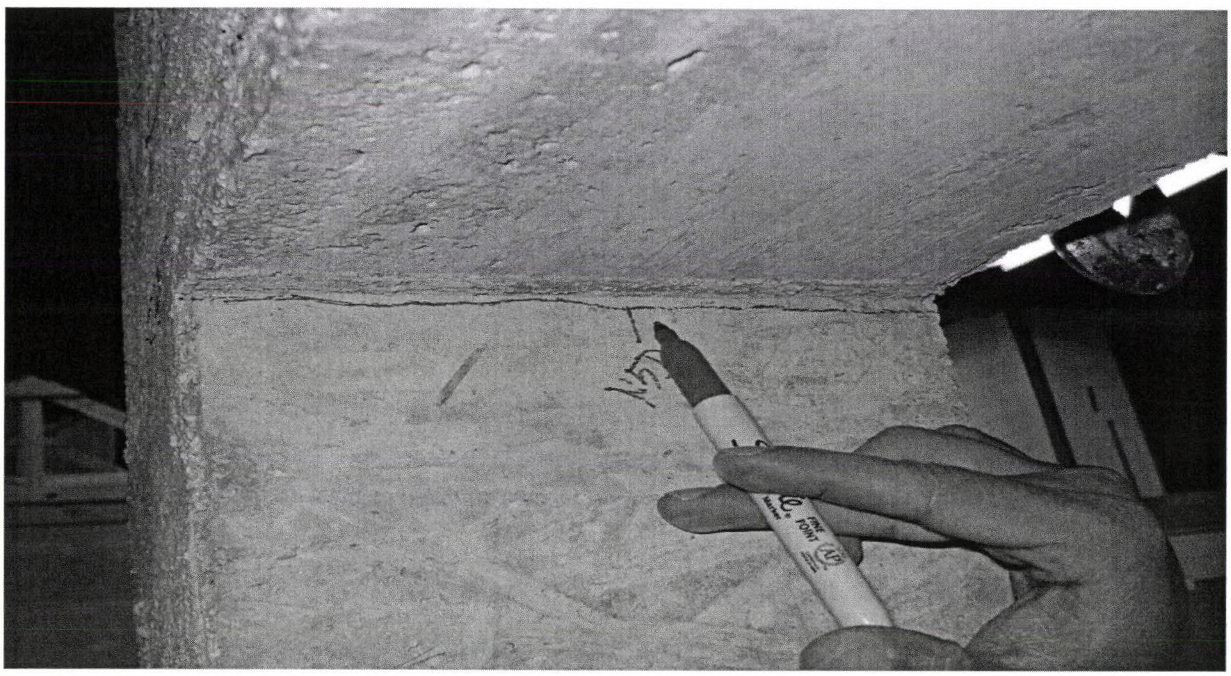

Figure F.23 Crack at beam-column joint in column C1 of SDA concrete frame after test sequence 5

APPENDIX G

DISPLACEMENT RESPONSE CURVES

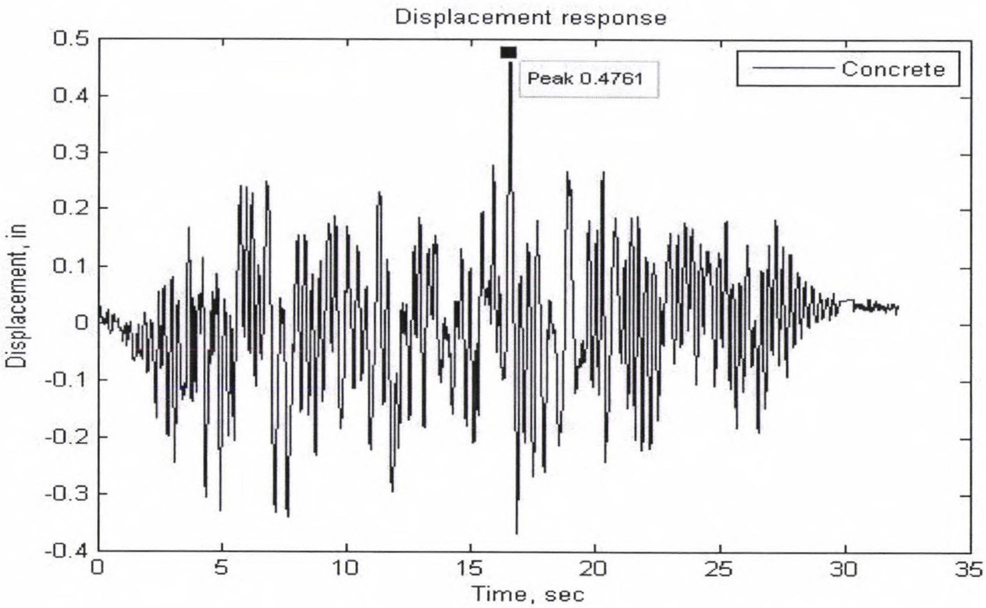

Figure G.1 Displacement response of concrete frame, Column C2 after test sequence 1

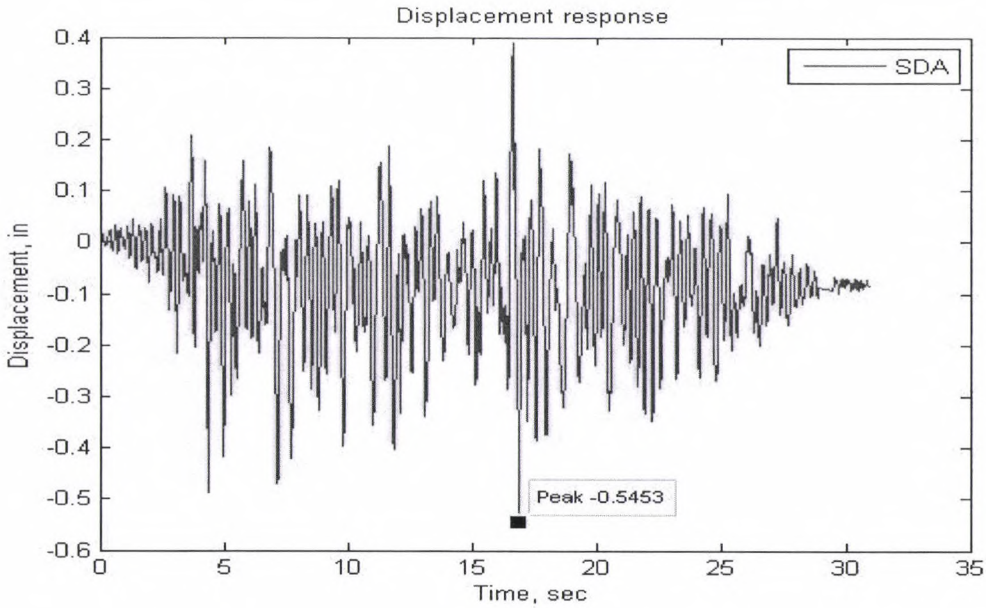

Figure G.2 Displacement response of SDA concrete frame, Column C2 after test sequence 1

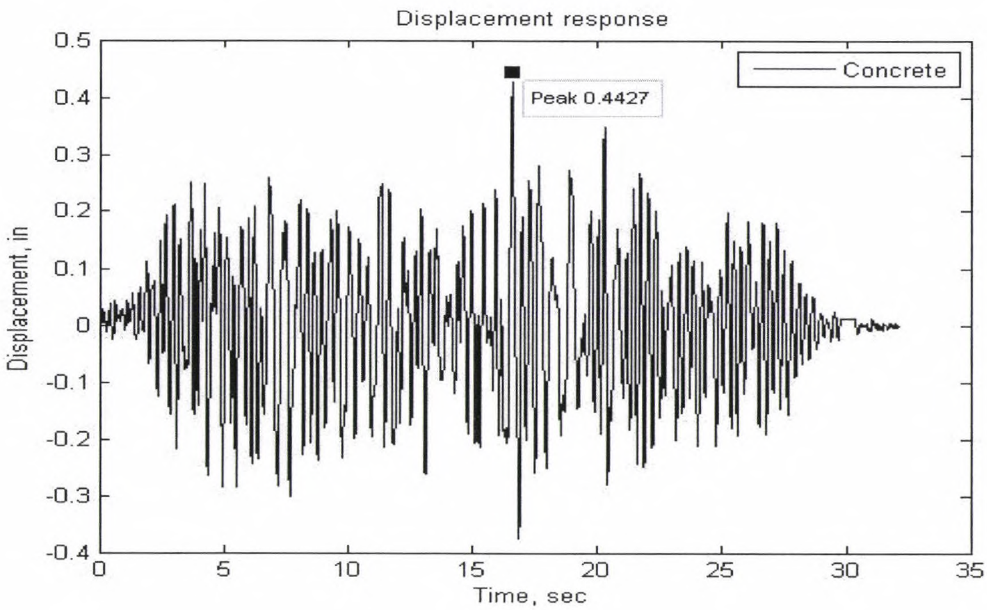

Figure G.3 Displacement response of concrete frame, Column C3 after test sequence 1

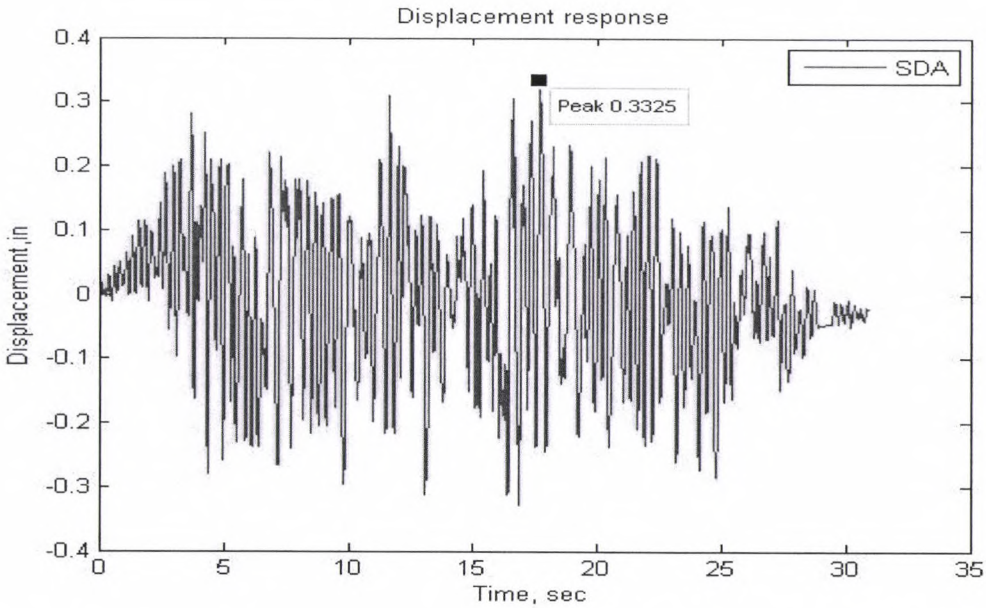

Figure G.4 Displacement response of SDA concrete frame, Column C3 after test sequence 1

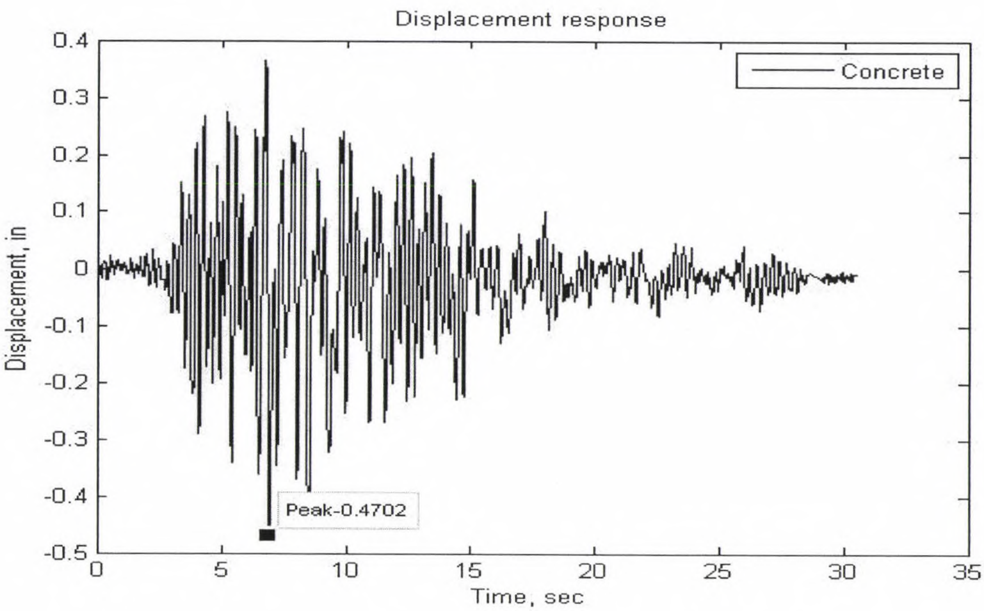

Figure G.5 Displacement response of concrete frame, Column C2 after test sequence 2

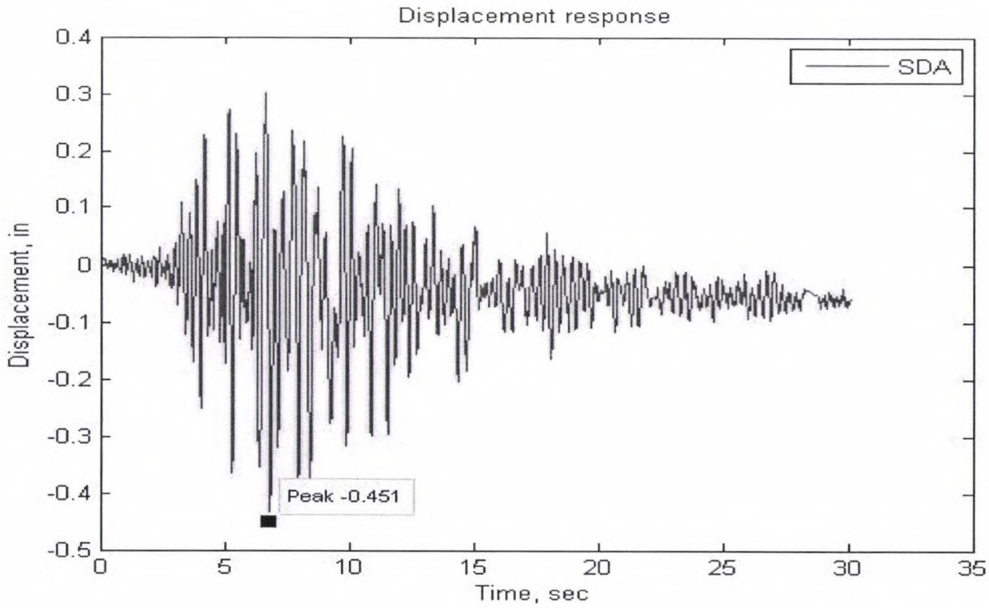

Figure G.6 Displacement response of SDA concrete frame, Column C2 after test sequence 2

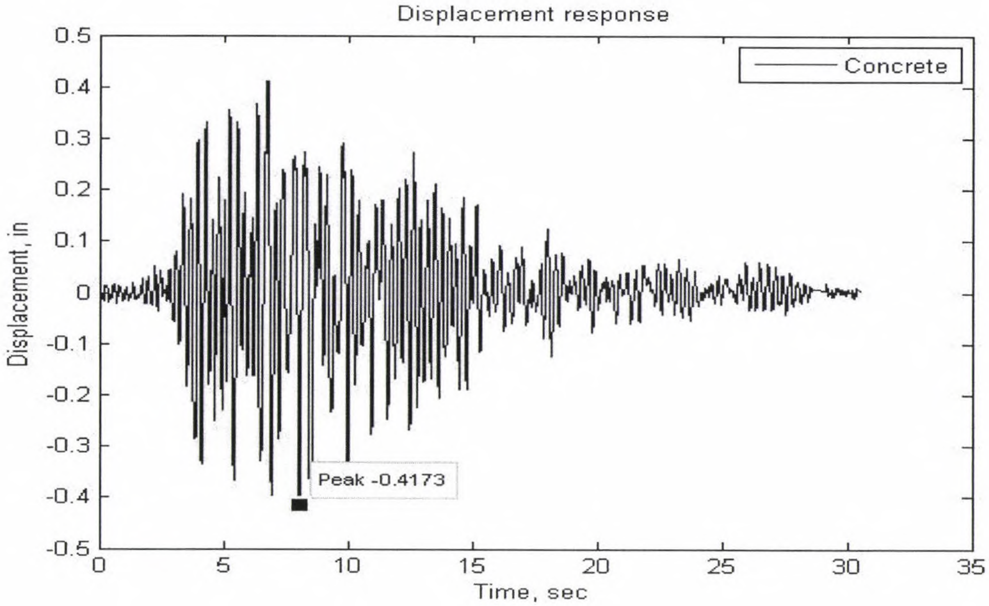

Figure G.7 Displacement response of concrete frame, Column C3 after test sequence 2

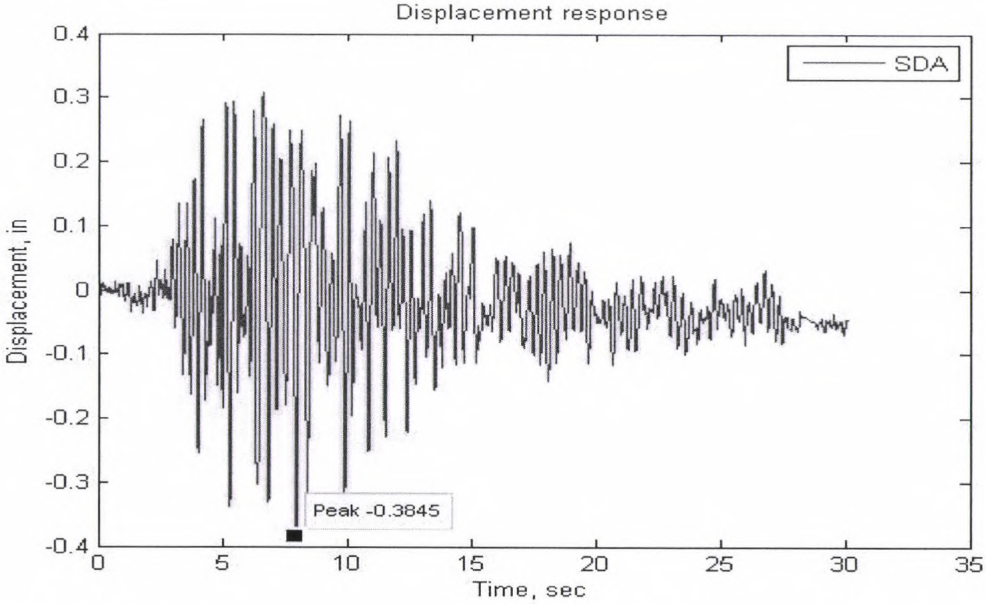

Figure G.8 Displacement response of SDA concrete frame, Column C3 after test sequence 2

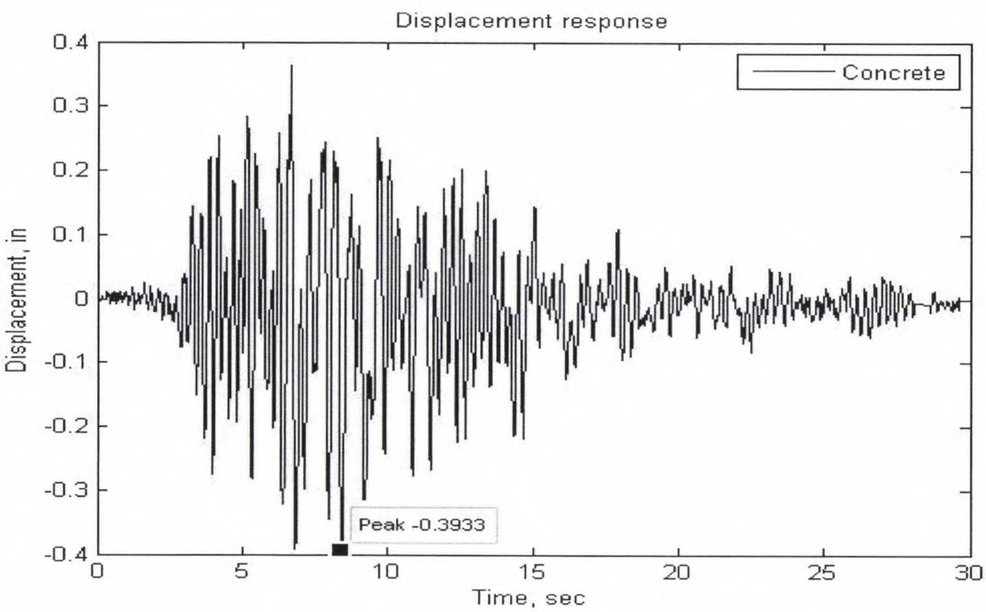

Figure G.9 Displacement response of concrete frame, Column C2 after test sequence 3

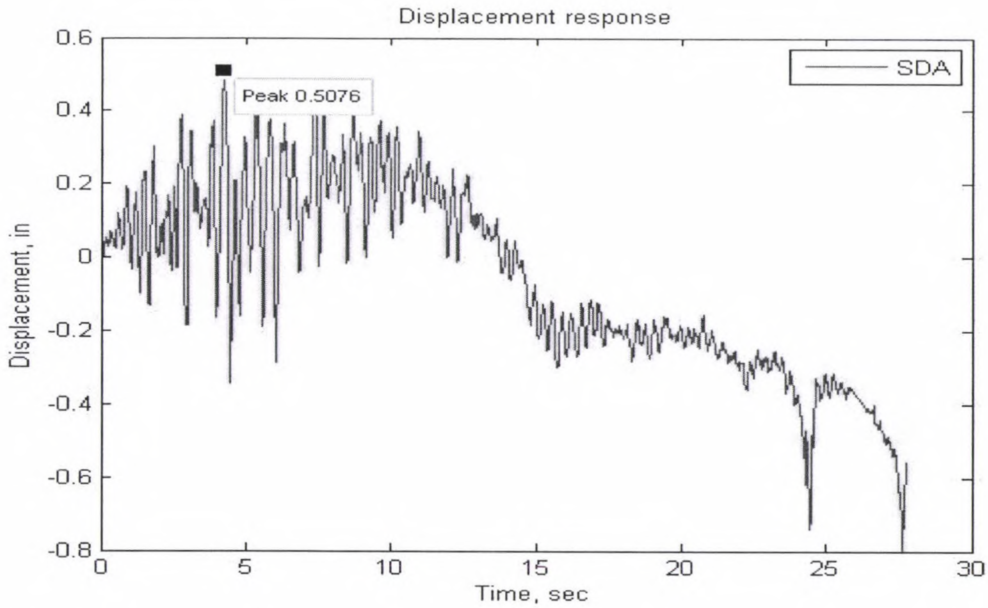

Figure G.10 Displacement response of SDA concrete frame, Column C2 after test sequence 3

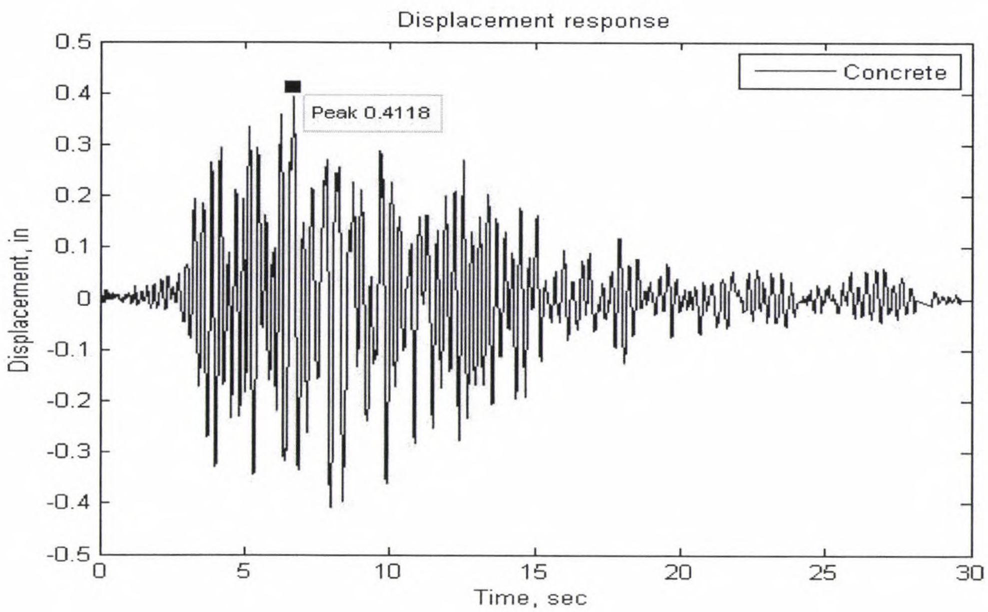

Figure G.11 Displacement response of concrete frame, Column C3 after test sequence 3

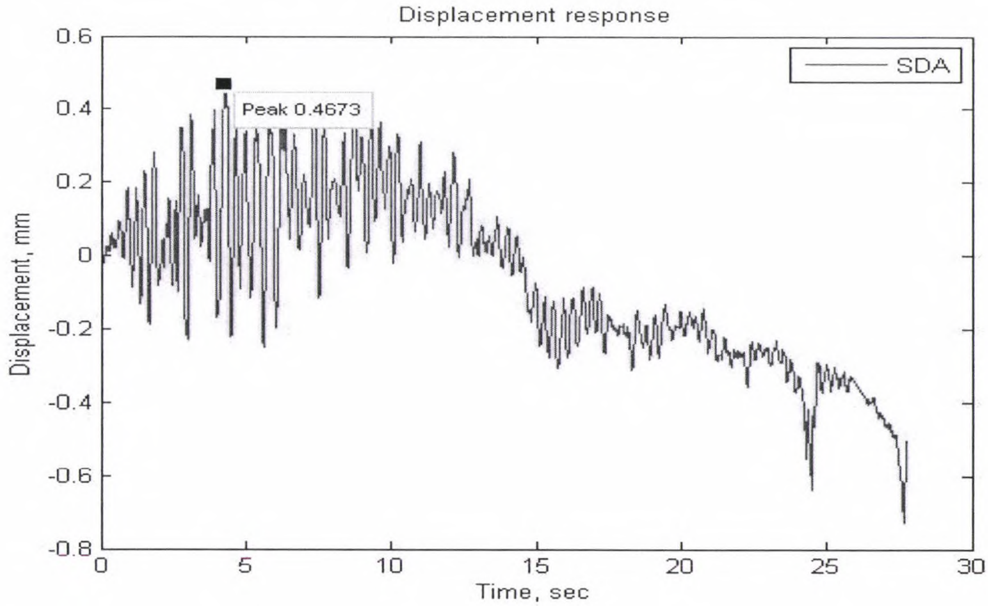

Figure G.12 Displacement response of SDA concrete frame, Column C3 after test sequence 3

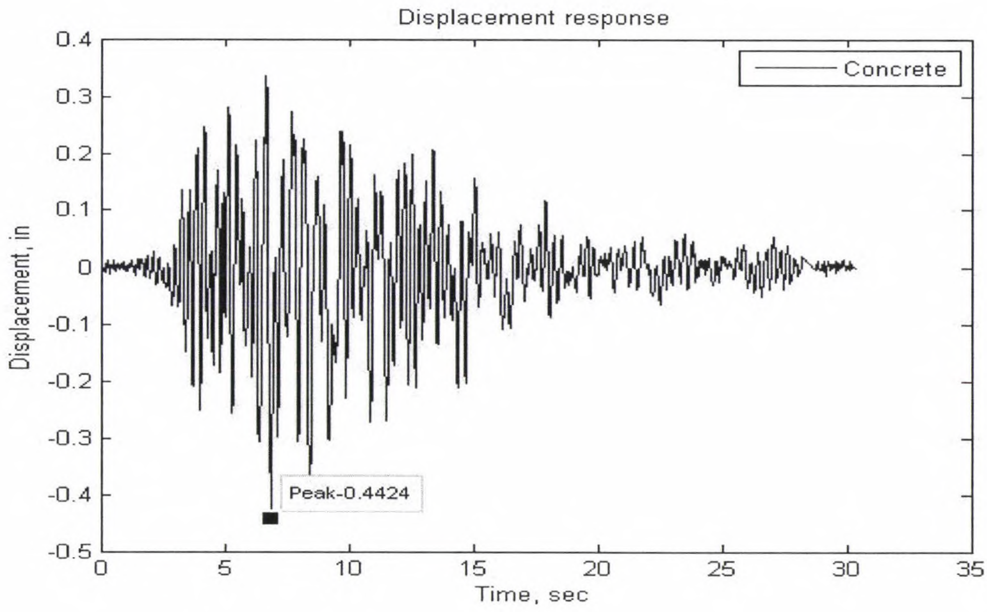

Figure G.13 Displacement response of concrete frame, Column C2 after test sequence 4

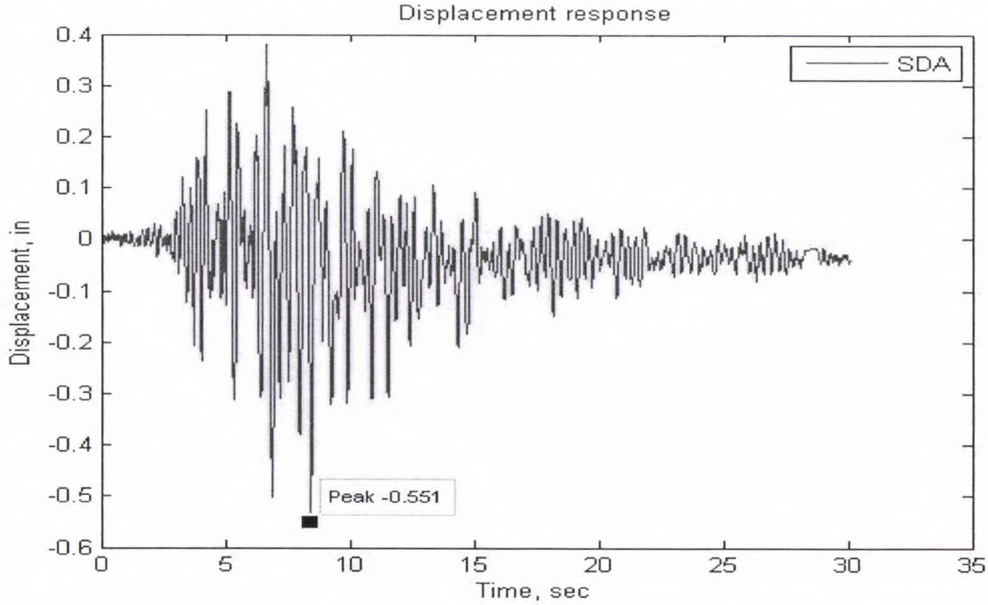

Figure G.14 Displacement response of SDA concrete frame, Column C2 after test sequence 4

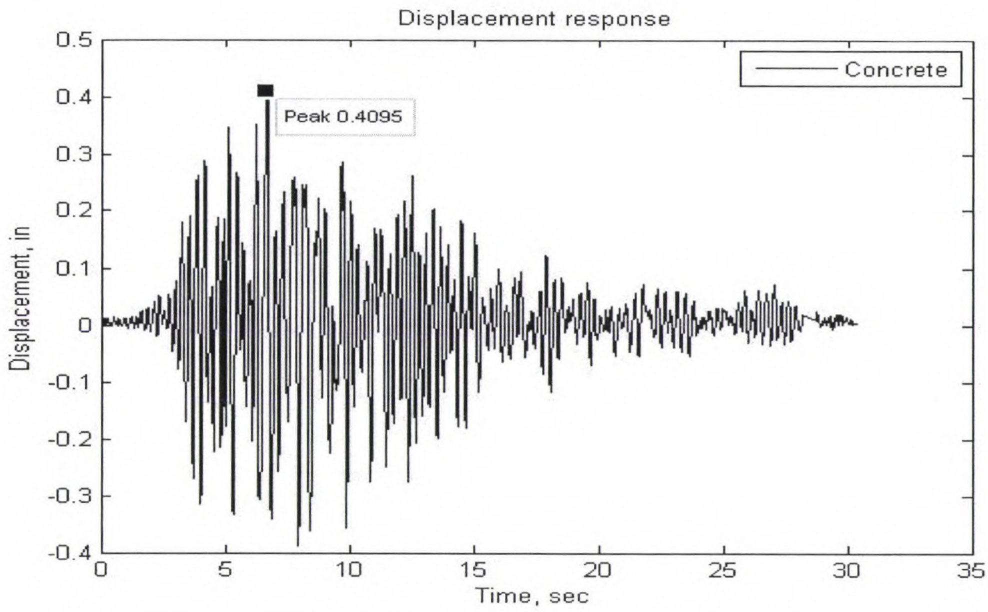

Figure G.15 Displacement response of concrete frame, Column C3 after test sequence 4

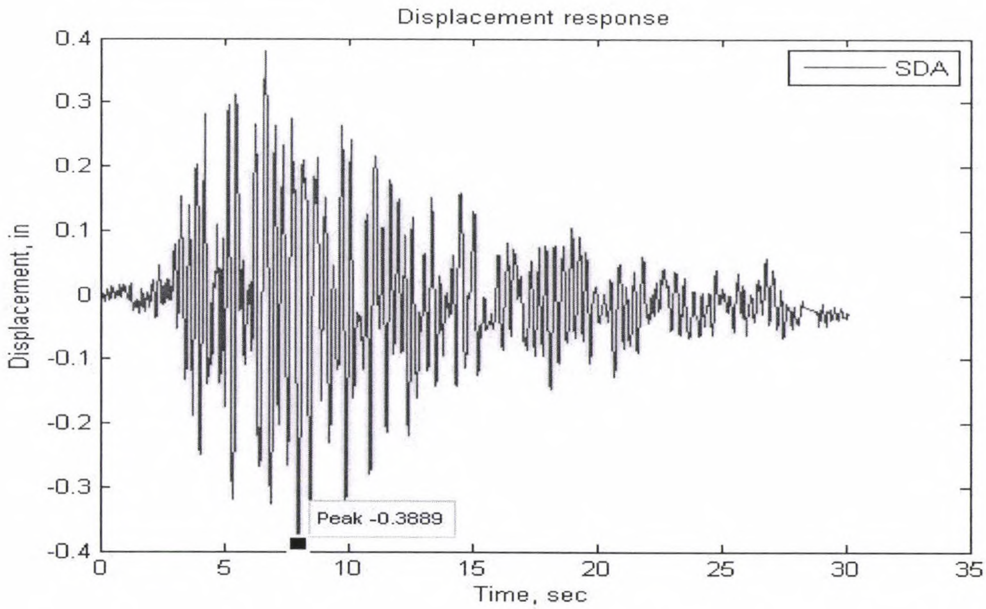

Figure G.16 Displacement response of SDA concrete frame, Column C3 after test sequence 4

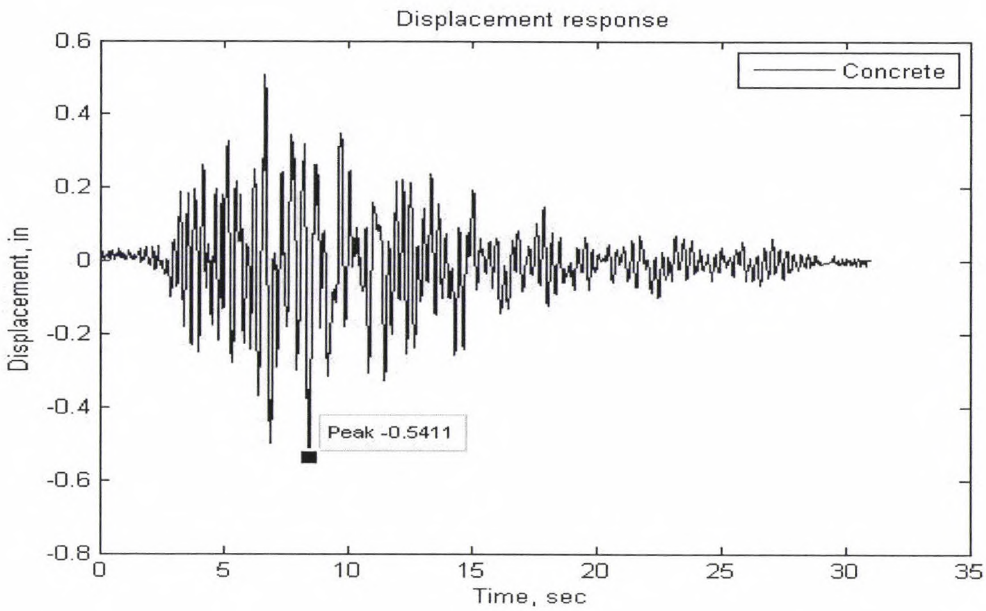

Figure G.17 Displacement response of concrete frame, Column C2 after test sequence 5

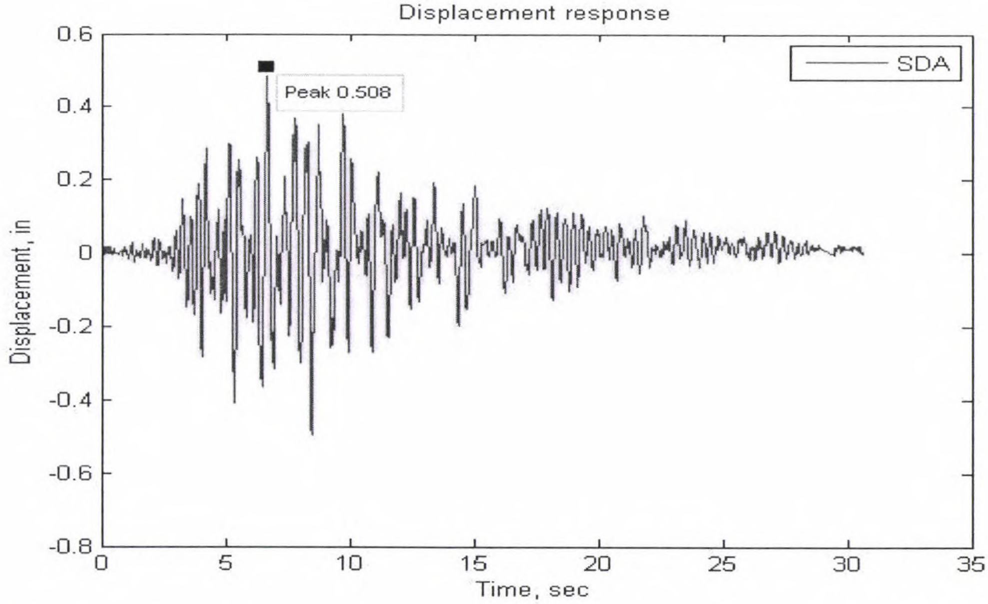

Figure G.18 Displacement response of SDA concrete frame, Column C2 after test sequence 5

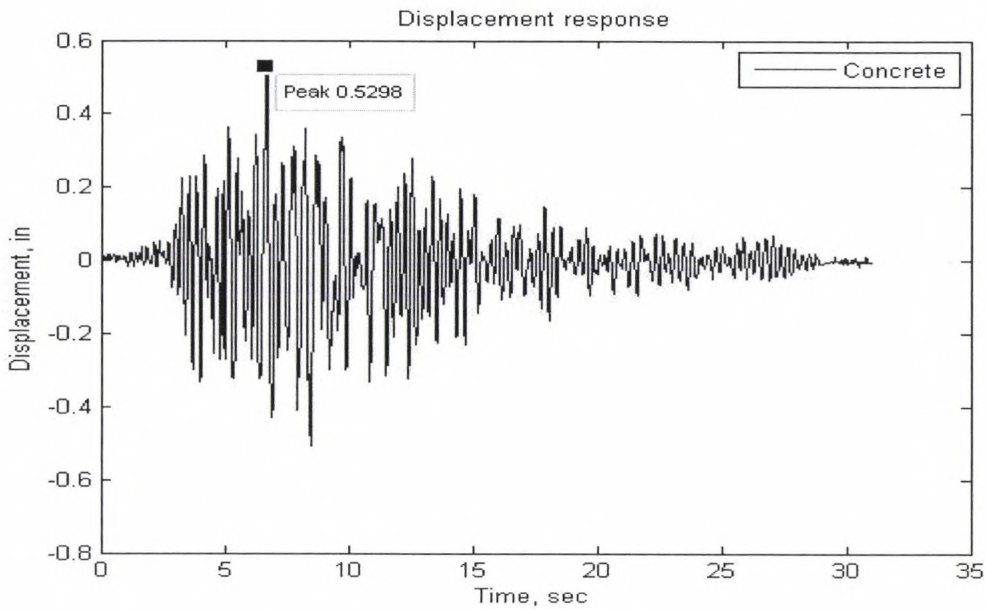

Figure G.19 Displacement response of concrete frame, Column C3 after test sequence 5

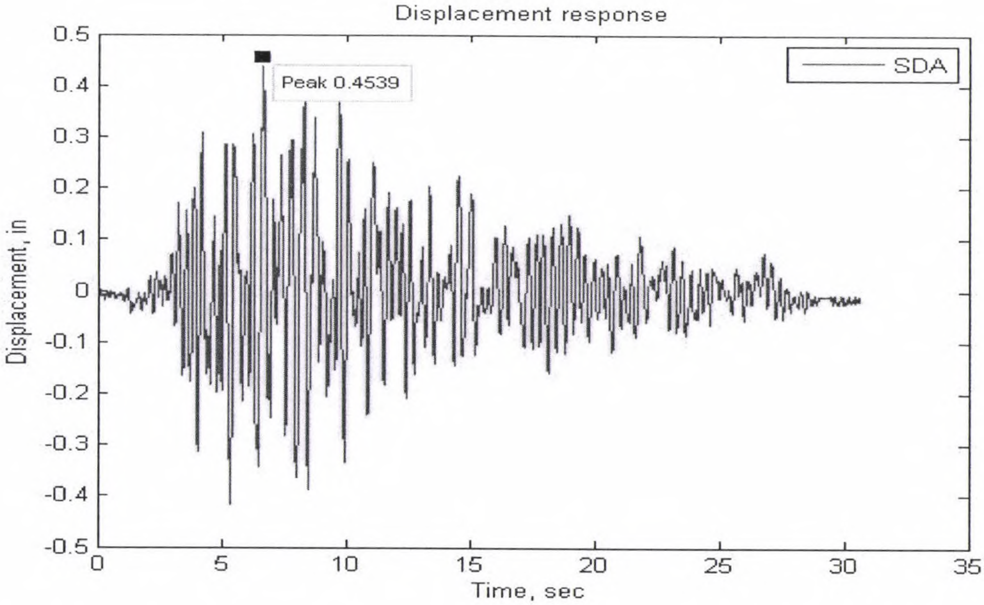

Figure G.20 Displacement response of SDA concrete frame, Column C3 after test sequence 5